The Pennsylvania State University
APPLIED RESEARCH LAB
P.O. Box 30
State College, PA 16804

Sensitivity Analysis of an Estimator-Correlator for the Detection of Spread Targets with Multiple Discrete Highlights

by

Roger W. Schwenke

Technical Report No. TR 00-006
December 2000

Supported by:
Office of Naval Research

L.R. Hettche, Director
Applied Research Laboratory

REPORT DOCUMENTATION PAGE

Form Approved
OMB No. 0704-0188

1. AGENCY USE ONLY (Leave blank)	2. REPORT DATE	3. REPORT TYPE AND DATES COVERED
	December 2000	Thesis in Acoustics

4. TITLE AND SUBTITLE
Sensitivity Analysis of an Estimator-Correlator for the Detection of Spread Targets with Multiple Discrete Highlights

5. FUNDING NUMBERS

6. AUTHOR(S)
Roger W. Schwenke

7. PERFORMING ORGANIZATION NAME(S) AND ADDRESS(ES)
Applied Research Laboratory
The Pennsylvania State University
PO Box 30
State College, PA 16804

8. PERFORMING ORGANIZATION REPORT NUMBER
TR 00-006

9. SPONSORING/MONITORING AGENCY NAME(S) AND ADDRESS(ES)
Office of Naval Research
Ballston Tower
800 North Quincy St.
Arlington, VA 22217 Mr. Les Jacobi

10. SPONSORING/MONITORING AGENCY REPORT NUMBER

11. SUPPLEMENTARY NOTES

12a. DISTRIBUTION/AVAILABILITY STATEMENT
Approved for public release: distribution unlimited

12b. DISTRIBUTION CODE

13. ABSTRACT (Maximum 200 words)

The maximum-likelihood sense optimum detector for the detection of randomly fluctuating multiple highlight objects in Gaussian reverberation and noise is an Estimator-Correlator (EC). If a large time-bandwidth product signal is used, a conventional matched-filter detector can spread scattered energy into multiple detector bins, resulting in lower output in each bin than if all the energy had been concentrated in just one.

The wideband, or Wavelet Transform Domain EC (WTD-EC) recombines the detection statistics from discrete highlights into a single detection statistic, possibly dramatically improving detector performance as characterized by the Receiver Operating Characteristics (ROC). Implementation of the estimator branch of the EC requires an
a priori estimate of the second order statistics of the echo, i.e. the covariance function or scattering function. Scattering functions are used as prior statistics because they are physically meaningful, robust statistical characterizations of distributed scatterers. A critical issue in the implementation of the WTD-EC is the sensitivity of its performance to the errors in the a priori statistical models. (Continued)

14. SUBJECT TERMS	15. NUMBER OF PAGES
Estimator-Correlator, Wavelet Transforms, Sensitivity Analysis, Detection, Scattering Functions, Ambiguity Functions, Receiver Operating Characteristic, ROC	105
	16. PRICE CODE

17. SECURITY CLASSIFICATION OF REPORT	18. SECURITY CLASSIFICATION OF THIS PAGE	19. SECURITY CLASSIFICATION OF ABSTRACT	20. LIMITATION OF ABSTRACT
UNCLASSIFIED	UNCLASSIFIED	UNCLASSIFIED	

This thesis analyzes the sensitivity of the WTD-EC to errors in the assumed scattering functions. Analytic expressions and verified numerical code are developed for the computation of ROC curves for arbitrary target scattering functions, reverberant scattering functions, and wideband transmitted signals. The sensitivity of the detector is found by deriving an expression for the ROC when the assumed scattering function is not the correct scattering function.

It is demonstrated that the WTD-EC cannot be characterized by a scalar figure of merit, and that only a ROC curve is adequate to characterize the performance of the detector. It is demonstrated that the sensitivity closely mimics the automabiguity function of the transmit signal. It is shown that, to some extent, one can trade time-bandwidth product for robustness to error. Compelling evidence is given that the WTD-EC does in fact retain it's advantages even when the a priori estimate contains large errors. Finally, it is shown that one need only estimate the position of target scatterers. It is not necessary t estimate the reverberation scatterers, or the relative magnitude of the target scattering highlights.

ABSTRACT

The maximum-likelihood sense optimum detector for the detection of randomly fluctuating multiple highlight objects in Gaussian reverberation and noise is an Estimator-Correlator (EC). If a large time-bandwidth product signal is used, a conventional matched-filter detector can spread scattered energy into multiple detector bins, resulting in lower output in each bin than if all the energy had been concentrated in just one.

The wideband, or Wavelet Transform Domain EC (WTD-EC) recombines the detection statistics from discrete highlights into a single detection statistic, possibly dramatically improving detector performance as characterized by the Receiver Operating Characteristics (ROC). Implementation of the estimator branch of the EC requires an a priori estimate of the second order statistics of the echo, i.e. the covariance function or scattering function. Scattering functions are used as prior statistics because they are physically meaningful, robust statistical characterizations of distributed scatterers. A critical issue in the implementation of the WTD-EC is the sensitivity of its performance to the errors in the a priori statistical models.

This thesis analyzes the sensitivity of the WTD-EC to errors in the assumed scattering functions. Analytic expressions and verified numerical code are developed for the computation of ROC curves for arbitrary target scattering functions, reverberant scattering functions, and wideband transmitted signals. The sensitivity of the detector is found by deriving an expression for the ROC when the assumed scattering function is not the correct scattering function.

It is demonstrated that the WTD-EC can not be characterized by a scalar figure of merit, and that only a ROC curve is adequate to characterize the performance of the detector. It is demonstrated that the sensitivity closely mimics the autoambiguity function of the transmit signal. It is shown that, to some extent, one can trade time-bandwidth product for robustness to error. Compelling evidence is given that the WTD-EC does in fact retain it's advantages even when the a priori estimate contains large errors. Finally, it is shown that one need only estimate the position of target scatterers. It is s not necessary to estimate the reverberation scatterers, or the relative magnitude of the target scattering highlights.

TABLE OF CONTENTS

LIST OF FIGURES

LIST OF TABLES

ACKNOWLEDGMENTS

I extend my sincere thanks to my thesis advisor Dr. Leon Sibul for his expert guidance and encyclopedic knowledge. I would like to thank Dr. Weiss for her guidance and help and for giving me my first opportunity in graduate school. I would like to thank Dr. Ricker for his thorough review. I would like to thank Dr. Tutwiler for their input and guidance. I thank Dr. Mike Roan for his encouragement and his professional and personal assistance.

I thank with all my heart my family and friends for their love and support. I thank my AP Physics teacher Dr. Dell for his inspiration. Finally, I owe a great debt to my sixth grade teacher Mr. Leshin for telling me I could do anything I set my mind to.

This material is based upon work supported by Mr. Les Jacobi, Code 333, the Office of Naval Research, through the Naval Sea Systems Command under contract No. N000-39-97-D-0042, Delivery Order No. 104.

"Worse than being blind
is being able to see
but have no vision."
- Helen Keller

Chapter 1

INTRODUCTION

1.1 Motivation

The process of transmitting a known signal into an environment and listening for its reflections is referred to generally as Range-Doppler detection. It is usually known under the more specific names SONAR, RADAR, Medical Ultrasound, SODAR, Non-Destructive Evaluation, etc. Advances in computer memory, computation speed, and transducer bandwidth have made possible (and will continue to make possible) higher Time-Bandwidth product (TB) transmit signals and therefore higher resolutions. Traditional Matched Filter (MF) and Estimator-Correlator (EC) methods have better performance with higher TB signals, as long as the resolution of the signal remains coarser than the size of the target. When the TB becomes high enough, resolution becomes finer than the size of the target, the reflected energy is spread across several detection bins and can result in lower probability of detection. This is sometimes referred to as "splitting loss" or "spreading loss". These distinctly resolved reflections will be called highlights. The purpose of this thesis is to use an EC structure to recombine the multiple discrete highlights of the signal, recover the splitting loss that comes with high resolution signals, and evaluate the performance of this EC. To do this, an a priori estimation of the target scattering function must be made, that is, one must make a guess as to where the highlights are. One of the risks in taking on this project is that errors in the scattering function estimate could cancel the gains made by recombining the energy, thus making this process useless in practice. Compelling evidence will be presented that highlight recombination retains its advantages even when the a priori estimate contains large errors.

1.2 Statement of Problem

Higher time-bandwidth product signals are desirable because they afford higher resolution and better probability of detection under correlated noise. With traditional detectors this is limited by splitting loss. A method is needed to recombine the energy split into different detection bins by the high resolution of the signal.

Two detection methods applicable to the Range-Doppler problem are considered. They are, the Estimator-Correlator (EC) and the Matched-Filter (MF). The matched filter simply

correlates the received signal with replicas of the transmit signal which have been delayed and frequency shifted (or scaled). The delay and frequency shift (or scale) of the replica of the transmit signal with the largest correlation represents the distance and radial velocity of the target. When the change in the reflected signal due to the velocity of the target is modeled as a frequency shift, this is called narrowband processing. When the change in the reflected signal due to the velocity of the target is modeled as a scaling of the signal, this is called wideband processing. Wideband processing is explained in section 2.3, narrowband in section 2.4.

The estimator-correlator uses the covariances of the received signal when the target is present, and when it is absent, to form an estimate of the target signal, which is then correlated with the received signal. The EC can also be implemented with either wideband or narrowband processing.

Recently, an implementation of the EC has been derived which represents a spread target as a scattering function in the Wavelet Transform Domain (WTD) [1]. Also, Dixon and Sibul have done work in parameter estimation for spread targets [2], [3]. In[4] Roan and Sibul derived the Receiver Operating Characteristics (ROC) of the WTD-EC, but they only computed the ROC for the case where the covariance eigenvalues are all equal, and they did not compute those eigenvalues from the scattering functions and autoambiguity function of the transmit signal. It is necessary to characterize the performance with the ROC and not with a scalar figure of merit because scatterers with different highlight structures but the same total energy have different ROC curves, and thus can not be described by a single parameter. Critical issues that remain to be addressed include: implementing WTD-EC for arbitrary eigenvalues which have been computed from the scattering functions and the autoambiguity function of the transmit signal, numerical problems in computing the eigenvalues from the scattering function estimates, and computing the Heaviside expansion of the probability distributions, analytic methods of validating the computation, computing ROC curves directly from scattering functions and signals of interest.

One is unlikely to ever estimate the scattering function exactly. It may be true that errors in the scattering function estimate cancel the benefits of attempting to recombine the highlights, making this process useless in practice. A sensitivity analysis of the WTD-EC needs to be derived which should include: general properties of the sensitivity, analytic special cases to validate the

sensitivity, and computations of the sensitivity for scattering functions and transmit signals of interest.

1.3 Original Contribution

The receiver operating characteristics of the wavelet transform domain estimator-correlator are computed for arbitrary covariance eigenvalues which have been computed from the scattering functions and autoambiguity function of the transmit signal. Numerical problems and solutions are identified. Analytic special cases are used to validate the numerical method. Performance of the WTD-EC is compared with the traditional (one highlight) estimator correlator. It is shown that the WTD-EC does in fact have a gain in performance proportional to the energy distributed between the highlights. It is demonstrated that the distance between highlights has little effect on the performance.

The Receiver Operating Characteristics (ROC) are derived for the case where the a priori estimate is not correct. This derivation is independent of the wavelet transform domain implementation of the EC, and is true regardless of how the eigenvalues of the covariances are computed. Analytic special cases are derived to validate the numerical implementation. Many properties of the sensitivity of the WTD-EC are shown. The sensitivity is related to the width of the autoambiguity function. One can trade off, to some extent, time-bandwidth product for robustness to error, but there is a minimum TB below which there is no performance advantage. The sensitivity does not depend on the input SNR. Compelling evidence is given to show that making a scattering function estimate is always better than not making one (assuming one highlight). Overestimating the overall magnitude of the target highlights does not significantly degrade the ROC curve, and thus, when implementing the detector, one need not make an estimate of the reverberant scatterers. Incorrectly estimating the relative magnitudes of highlights with respect to each other also does not significantly degrade the probability of detection, unless the estimate is so small that it is equivalent to guessing that there is no highlight at all.

1.4 Assumptions

It is assumed that the propagation medium is isovelocity, homogeneous, and has no frequency dependent attenuation. Scattering is assumed to be wide-sense stationary and uncorrelated(WSSUS) [5]. This allows for a convenient matrix formulation connecting the wideband scattering function to the covariance matrices. Since no phase information about the highlights is necessary, this makes for a robust model for the recombination of the energy split into highlights. The wideband scattering model is assumed, which implies that the acceleration of the targets is smaller than a limit set by the time bandwidth product, and that the transmit signal is finite energy and square integrable. The scattering function model is very comprehensive. The target object, channel, and unwanted scatterers are modeled with scattering functions to represent highlights, multipath, biologics in underwater, etc. The total scattering function is the convolution of all the component scattering functions [6]. In this thesis the target and reverberation are modeled with scattering functions, therefore one is not limited to assuming uncorrelated Gaussian white noise.

1.5 Overview

Chapter 2 reviews the literature on the topics of signal design and wideband sonar processing. Prerequisite results and theories in wideband processing and estimation are derived. In Chapter 3 various numerical difficulties are overcome, a computational code for calculating the ROC curve is implemented, several analytic cases are derived to validate the code, and ROC curves are computed and compared to traditional methods. In Chapter 4 the sensitivity of the detector to errors in the scattering function estimate is derived, computation code is implemented, analytic cases are used to validate it, and the sensitivity of the detector for several interesting kinds of errors is computed. Appendix B covers the numerical difficulties of computing the Heaviside expansion when poles are close together.

Chapter 2

BACKGROUND

2.1 Wideband Processing

One way to model the reflection from a moving target is to say that it imparts a frequency shift to the reflected signal. This is called narrowband processing, and is discussed in more detail in section 2.4. When the velocity of the target is very high, or when the time-bandwidth product of the signal is very large, the amount by which a signal shrinks or stretches in duration (called time dilation) becomes significant. A reflection model that includes time dilation is called wideband processing, and is discussed in section 2.3.

Several papers have been written by Weiss showing how wideband processing can be implemented as a wavelet transform [7], [8], [9], [10]. Jin et. al. have also shown this [11]. Altes has derived a set of signal transforms which leaves the wideband ambiguity function unchanged [12].

Jourdain and Henrioux have investigated the wideband auto-ambiguity properties of BPSK signals, linear FM, Hyperbolic FM, and Costas Codes [13]. Modulating a BPSK with a Gaussian window and repeating small sections of the code produces higher peak to sidelobe levels than other signal types. Methods of approximating the wideband ambiguity function have been investigated by Ricker [14] and Glisson et. al.[15]. In these schemes scaled versions of the transmit signal are pre-fabricated and the received signal is narrow band correlated around each replica.

In "Wavelet Domain Implementation of the Estimator-Correlator and Weighted Wavelet Transforms", Sibul et. al. [1] derive a continuous wavelet domain estimator correlator for signals propagated in stochastic scattering channels. They show that the detection statistic must be defined using a reproducing kernel Hilbert space. Tague and Sibul [16] have developed a canonical Estimator-Correlator array processor.

In Roan's dissertation [17] a Kalman filter method is used to track changes in the scattering function. ROC curves are not derived, nor is the detection statistic's sensitivity to error in the scattering function estimate computed.

In Grove's dissertation [18] the relationship between errors in physical parameter measurements and errors in the resulting scattering function estimate are derived. Analysis of the change in the detection statistic due to these errors is not conducted in detail.

Very recently Ricker and Cutezo have published a paper [19] where ROC curves are computed for the case where the assumed scattering function is not the correct scattering function. They give three examples each with greater than five highlights. This thesis takes the approach of looking at examples with a very small number of highlights to clearly show relationships such as: errors in position and the autoambiguity function, and errors in highlight magnitude and performance.

In Roan and Sibul's "Performance Quantification for the Wavelet Transform Domain Estimator-Correlator" [4] the ROC is calculated for a high time-bandwidth product signal where the noise covariance eigenvalues all have the same value. The calculation of these ROC curves did not use an actual transmit signal and target and reverberant scattering functions, but rather used eigenvalues that were thought to be representative of a typical system. This thesis expands on that work by creating a method for calculating the ROC from the actual transmit signal, target, and reverberant scattering functions, and deriving the numerical limitations on that calculation imposed by the Heaviside expansion.

2.2 Signal Design

Being able to find the sensitivity of the WTD-EC for an arbitrary transmit signal has important implications for signal design. Future researchers could use the sensitivity analysis of this thesis to find new transmit signals with new qualities. It is important to put such an optimization in the context of signals optimized for other qualities. To this end, a review of signal design literature is given in Appendix A.

The results of this thesis show that, to maximize the ability to discern between similar scatterers (maximum sensitivity to error), one should use high time-bandwidth product signals which have an autoambiguity mainlobe which is as narrow as possible in the direction where you expect error. Signals with "thumb-tack" like autoambiguities, such as FSK signals or Costas codes, are applicable if one is concerned with errors in both range and velocity. If one is only concerned with errors in range, LFM or HFM (velocity tolerant) signals would do well. One

needs a signal which has the widest autoambiguity mainlobe for a given time-bandwidth product in order to maximize robustness to error. This is not a type of signal which has previously been derived, and thus this thesis shows that there may be signals yet to be found which have superior robustness to error in the a priori scattering function estimate than any used today.

The product of the total time-duration of a signal and its total bandwidth, called Time-Bandwidth product (TB), is an important characteristic of a signal. For many years, it was a "folk theorem" that the number of degrees of freedom of a signal equaled 2TB. This was made rigorous by Slepian, Landau, and Pollack [20], [21], [22], [23], [24] . Generally, the higher the TB, the sharper the resolution in the time-scale, or time-frequency plane.

Given a digital signal with N sample points, one could "play it back" through a Digital to Analog Converter (DAC) at a low sampling frequency, and get an analog signal with a long time duration and low bandwidth. Conversely, one could play it back with a high sampling frequency and get a signal with a short time duration and large bandwidth. Because a digital signal with N samples has the same TB regardless of the sampling frequency used to play it back through a Digital to Analog Converter (DAC), this thesis will usually characterize a signal by its TB, and not mention the time duration or bandwidth it would have if transmitted at a particular sampling frequency.

2.3 Wideband Derivation

In order to implement an estimator correlator one must have a model for how signals are reflected by scatterers. Consider a signal f(t) transmitted from a stationary position and reflected from a stationary object. The return signal g(t) will be delayed by a factor $\tau = 2R/c$ so that $g(t) = f(t-\tau)$. Here R is the distance between the transmitter and reflector, and c is the propagation speed of the signal [25], [26], [27].

More generally, if R is expressed as a function of time, as in the case of a moving scatterer, then the round-trip travel time is:

$$\tau(t) = \frac{2}{c} R(t - \frac{\tau(t)}{2}) \qquad (1)$$

Then $\tau(t)$ can be solved for by differentiating with respect to time (denoted by prime)

$$\tau'(t) = \frac{2}{c} R'(t - \frac{\tau(t)}{2})[1 - \frac{\tau'(t)}{2}] \quad (2)$$

In this derivation parenthesis denote arguments of functions and brackets denote groups of terms. Assuming the velocity $v = R'(t)$ is nearly constant (i.e., no acceleration) over the length of the signal

$$\tau'(t) = \frac{2v}{c+v} \quad (3)$$

Integrating and choosing $\tau(\tau_0) = \tau_0$, yields

$$\tau(t) = \tau_0 + \frac{2v}{c+v}[t - \tau_0] \quad (4)$$

Substituting into $g(t) = f(t - \tau(t))$ yields

$$g(t) = f(s[t - \tau]) \text{ where } s = \frac{c-v}{c+v}.$$

This is the wideband model for signal reflection. It is easy to see that the signal is stretched or contracted by the scale factor s. This scale factor is analogous to the scale factor of the wavelet transform. It will be shown that wideband correlation is the same as a wavelet transform.

The restriction that the velocity be nearly constant (or nearly no acceleration) is more precisely stated as [50]:

$$TB^{\frac{1}{2}} < \sqrt{\frac{c}{2a}}, \quad (5)$$

where T is the time length of the signal, B is the bandwidth, and a is the acceleration of the object.

In order to estimate the range and velocity of an object, the received signal g(t) must be correlated with hypothesized scaled and time shifted versions of the transmitted signal. The maximum of this wideband correlation will correspond to the velocity and displacement of the object. The wideband correlation of two functions f(t) and g(t) is given by:

$$WC(s,\tau)_{fg} = s^{\frac{1}{2}} \int g(t) f^*(s[t-\tau])dt, \tag{6}$$

where the factor $s^{1/2}$ has been added to preserve energy. The wavelet transform is defined as [28]

$$W_f g(s,\tau) = \frac{1}{s^{1/2}} \int g(t) f^*(\frac{t-\tau}{s})dt \tag{7}$$

It can be seen that the wideband correlation (or wideband matched filter) is identical to a continuous wavelet transform with the change of variables $s \rightarrow 1/s$

2.4 Narrowband Derivation

For many years wideband processing was considered too computationally expensive. As such, an approximation was made so that the processing could be carried out using a Fourier Transform instead of a Wavelet transform. In this processing, the time-bandwidth product and the velocity are further restrained. Assuming the transmitted signal is of the form of a pure tone of center frequency ω_c modulated by a complex envelope function w(t), f(t) can be written as:

$$f(t) = w(t)e^{i\omega_c t} \tag{8}$$

The time delayed and time scaled received signal, g(t) then becomes

$$g(t) = w(s[t-\tau])e^{i\omega_c s[t-\tau]} \tag{9}$$

Defining $s = 1-\delta$ and $\delta = 2v/(c+v)$, g(t) can be written as:

$$g(t) = w([1-\delta][t-\tau])e^{i\omega_c [t-\tau]}e^{i\omega_c \delta[t-\tau]} \tag{10}$$

Defining the Doppler shift along the line of sight to be $\omega_d = \omega_c \delta$, and assuming v/c<<1, yields:

$$g(t) \approx w(t-\tau) e^{i\omega_c[t-\tau]} e^{i\omega_d[t-\tau]} \tag{11}$$

or,

$$g(t) \approx f(t-\tau) e^{i\omega_d[t-\tau]} \tag{12}$$

This is the narrowband model for signal reflection. The signal has been delayed by τ and shifted in frequency by an amount ω_d. It can be shown [29] that this constrains the time-bandwidth product such that:

$$TB << \frac{c}{2v} \tag{13}$$

Again, in order to detect the range and velocity of an object, the received signal g(t) must be correlated with hypothesized scaled and time shifted versions of the transmitted signal. The maximum of the magnitude of this narrowband correlation will correspond to the velocity and displacement of the object.

2.5 Wideband and Narrowband Differences: an Example

Consider a linear frequency modulated signal with center frequency 50Hz, and bandwidth of 80Hz (frequency changes from 10Hz to 90Hz). If this signal were frequency shifted by 100Hz, its time duration would be the same, its center frequency would be 150Hz, and its bandwidth would remain 80Hz (frequency sweeps from 110Hz to 190Hz). If, instead, this signal were scaled by a factor of three, its time duration would be one third of the original, its center frequency would still be 150Hz, however its bandwidth would be 240Hz (sweep from 30Hz to 270). This is shown in figure 1. This shows that scaling a signal yields a different time series than when applying a Doppler shift to that same signal. Thus, it is important to process wideband signals with time-scale methods rather than with narrowband techniques.

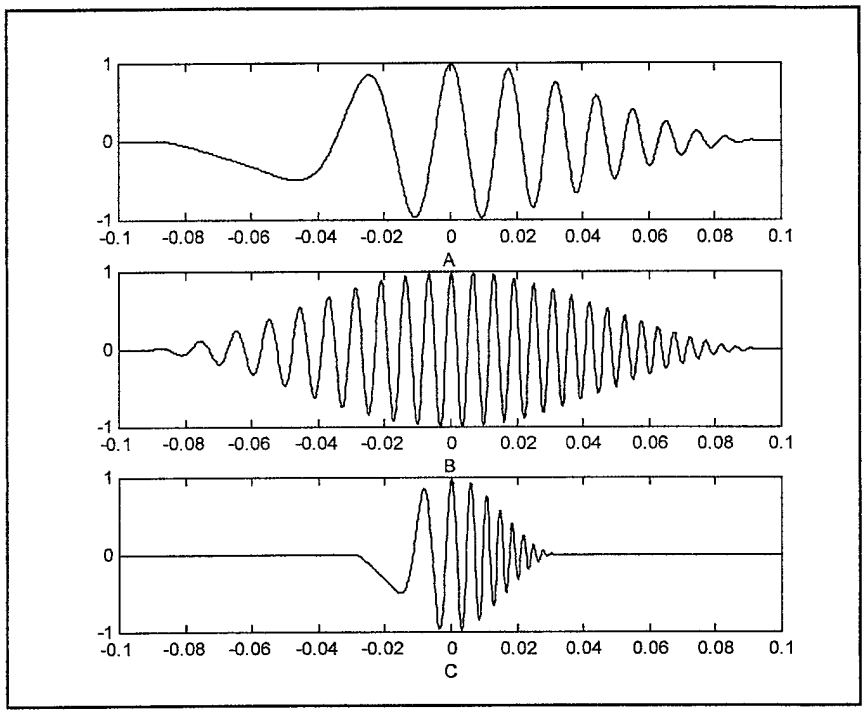

Figure 1 A comparison of frequency shifting and scaling. A)LFM with center frequency 50Hz and bandwidth of 80Hz. B)Frequency shifted by 100Hz. C)Scaled by a factor of 3.

2.6 Deriving the Likelihood Ratio

Now that it has been shown how the scattering process affects the transmit signal, a detector to estimate the scattering processes can be derived. Basic detection and estimation theory has been thoroughly laid out in books such as Van Trees [30], [31] and McDonough and Whalen [32]. This derivation follows the one in Van Trees [30] chapter 2. In an active system, a known signal, f(t), is transmitted into a channel and reflected by scatterers and received as, $r_u(t)$:

$$r_u(t) = y_u(t) + n_u(t) \tag{14}$$

where $n_u(t)$ is unwhitened noise, and $y_u(t)$ is that part of the received signal caused by the reflection and reverberation of the transmit signal. The subscript u denotes the unwhitened input

signal. The Likelihood ratio is:

$$\Lambda(r) \equiv \frac{p_{r|H_1}(r|H_1)}{p_{r|H_0}(r|H_0)}$$

where H_1 denotes the hypothesis that a scatterer is present at a particular scale and delay, and H_0 denotes the hypothesis that there is no scatterer present. The expression $p_{r|H_i}(r|H_i)$ denotes the probability that the observed vector r occurred given hypothesis H_i is true (i=0,1). When the components of the vector r are jointly Gaussian the likelihood ratio can be written

$$\Lambda(r) = \frac{|R_0| \exp\left[(r^H - m_1^H) R_1^{-1} (r - m_1)\right]}{|R_1| \exp\left[(r^H - m_0^H) R_0^{-1} (r - m_0)\right]} \underset{>}{<} \eta \qquad \textbf{(16)}$$

where R_0 and R_1 are the covariance matrices for the received signal under H_0 and H_1 respectively, and m_0 and m_1 are the mean vectors of the received signal, H represents the Hermitian transpose (complex conjugate transpose), and η is the threshold. Taking the log, assuming the means are zero($m_0 = m_1 = 0$), and moving constant coefficients to the right hand side, the log likelihood ratio is

$$l(r) = \log \Lambda(r) = r^H (R_0^{-1} - R_1^{-1}) r \underset{>}{<} \gamma \qquad \textbf{(17)}$$

where γ is η divided by all the constant coefficients of equation 16. For the signal defined in equation 14, the covariances are:

$$R_0 = R_{n_u n_u} \text{ and } R_1 = R_{r_u r_u} = R_{y_u y_u} + R_{n_u n_u}$$

Here $R_{n_u n_u}$ is the unwhitened noise covariance, $R_{y_u y_u}$ is the total echo covariance, and $R_{r_u r_u}$ is the received signal covariance. Substituting these into equation 17 yields:

$$l = r^H (R_{n_u n_u}^{-1} - R_{r_u r_u}^{-1}) r$$

Rearranging yields

$$l = r^H R_{r_u r_u}^{-1} (R_{r_u r_u} - R_{n_u n_u}) R_{n_u n_u}^{-1} r$$

Using $R_{r_u r_u} = R_{y_u y_u} + R_{n_u n_u}$ yields:

$$l = r^H R_{r_u r_u}^{-1} (R_{y_u y_u} + R_{n_u n_u} - R_{n_u n_u}) R_{n_u n_u}^{-1} r$$

which can be simplified to:

$$l = r^H R_{r_u r_u}^{-1} R_{y_u y_u} R_{n_u n_u}^{-1} r \tag{21}$$

Identifying that the estimate of the target signal $\hat{y}$ is:

$$\hat{y} = R_{r_u r_u}^{-1} R_{y_u y_u} r$$

the likelihood ratio can be written:

$$l = \hat{y}^H R_{n_u n_u}^{-1} r$$

This detector is referred to as the estimator-correlator, because it first makes an estimate of the target signal ($\hat{y}$) and then correlates it with the whitened received signal ($R_{n_u n_u}^{-1} r$). This was first brought to light by Price [33] for Gaussian signals in Gaussian noise. Work has been done to extend this to other models of continuous signals by Esposito [34] and Kailath [35], [36], and discrete signals by Schwartz [37], [38]. Middleton [39] has analyzed simultaneous detection and estimation

2.7 The Whitening Process

To derive a detector for a signal in colored noise, a detector is proposed (without explanation), and then shown to have suitable detector qualities. This derivation follows the one in Van Trees 30 section 4.3.1. Consider a received signal, $r_u(t)$, which consists of a desired signal $y_u(t)$, and colored noise, $n_u(t)$

$$r_u(t) = y_u(t) + n_u(t)$$

The filter $h_w(t,u)$ which is known to whiten $n_u(t)$, is now applied to $r_u(t)$

$$r(t) = \int h_w(t,u) r_u(u) du$$

The subscript u is dropped from whitened variables. Expanding yields:

$$r(t) = \int h_w(t,u) y_u(u) du + \int h_w(t,u) n_u(u) du$$

The integrals are now renamed

$$r(t) = y(t) + n(t)$$

Thus the problem has been reduced to detecting a known signal in white noise. The sufficient statistic Λ for a known signal in white noise is:

$$\ln \Lambda[r(t)] = \int r(t) y(t) dt - \frac{1}{2} \int y^2(t) dt$$

The whitened known signal $y(t)$ can be pre-computed before the likelihood ratio is computed so that only the first term on the right hand side needs to be computed in real time. However, in this formulation the received signal must be whitened in real time for the likelihood ratio to be computed. This is known as the Whitening realization. Another realization can be derived which does not require whitening the received signal in real time. Substituting in the expression for the whitened variables:

$$\ln \Lambda[r(t)] = \int dt \int du\, h_w(t,u) r_u(u) \int dv\, h_w(t,v) y_u(v) - E_s$$

where E_s is the energy in the transmit signal. Changing the order of integration (which can be done because the signals are of finite duration) yields:

$$\ln \Lambda[r_w(t)] = \int du\, r_u(u) \int dv\, y_u(v) \int h_w(t,u) h_w(t,v) dt$$

Defining:

$$Q(u,v) = \int h_w(t,u)h_w(t,v)dt$$

Substituting this into the log-likelihood yields:

$$\ln \Lambda[r(t)] = \int dur_u(u) \int y_u(v)Q(u,v)dv$$

This can be further simplified by defining

$$g(u) = \int y_u(v)Q(u,v)dv$$

which yields

$$\ln \Lambda[r(t)] = \int r_u(u)g(u)du$$

This is called the correlator realization, or the mismatched filter for colored noise. It is used throughout this work. Because g(u) can be pre-computed, this realization has the same real-time computational complexity as standard detection in white noise.

2.8 Calculating the Eigenvalues of the Noise Covariance

The inputs to the likelihood ratio (equation 14) are the received signal covariance and the noise covariance. It is now shown that the noise covariance can be calculated from the scattering function and the transmit signal autoambiguity function. The following development comes from personal communication with L. H. Sibul. For a good review of eigenvalue decomposition see [45]. The eigenvalues λ_k and eigenvectors $u_k(t)$ of the unwhitened noise covariance $R_{n_u n_u}$ are:

$$\lambda_k u_k(t) = \int R_{n_u n_u}(t,\tau)u_k(\tau)d\tau$$

The noise covariance is composed of white noise and a component due to unwanted scatterers and reverberation in the channel:

$$n_u(t) = n_w(t) + reverb(t)$$

where $n_w(t)$ jointly Gaussian white noise, and $reverb(t)$ is the signal reflected by the reverberant scatterers. Therefore $R_{n_u n_u}$ can be decomposed as:

$$R_{n_u n_u} = \frac{N_0}{2}\delta(t-\tau) + R_{reverb}(t,\tau)$$

Where $(N_0/2)\delta(t-\tau)$ denotes the white noise component, and $R_{reverb}(t,\tau)$ is the covariance of the reverberant signal. The eigenvalues now become:

$$\lambda_k u_k(t) = \frac{N_0}{2}u_k(t) + \int R_{rev}(t,\tau)u_k(\tau)d\tau$$

The eigenvalues are now defined in terms of a white and reverberant component:

$$\lambda_k = \frac{N_0}{2} + \lambda_k^{rev}$$

The reverberant eigenvalues are then:

$$\lambda_k^{rev} u_k(t) = \int R_{rev}(t,\tau)u_k(\tau)d\tau \qquad \textbf{(40)}$$

The reverberant time signal can be represented in terms of the reverberant scattering function, from Sibul, et. al. [1] as:

$$reverb(t) = \int w_{rev}(x)[U(x)f(t)]d\mu(x) \qquad \textbf{(41)}$$

where $w_{rev}(x)$ is the narrowband or wideband reverberant spreading function, $d\mu(x)$ is the left invariant Haar measure on the appropriate (narrowband/Heisenberg or wideband/affine) group G, U(x) is a unitary representation of the corresponding group, f(t) is the transmit signal, and the

vector x represents either (τ, ϕ) or (τ, s) where τ is time delay, ϕ is frequency shift, and s is scale. The spreading function w(x) can be estimated by wavelet transform of the reverberant signal. Equation 41 is essentially representing reverb(t) in terms of the inverse wavelet transform of the spreading function. U(x) is an operator which represents the transformation $f(t) \Rightarrow f(s(t-\tau))$. A good review of a group theory approach to the ambiguity function can be found in Grove [18] or Chaiyasena [40]. The covariance of the reverberation is:

$$R_{rev}(t,\tau) = E\{rev(t)rev^*(\tau)\}$$

Rewriting this is terms of the scattering function yields:

$$R_{rev}(t,\tau) = \int\int E\{w(x)w^*(x')\}[U(x)f(t)][U(x')f(\tau)]^* d\mu(x)d\mu(x')$$

Defining the reverberant scattering function as $S_{rev}(x,x') = E\{w(x)w^*(x')\}$ yields:

$$R_{rev}(t,\tau) = \int\int S_{rev}(x,x')[U(x)f(t)][U(x')f(\tau)]^* d\mu(x)d\mu(x')$$

Assuming uncorrelated scattering (WSSUS), i.e., $S(x,x') = S(x,x)\delta(x-x')$, the reverberation covariance becomes:

$$R_{rev}(t,\tau) = \int S_{rev}(x,x)[U(x)f(t)][U(x)f(\tau)]^* d\mu(x)$$

Substituting this into the eigenvalue equation 40 yields:

$$\lambda_k^{\ rev} u_k(t) = \int\int S_{rev}(x,x)[U(x)f(t)][U(x)f(\tau)]^* u_k(\tau)d\tau d\mu(x)$$

Taking the wavelet transform of both sides with respect to f(t) yields:

$$\lambda_k^{rev} \int [U(x')f(t)]^* u_k(t)dt =$$
$$\int\int\int S_{rev}(x,x)[U(x)f(t)][U(x')f(t)]^*[U(x)f(\tau)]^* u_k(t)d\tau dt d\mu(x)$$

Using the definition of the reproducing kernel for the space spanned by $\langle g, U(x)f \rangle$, we identify:

$$K(x,x') = \langle U(x)f, U(x')f \rangle_H$$

where $\langle \bullet, \bullet \rangle_H$ denotes the inner product on the Hilbert space H. K contains all the information about the transmit signal and its autoambiguity function. The eigenvalue equation becomes

$$\lambda_k^{rev} W_f u_k(x') = \int S_{rev}(x,x) K(x,x') W_f u_k(x) d\mu(x)$$

where W_f denotes the wavelet transform with respect to f(t). The above can be discretized by only considering the points (x_j) where scatterers (highlights) exist.

$$\lambda_k^{rev} W_f u_k(x_i) = \sum_j K(x_i, x_j) S_{rev}(x_j, x_j) W_f u_k(x_j) \qquad \textbf{(50)}$$

where x_j represents the scale and delay of each highlight and $S(x_j, x_j)$ represents the strength of each highlight. In section 3.6 it is shown that this discretization may dramatically reduce the computation time that might have otherwise been needed. Using $\bar{\psi}_k = W_f u_k(x_j)$ the reverberation covariance eigenvalues can be written as

$$\lambda_k^{rev} \bar{\psi}_k = \underline{\underline{K}} \underline{\underline{S_{rev}}} \bar{\psi}_k \qquad \textbf{(51)}$$

These eigenvalues and eigenfunctions will be used to whiten the received signal covariance and target scattering signal covariance. Similarly, the eigenvalues for $R_{y_i y_i}$ are:

$$\lambda_k^{y} \bar{\psi}_k = \underline{\underline{K}} \underline{\underline{S_{\text{target}}}} \bar{\psi}_k$$

where S_{target} denotes the target scattering function $S_{\text{target}} = E\{w_{\text{target}}(x) w_{\text{target}}(x')\}$.

The scattering function of the reverberation and of the target are physical models of targets of interest and the environments in which they might be found. The likelihood function

will now be derived in terms of these eigenvalues.

The unwhitened noise covariance matrix can be represented in terms of its eigenvalues and eigenvectors as:

$$R_{n_u n_u} = U_{n_u} \Lambda_{n_u} U_{n_u}^{-1}$$

where Λ_{n_u} is the diagonal matrix of eigenvalues, and U_{n_u} is a matrix whose columns are the eigenvectors $\bar{u}_k$, which in turn is computed from $\bar{u}_k = W_f^{-1} \bar{\psi}_k(x_j)$. A transformation is now presented that will map $R_{n_u n_u}$ into the identity matrix and this transformation is then applied to all other variables. These whitened variables will not have the subscript u.

$$R_{nn} = \Lambda_{n_u}^{-1/2} U_{n_u}^H R_{n_u n_u} U_{n_u} \Lambda_{n_u}^{-1/2}$$

Expanding $R_{n_u n_u}$ yields:

$$R_{nn} = \Lambda_{n_u}^{-1/2} U_{n_u}^H [U_{n_u} \Lambda_{n_u} U_{n_u}^H] U_{n_u} \Lambda_{n_u}^{-1/2} = I$$

Applying the whitening filter to $R_{y_u y_u}$ yields:

$$R_{yy} = \Lambda_{n_u}^{-1/2} U_{n_u}^H R_{y_u y_u} U_{n_u} \Lambda_{n_u}^{-1/2}$$

Expanding $R_{y_u y_u}$ yields:

$$R_{yy} = \Lambda_{n_u}^{-1/2} U_{n_u}^H [U_{y_u} \Lambda_{y_u} U_{y_u}^H] U_{n_u} \Lambda_{n_u}^{-1/2}$$

To calculate the likelihood ratio, R_{rr} must first be found

$$R_{rr} = R_{yy} + R_{nn}$$

Because R_{nn} is white and the eigenvalues of the received signal covariance can be calculated

from the scattering function, the following holds:

$$R_{rr} = U_y \Lambda_y U_y^H + I$$

By noting

$$U_y I U_y^H = U_y U_y^H = I$$

The identity matrix can be brought inside

$$R_{rr} = U_y [\Lambda_y + I] U_y^H$$

The likelihood ratio derived in equation 14 was

$$l = r^H R_{nn}^{-1} R_{yy} R_{rr}^{-1} r$$

Substituting in expressions for the whitened variables yields:

$$l = r^H [I][U_y \Lambda_y U_y^H][U_y (\Lambda_y + I)^{-1} U_y^H] r$$

which can be simplified to:

$$l = r^H U_y \Lambda_y (\Lambda_y + I)^{-1} U_y^H r$$

Defining

$$z = U_y^H r$$

the likelihood becomes:

$$l = z^H \Lambda_y (\Lambda_y + I)^{-1} z$$

The covariance of z is now computed for later use:

$$R_{zz} = U_y^H R_{rr} U_y$$

Expanding R_{rr} yields:

$$R_{zz} = U_y^H [R_{yy} + I] U_y$$

or more simply:

$$R_{zz} = \Lambda_y + I$$

We have now come quite a ways from our original expression for the likelihood function. We will now condense together only the terms needed to calculate the likelihood ratio in practice. First, the likelihood function itself is:

$$l = z^H \Lambda_y (\Lambda_y + I)^{-1} z$$

where z is the whitened received signal:

$$z = U_y^H r$$

U_y^H and Λ_y are the eigenfunctions and eigenvalues of the whitened target scattering signal covariance which is:

$$R_{yy} = \Lambda_{n_u}^{-1/2} U_{n_u}^H R_{y_u y_u} U_{n_u} \Lambda_{n_u}^{-1/2}$$

U_{n_u} and Λ_{n_u} are the eigenfunctions and eigenvalues of the unwhitened noise covariance which are derived from the reverberation scattering function and the transmit signal autoambiguity function:

$$\lambda_k^{rev} \bar{\psi}_k = \underline{\underline{K}} \underline{\underline{S}}_{rev} \bar{\psi}_k$$

Likewise the unwhitened target scattering signal covariance $R_{y_u y_u}$ is computed from the target scattering function and the transmit signal autoambiguity function:

$$\lambda_k^{y} \bar{\psi}_k = \underline{\underline{K}} \underline{\underline{S}}_{\text{target}} \bar{\psi}_k$$

Thus the inputs to the likelihood function consist of the received signal, the transmit signal auto-

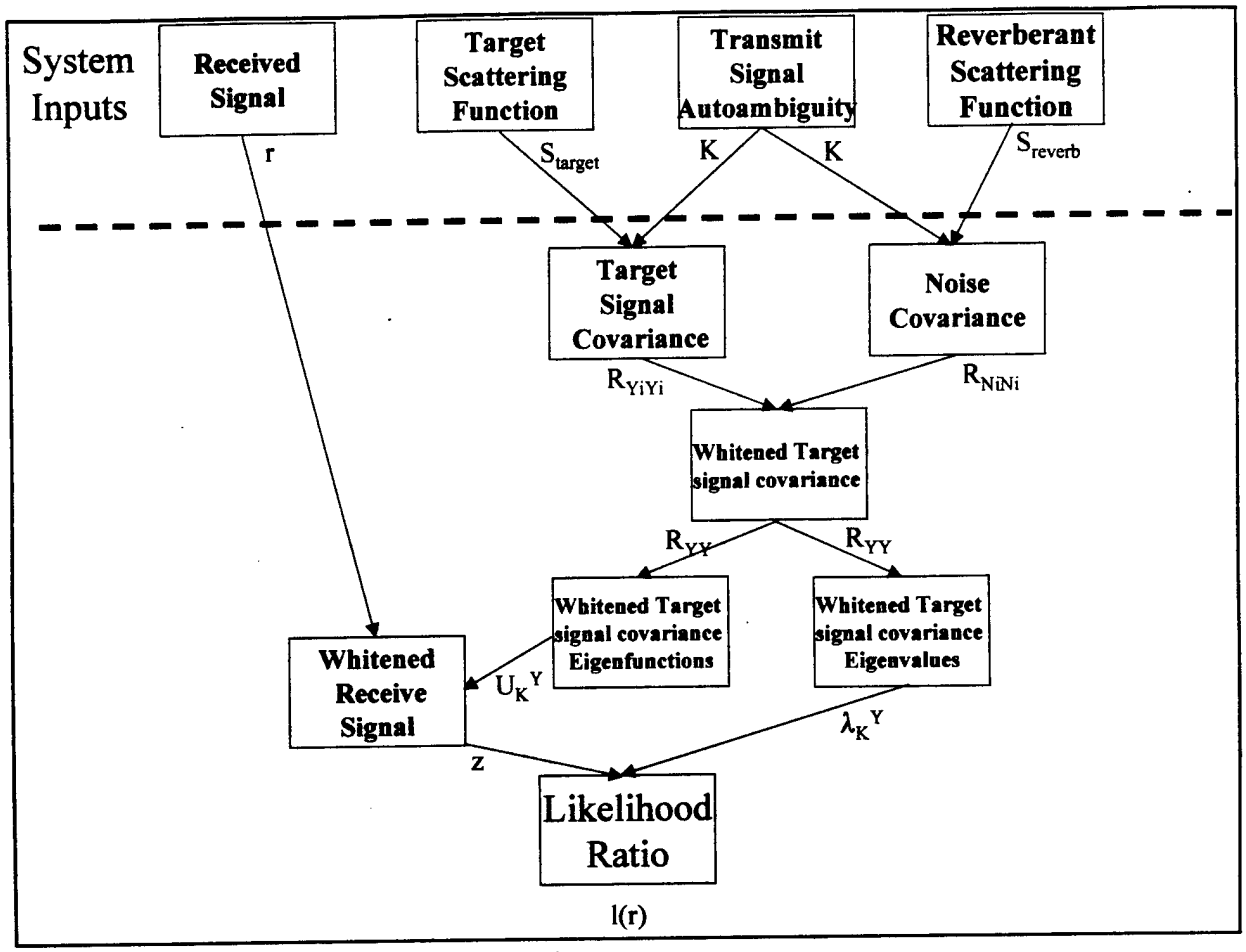

Figure 2 Ingredients of the Likelihood Ratio

ambiguity function, the target scattering function, and the reverberation scattering function. This is shown graphically in figure 2 .

2.9 Calculating the Receiver Operating Characteristics

To evaluate the performance of the likelihood detector that has been derived in the previous section, it is necessary to find the Receiver Operating Characteristics. The following derivation of the ROC comes from personal communication with L. H. Sibul. First, the characteristic function of the probability density of the likelihood function is found. The probability density will be evaluated by taking a Heaviside expansion of the characteristic function. Finally, the probabilities of detection and false alarm will be computed from the

probability density function. The log likelihood can be written in scalar form as:

$$l = \sum_{k=1}^{N} |z_k|^2 \frac{\lambda_k^y}{\lambda_k^y + 1}$$

where N is the number samples in the received vector (as explained in section 3.1), z_k are the individual samples in the whitened received vector $\bar{z}$, and $\Lambda_y = diag(\lambda_k^y)$. Using

$$E\{|z_k|^2 | H_0\} = 1 \text{ and } E\{|z_k|^2 | H_1\} = \lambda_k^y + 1$$

Unit variance white Gaussian random variables can be written in terms of z_k

$$v_{k_0} = \frac{z_k}{1} \text{ and } v_{k_1} = \frac{z_k}{\lambda_k + 1}, \; k = 1,\ldots,N$$

where sub-subscript 0 or 1 indicates that this variable corresponds to H_0 or H_1 respectively. Using these, the likelihood ratio can be rewritten such that the magnitude of each term in the sum is expressed solely in terms of the eigenvalues

$$l|H_0 = \sum_{k=1}^{N} |v_{k_o}|^2 \frac{\lambda_k^y}{\lambda_k^y + 1} \text{ and } \quad l|H_1 = \sum_{k=1}^{N} |v_{k_1}|^2 \lambda_k^y$$

Using i=0,1, and rewriting the complex variable $v_{k_i} = c_{k_i} + jd_{k_i}$ yields:

$$l|H_0 = \sum_{k=1}^{N} (c_{k_0}{}^2 + d_{k_0}{}^2) \frac{\lambda_k^y}{\lambda_k^y + 1} \text{ and } l|H_1 = \sum_{k=1}^{N} (c_{k_1}{}^2 + d_{k_1}{}^2) \lambda_k^y$$

Each term in the sum is of the form $y = A_{k_i} x^2$ where:

$$A_{k_0} = \frac{\lambda_k^y}{\lambda_k^y + 1} \text{ and } A_{k_1} = \lambda_k^y .$$

We may now use the property that any random variable that is the sum of independent random

variables, has a probability density which is the convolution of the probability densities in the sum. This can be found in standard texts such as Papoulis [41], or Bendat and Piersol [5]. In other words, for general random variables x, y, z with probability density function p_x, p_y, p_z, if:

$$z(k) = x(k) + y(k)$$

then

$$p(z) = \int p_x(x) p_y(z - x) dx$$

or

$$\phi_z(\omega) = \phi_x(\omega)\phi_y(\omega)$$

where $\phi(\omega)$ is the Fourier transform of a probability density, and is called the characteristic function:

$$\phi(\omega) = E[e^{j\omega x}] = \int p(x) e^{j\omega x} dx$$

The Characteristic function of one term of the likelihood ratio is:

$$\phi_y = \frac{1}{\sqrt{2\pi}} \int e^{j\omega A_{k_i} x^2} e^{-x^2/2} dx \text{ or } \phi_y = (1 - j2\omega A_{k_i})^{-1/2}$$

Using the property that functions convolved in the probability domain are multiplied in the characteristic domain yields:

$$\phi_{l_i} = \prod_{k=1}^{N} (1 - j2\omega A_{k_i})^{-1/2} (1 - j2\omega A_{k_i})^{-1/2}$$

or

$$\phi_{l_i} = \prod_{k=1}^{N} (1 - j2\omega A_{k_i})^{-1}$$

By using the Heaviside Partial Fraction Expansion [42], this can be written as

$$\phi_{l_i} = \sum_{k=1}^{N} \frac{K_{k_i}}{1 - j2\omega A_{k_i}} \tag{82}$$

where

$$K_{k_i} = (1 - j2\omega A_{k_i}) \prod_{j=1}^{N} \frac{1}{(1 - j2\omega A_{j_i})} \Big|_{\omega = 1/(j2A_{k_i})}$$

Subsequently:

$$p_{l|H_1}(l|H_1) = \frac{1}{2\pi} \int \sum_{k=1}^{N} \frac{K_{k_1} e^{j\omega l}}{1 - j2\omega A_{k_1}} d\omega$$

This integral is often listed in Laplace transform tables, such as Spiegel [43], so the following substitutions are made: $s = j\omega$, $ds = jd\omega, d\omega = ds/j$

$$p_{l|H_1}(l|H_1) = \sum_{k=1}^{N} K_{k_1} \frac{1}{2\pi j} \int \frac{e^{sl}}{1 - 2sA_{k_1}} ds$$

Letting $\mathcal{L}$ denote the Laplace transform yields:

$$p_{l|H_1}(l|H_1) = \sum_{k=1}^{N} K_{k_1} \mathcal{L}^{-1} \left\{ \frac{1}{1 - 2sA_{k_1}} \right\}$$

or

$$p_{l|H_1}(l|H_1) = \sum_{k=1}^{N} K_{k_1} \mathcal{L}^{-1} \left\{ \frac{1}{-2A_{k_1}(s - 1/2A_{k_1})} \right\}$$

Evaluating the inverse Laplace transform yields:

$$p_{l|H_1}(l|H_1) = \sum_{k=1}^{N} \frac{K_{k_1}}{-2A_{k_1}} e^{-l/2A_{k_1}} \tag{88}$$

The probability of detection is defined as:

$$P_d = \int_{\gamma}^{\infty} p_{l|H_1}(l|H_1)dl$$

Where γ is the threshold from equation 17. Substituting equation 88 into the above yields:

$$P_d = \int_{\gamma}^{\infty} \sum_{k=1}^{N} \frac{K_{k_1}}{-2A_{k_1}} e^{-l/2A_{k_1}} dl$$

or

$$P_d = \sum_{k=1}^{N} \frac{K_{k_1}}{-2A_{k_1}} \int_{\gamma}^{\infty} e^{-l/2A_{k_1}} dl$$

Integrating over l yields:

$$P_d = \sum_{k=1}^{N} \frac{K_{k_1}}{-2A_{k_1}} \frac{e^{-\gamma/2A_{k_1}}}{-1/2A_{k_1}}$$

or

$$P_d = \sum_{k=1}^{N} K_{k_1} e^{-\gamma/2A_{k_1}} \quad \textbf{(93)}$$

Similarly, the probability of false alarm is:

$$P_f = \sum_{k=1}^{N} K_{k_0} e^{-\gamma/2A_{k_0}} \quad \textbf{(94)}$$

A ROC curve is the plot of probability of false alarm versus the probability of detection. Equations 93 and 94 are what are used to compute all of the ROC curves in this thesis. Because of the form of equations 93 and 94 two scatterers that have the same amount of energy in the whitened eigenvalues will have different ROC curves if the energy is distributed differently between the eigenvalues. This is why a scalar figure of merit can not be used to characterize the

WTD-EC. In short, the performance can not be characterized by a scalar because the scatterer can not be characterized by a scalar.

One of the original contributions of this thesis is that these curves are not using equal eigenvalues as in Roan and Sibul [4].

Chapter 3

IMPLEMENTING THE WAVELET TRANSFORM DOMAIN ESTIMATOR CORRELATOR

3.1 Implementing the WTD-EC

One decision to be made in implementing the WTD-EC is deciding how large the matrices will be. It is easiest to start at the end. When the detector is actually implemented it will have to compute:

$$l = r^H R_{nn}^{-1} R_{yy} R_{rr}^{-1} r$$

In order to include all of the energy reflected from the target, the received vector r has to be at least as long as the transmit signal convolved with the scattering function. We will call this length N. Now let's go to the beginning. To find the unwhitened covariance eigenvalues, we must implement the equation:

$$\lambda_i \psi_i(x_i) = \sum_{j=1}^{N} K(x_i, x_j) S(x_j, x_j) \psi_i(x_j) \qquad \textbf{(96)}$$

where each x_j is a position in scale and delay space $x_j = (s_j, \tau_j)$. There is no restriction on where these positions should be, or what order they should be in, only that there should be at least N of them. Again, in order to capture all of the energy in the target, there should be an x_j for each highlight.

Theoretically it is possible for there to be more than N highlights (if there are many highlights at many scales). In this case it would be necessary to make the received vector longer.

Equation 96 is easily implemented as a matrix equation:

$$\lambda_i \psi_i = \underline{\underline{KS}} \psi_i \qquad \textbf{(97)}$$

In our case, this equation is implemented with the Matlab eig() function. Matlab will automatically normalize ψ_i. In practice there is one large eigenvalue for each highlight, and the

eigenvector for that eigenvalue looks like the autoambiguity function centered on the highlight position. Note that even though x_j does not enter into equation 97, one must still keep track of it in order to take the inverse wavelet transform of ψ_i.

$$u_i = W_f^{-1}\psi_i(x_j)$$

or

$$u_i = \sum_{j=1}^{N}[U(x_j)f(t)]\psi_i(x_j)$$

so u_i is composed of scaled and delayed versions of the transmit signal, weighted by $\psi_i(x_j)$. Again, this necessitates u being at least N long. Also, the vectors u_i are not unit normalized. Next, the unwhitened target signal covariance is computed

$$R_{y_u y_u} = U_{y_u}\Lambda_{y_u}U_{y_u}^{-1}$$

where U_{y_u} is a matrix whose columns are the eigenvectors u_i. Because u_i are not unit normalized it is not true that $U_{y_u}^{-1} = U_{y_u}^{H}$. Also, because its condition number is infinite the inverse can not be found in the normal way (such as the Matlab inv() routine). In practice it is found that it is nearly true that $U_{y_u}U_{y_u}^{H} = cI$ where k is a positive real number (this is shown in section 3.3). In the code used for this thesis we use $U_{y_u}^{-1} = (1/c)U_{y_u}^{H}$, and similar expression for the noise covariance eigenvectors.

3.2 Input SNR

Throughout this work the input SNR will be used to quantify the received signal seen by the detector. It is not clear how to apply the traditional definition of the input SNR to a scatterer

with more than one highlight. The traditional definition of Input SNR is:

$$InputSNR = \frac{E_s}{E_n} \tag{101}$$

where E_s is the energy in the transmit signal reflected by the target, and E_n is the noise energy integrated over the duration of the received signal (this duration is called the processing window). The difficulty is that when a target is spread, the length of the received signal will be longer than if the target can accurately be modeled as a point scatterer, and will only have the same input SNR if the processing window is increased for the spread target, and not for the point target. This is not necessarily a fair comparison.

One can rewrite the energies in equation 101 as an average power times the processing window duration. The processing window duration in the numerator and denominator then cancel out, and you get a definition of the input SNR which is independent of the processing window

$$InputSNR = \frac{P_s}{P_n}$$

This is the definition preferred by Scharf [44]. This definition has the advantage that, when the energy in a target is spread among several highlights, the average power goes down while the noise variance remains the same, causing the input SNR to decrease. This reflects the fact that the matched-filter output SNR would also decrease due to the splitting loss incurred by having several highlights.

In terms of the scattering function, the signal power is equal to the magnitude of the average target scattering function highlight divided by the number of sample points in the transmit signal. This is because the magnitude of the scattering function at a point is the total energy reflected by that highlight. Because the highlight is reflecting the transmit signal, that energy is distributed across the duration of the transmit signal.

In all of the examples in this thesis, the reverberant scattering function is equal to one at each sample point. Because each reverberant highlight is reflecting the transmit signal, it is

contributing noise to all the sample points around it. For this reason the noise power is also one. Note that if the target scattering function also had a large number of highlights very close together, its signal power would have to be found in this way.

Combining these definitions, the input SNR is $InputSNR = 10\log 10[s^t_{ave} / (N_s s^n_{ave})]$ where s^t_{ave} is the magnitude of the largest target highlight, N_s is the number of sample points in the transmit signal, and s^n_{ave} is the average reverberant scattering magnitude. $10\log_{10}$ is used and not $20\log_{10}$ because the scattering function is a second order statistic. Note that if you multiply the target and reverberant scattering functions by constants the resulting input SNR is:

$$InputSNR = 10\log_{10}\left[\frac{(as^t_{ave})}{(bs^n_{ave})N_s}\right] = 10\log_{10}[s^t_{ave} / (s^n_{ave}N_s)] + 10\log_{10}[a/b]$$

The signal powers corresponding to a target and reverberant scatterer, and transmit signal with 50 sample points are shown in figure 3 (only the real part of the complex envelope is shown). A single target highlight of magnitude 50, results in a target signal of power one that is 50 sample points long. A reverberant scattering function which is one everywhere, produces a reverberant signal with power equal to one everywhere. Therefore, both have the same total energy in both the scattering functions and time series.

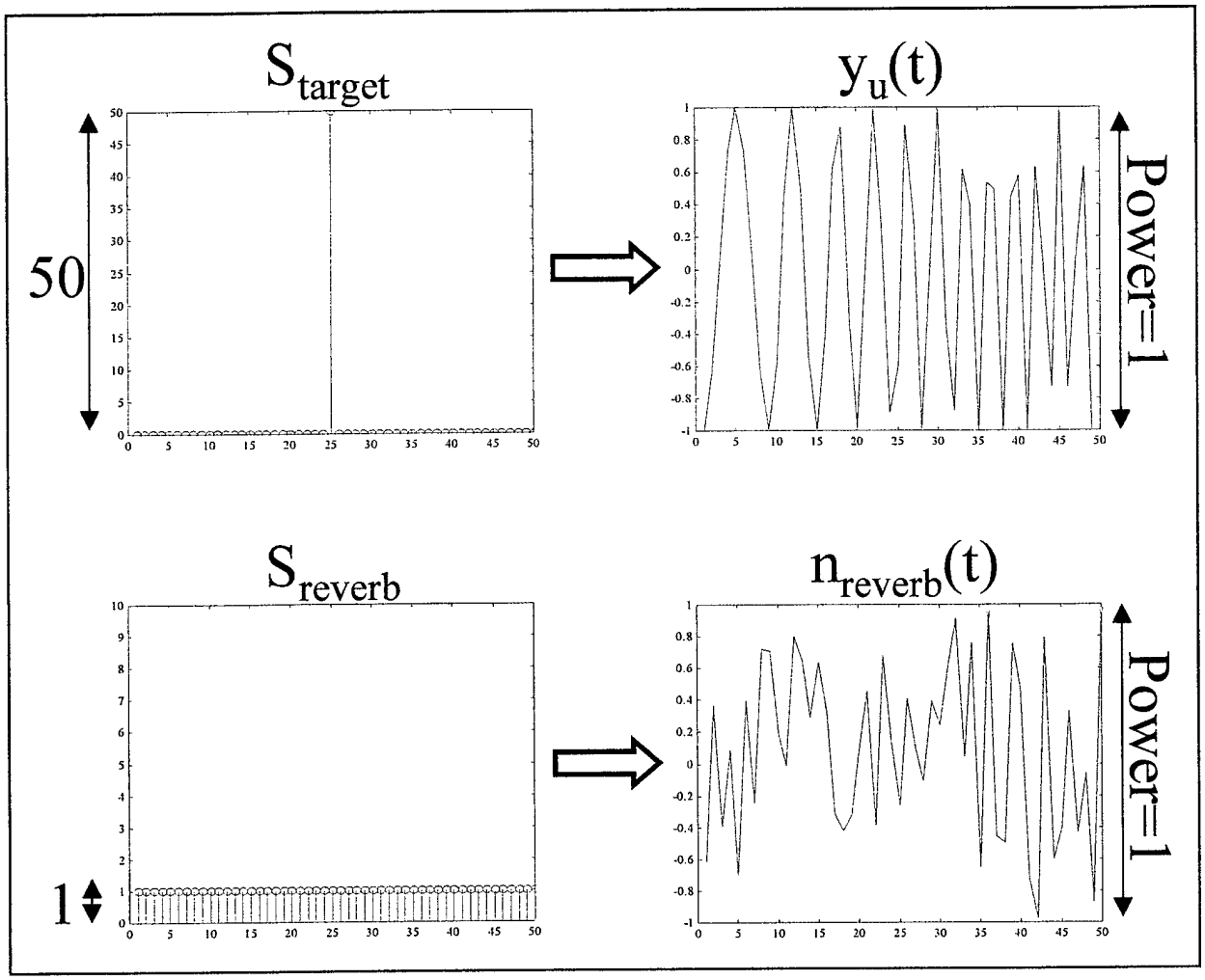

Figure 3 Explaining Input SNR

It can be shown that one need not rerun the entire calculation if the only change is the input SNR. If the scattering function in equation 97 is multiplied by a constant

$$\lambda_i^t \psi_i^t = \underline{\underline{K}}(a\underline{\underline{S}}^t)\psi_i^t \text{ and } \lambda_i^{rev}\psi_i^{rev} = K(bS^{rev})\psi_i^{rev}$$

the new eigenvalues are

$$\lambda_i^t = a\lambda_i^{to} \text{ and } \lambda_i^{rev} = b\lambda_i^{revo}$$

where λ_i^{to} and λ_i^{revo} are the old eigenvalues, that is, the eigenvalues that would result if one had not multiplied the scattering functions by a constant. The eigenvectors remain the same.

Subsequently, the whitened covariance matrix is:

$$R_{yy} = (b\Lambda_{n_i})^{-1/2} U_{n_i}^H [U_{y_i} (a\Lambda_{to}) U_{y_i}^H] U_{ni} (b\Lambda_{n_i})^{-1/2}$$

or

$$R_{yy} = (a/b) R_y^{old}$$

and therefore

$$\Lambda_y = (a/b)\Lambda_{yo}$$

Thus if you want to know the ROC for a given scattering function and transmit signal, but for a different input SNR, simply multiply the old eigenvalues by the ratio of the constants and generate a ROC curve from the resulting eigenvalues.

3.3 Numerical Problems Computing the Heaviside Expansion

The probability of detection and false alarm depend directly on computing a Heaviside expansion of the characteristic function of the probability density. While the Heaviside Expansion is an elegant mathematical procedure on paper, it can be difficult to implement in practice. It turns out that there can be numerical problems in computing the probability of false alarm. It will be shown that this only happens when the number of target highlights approaches the number of digits of precision of the computer doing the calculation. When this occurs, the probability of false alarm can be approximated with a chi squared distribution. Details are given in Appendix B. All of the examples in this thesis have a number of highlights less than this limit.

The probability of false alarm depends on K_{k_0} which in turn depends on A_{k_0}. Because $A_{k_0} = \lambda_k^y / (\lambda_k^y + 1)$, when the eigenvalues are much larger than one, all of the A_{k_0}'s are approximately equal to 1. This can lead to subtracting two numbers which are close together in a

denominator, a situation that introduces numerical noise into the calculation

$$K_{k_0} = \prod_{j \neq k} \frac{1}{1 - j2\omega A_{j_0}} \Bigg|_{\omega = 1/j2A_{k_0}}$$

or

$$K_{k_0} = \prod_{j \neq k} \frac{1}{1 - j2A_{j_0} / j2A_{k_0}}$$

For almost all A_{k_0} the term in the denominator is 1 minus a number close to 1. This can be avoided by writing A_{k_i} in terms of the eigenvalues and rearranging.

$$A_{k_0} = \frac{\lambda_k^y}{\lambda_k^y + 1}$$

$$K_{k_0} = \prod_{j \neq k}^{N} \left(1 - \frac{1 + \lambda_k^y}{j2\lambda_k^y} \frac{j2\lambda_j^y}{1 + \lambda_j^y} \right)^{-1}$$

$$K_{k_0} = (\lambda_k^y)^{N-1} \prod_{j \neq k}^{N} \left(\frac{1 + \lambda_j^y}{\lambda_k^y - \lambda_j^y} \right) \qquad \textbf{(111)}$$

This alleviates the problem of subtracting two close numbers in the denominator, and this is how the Heaviside coefficients are computed for the examples in this thesis. However, equation 111 reveals a deeper problem. If λ_k^y is of order one (of which many are) then K_{k_0} will be of order 10^N, where N is the number of eigenvalues. This is a problem because the K_{k_0} 's must sum to 1. Because $\phi_{l_i}(\omega)$ is a characteristic function, it must be true that $\phi_{l_i}(\omega = 0) = 1$.

Substituting this into equation 82 yields:

$$\phi_{l_i}(0) = \sum_{k}^{N} \frac{K_{k_i}}{1 - j2(0)A_{k_i}} = 1$$

$$\sum_{k}^{N} K_{k_i} = 1$$

Since the K_{k_0} s must sum to one, the computer must be able to represent a difference of 1 between two numbers of order 10^N . Therefore N must be less than the number of digits of precision of the computation. This limits the number of eigenvalues to the number of digits of precision of the calculation. As will be shown in section 3.3 the number of significant eigenvalues is approximately equal to the number of target highlights. Therefore, in order to compute ROC curves for a target with more than N highlights an approximation to the Heaviside function must be used.

This problem persists in other ways of writing the Heaviside expansion, such as:

$$\phi_{l_i} = \prod_{k=1}^{N} \frac{-(j2A_{k_i})^{-1}}{(\omega - (j2A_{k_i})^{-1})}$$

The Heaviside Expansion would then be

$$\phi_{l_i} = \sum_{k=1}^{N} \frac{C_k}{(\omega - (j2A_{k_i})^{-1})}$$

where

$$C_k = (\omega - (j2A_{k_i})^{-1}) \prod_{j}^{N} \frac{-(j2A_{j_i})^{-1}}{(\omega - (j2A_{j_i})^{-1})} \Big|_{\omega=(j2A_{k_i})^{-1}} \quad \textbf{(116)}$$

and

$$\phi_{l_i}(0) = \sum_{k=1}^{N} \frac{C_k}{(0) - (j2A_{k_i})^{-1}} = \sum_{k=1}^{N} -j2A_{k_i}C_{k_i} = 1$$

where

$$C_{k_0} = (-\lambda_k^y)^{N-1} \prod_{j \neq k}^{N} \frac{(\lambda_j^y + 1)}{\lambda_j^y - \lambda_k^y} \tag{118}$$

Again the coefficients are of the order 10^{N-1}.

It is important to note that computing the probability of detection does not have this problem and can be computed exactly. This is because $A_{k_1} = \lambda_k^y$ and thus they are not necessarily all nearly equal. This allows us to find an approximation to the false alarm that does not necessarily have any information about the eigenvalues in it. The ROC will still contain information about the eigenvalues because they are contained in the probability of detection.

If all of the A_{k_0}'s were precisely equal, the corresponding probability function would be a Chi Squared distribution. This method is not used in this thesis, but may be useful in the future, and so details are given in Appendix B.

3.4 Validating the numerical calculation

One of the contributions of this thesis is the numerical computation of the Wavelet Transform Domain Estimator-Correlator from the transmit signal and scattering functions when the covariance eigenvalues are not all equal. In this section an analytic special case is derived to validate the numerical calculation. Consider the case where the autoambiguity matrix $\mathbf{K}$ is the identity matrix $\mathbf{I}$. Substituting into equation 51 yields:

$$\lambda^t \psi^t = \mathbf{S}^t \psi^t \text{ and } \lambda^n \psi^n = \mathbf{S}^n \psi^n$$

because the WSSUS assumption means that $\mathbf{S}$ is diagonal (i.e. $S = diag(s_k)$), the eigenvalues become the scattering strengths, and the eigenvectors become the usual basis functions

$$\lambda_k^t = s_k^t \text{ and } \lambda_k^n = s_k^n$$

where

$$\Psi^t = \Psi^n = \mathbf{I}$$

where the Ψ are the matrices formed from the corresponding eigenvectors ψ. Recall that, in order to find the eigenvalues from the scattering function, the wavelet transform of the covariance eigenvalues was taken. Thus the vectors ψ_k are really the wavelet transform of the eigenvectors of the covariance matrices. The matrix of inverse wavelet transformed vectors will be called $\mathbf{U}$. Note that $\mathbf{U}$ does not equal $\mathbf{I}$, but that $\mathbf{U}_t = \mathbf{U}_n$. Thus this is not an entirely unrealistic case. It is not required that the autoambiguity function of the transmit signal be a delta function, just that its autoambiguity function has insignificant sidelobes at delays and scales corresponding to the distance between highlights (the x_j from equation 50). The unwhitened target signal covariance is:

$$\mathbf{R}_{yiyi} = \mathbf{U}_u \Lambda_u \mathbf{U}_u^H \tag{119}$$

The whitened signal covariance is:

$$\mathbf{R}_{yy} = \Lambda_n^{-1/2} \mathbf{U}_n^H \mathbf{U}_t \Lambda_t \mathbf{U}_t^H \mathbf{U}_n \Lambda_n^{-1/2} \tag{120}$$

But since $\mathbf{U}_n$ and $\mathbf{U}_t$ are equal, all of the $\mathbf{U}$ terms cancel and

$$\mathbf{R}_{yy} = diag(\lambda^t / \lambda^n) \tag{121}$$

Since $\mathbf{R}_{yy}$ is diagonal its eigenvalues are just the diagonal elements

$$\lambda_k^y = \frac{\lambda_k^t}{\lambda_k^n} = \frac{s_k^t}{s_k^n} \tag{122}$$

The eigenvalues generated by the numerical code used in this paper have been compared to the above analytical method for many different scattering functions and they agree to within machine numerical precision.

For the case where K is not the identity matrix, one can check to make sure that the matrices involved conform to constraints on eigenvectors and covariance matrices. To check that the inverse wavelet transform of $\vec{u}$ is done correctly, one can use the property that a matrix of eigenvectors is Hermitian. As shown before, one starts with the autoambiguity matrix K and the scattering function S, and finds:

$$\lambda\psi = KS\psi$$

where the λ 's are the eigenvectors of the covariance matrix and the ψ 's are the wavelet transformed eigenvectors of the covariance matrix (each of which has either the subscript t or n to indicate the target signal covariance or noise covariance). The actual covariance eigenvectors are:

$$\vec{u} = W_f^{-1}\psi(x)$$

Because it is the result of this inverse wavelet transform, the vectors $\vec{u}$ are not unit normalized. U is defined to be the matrix of eigenvectors $\vec{u}$, and should be Hermitian. That is

$$U^H = U^{-1} \text{ or } UU^H = I$$

But because the eigenvectors are not normalized it is actually the case that $UU^H = cI$. The product $O_{ij} = UU^H$ for a typical set of eigenvectors is shown in figure 4. All of the information about the magnitude of the received signal is in the scattering function. The normalization of the transmit signal doesn't matter. Therefore, it may be possible to normalize the transmit signal such that c = 1. This would save computation time by not having to compute the product UU^H in order to find c.

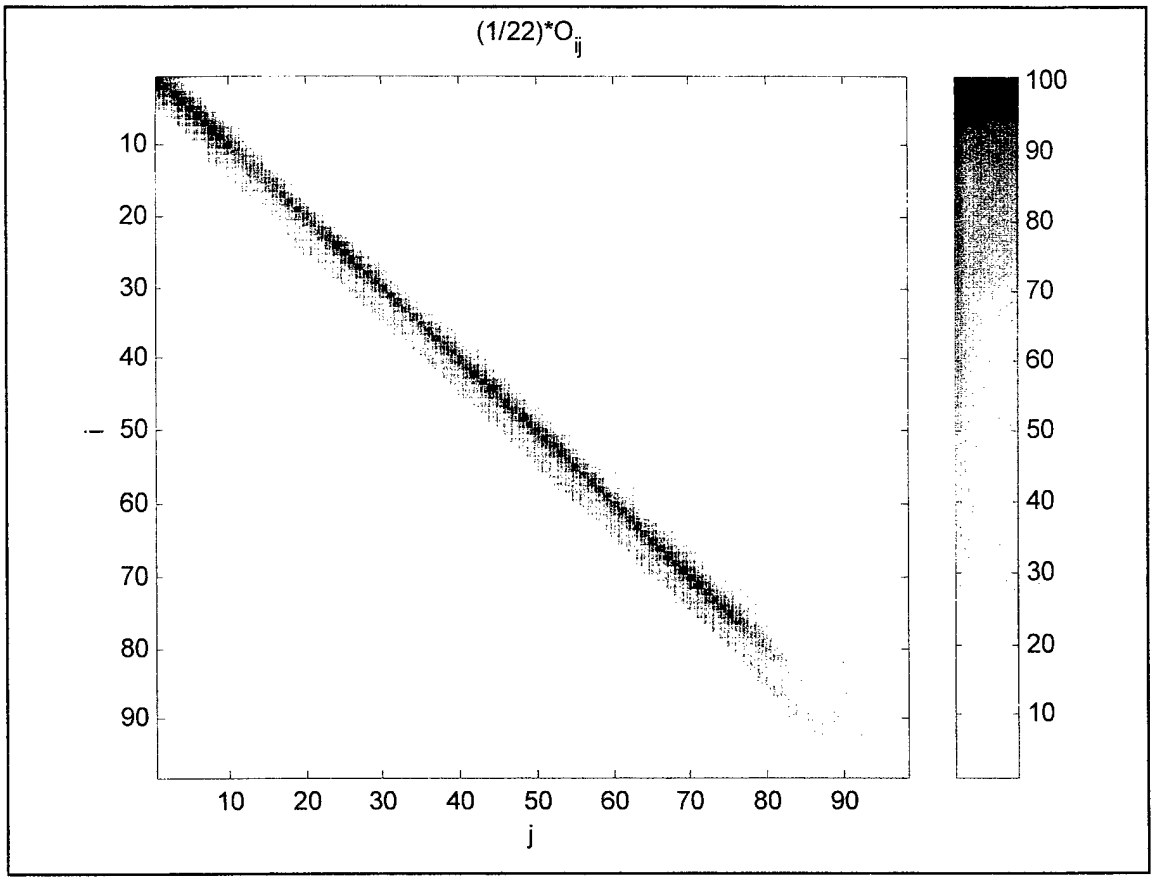

Figure 4 The product UU^H for a typical set of eigenvectors

The covariance matrices $R_{y_u y_u}$, $R_{n_u n_u}$ and R_{yy} can also be checked. Covariance matrices must be positive definite, which in turn means that their eigenvalues must be positive and real [45]. The computation can be checked by seeing how close the eigenvalues come to being positive and real.

Table 1 Closeness of eigenvalues to being real and positive

	Negative	Imaginary
λ^{rev}	6.62E-02	0.00E+00
λ^{t}	3.26E-06	0.00E+00
λ^{y}	1.19E-17	3.18E-16

Table 1 shows how close the various eigenvalues come to being purely positive and real. The "Negative" column shows the ratio of the largest negative eigenvalue to the largest eigenvalue. The "Imaginary" column shows the ratio of the largest imaginary component of an eigenvalue to the largest eigenvalue. The fact that λ^{y} has such small negative eigenvalues is at least in part due to the fact that all of the negative eigenvalues were removed from λ^{t} and λ^{rev} before λ^{y} was computed. The largest negative reverberant eigenvalue may not seem clearly negligible in and of itself, however the sum of the negative eigenvalues only constitutes 5% of the reverberant eigenvalue energy. Negative eigenvalues only constitute 0.01% of the target eigenvalue energy. Negative eigenvalues are the result of numerical noise in the eigenvalue decomposition process. They must be thrown out because they make the probability of detection and false alarm diverge.

The code to calculate the WTD-EC is broken roughly into two parts, the first to generate the whitened target covariance eigenvalues, and the second to generate the Heaviside expansion and ROC curve from those eigenvalues. This section can also be validated. When there is only one significant eigenvalue, there is only one term in the characteristic function, so the Heaviside coefficient must equal 1

$$\phi_{l_i} = \prod_{k=1}^{1} \frac{1}{1 - j2\omega \mathrm{A}_{k_i}} = \frac{1}{1 - j2\omega \mathrm{A}_{1_i}}$$

The Heaviside expansion of this is:

$$\phi_{l_i} = \frac{1}{1 - j2\omega A_{1_i}} = \sum_{k=1}^{1} \frac{K_{k_i}}{1 - j2\omega A_{k_i}} = \frac{K_{1_i}}{1 - j2\omega A_{1_i}}$$

meaning $K_{1_i} = 1$. The code used to generate the examples in this thesis complies with this constraint.

In [30] pg 108, Van Trees shows that the probability distribution of the likelihood function reduces to a Chi Square distribution for the case where all the eigenvalues are the same (equal

covariances). His expression for the probability of false alarm is:

$$P_f = 1 - I_r\left(\frac{\gamma'''}{\sqrt{M+1}}, M\right)$$

where I_r is the incomplete gamma function, γ''' is the threshold, and M=N/2 -1 where N is the number of eigenvalues. A similar expression is used for P_d with a slightly different γ'''. The code used in this thesis can obviously not compute a ROC curve for eigenvalues that are exactly equal, but for a small number of eigenvalues that are close together (in this case within 5%) it should yield similar results. A comparison is shown in figure 5. Because only the subroutine that takes the eigenvalues as inputs and generates the ROC curves is being validated, the eigenvalues used are made up, and do not correspond to any particular transmit signal or scattering functions. Note that these curves are not meant to be exactly the same, just to show that no gross coding errors were made that might cause the computation to be orders of magnitude wrong.

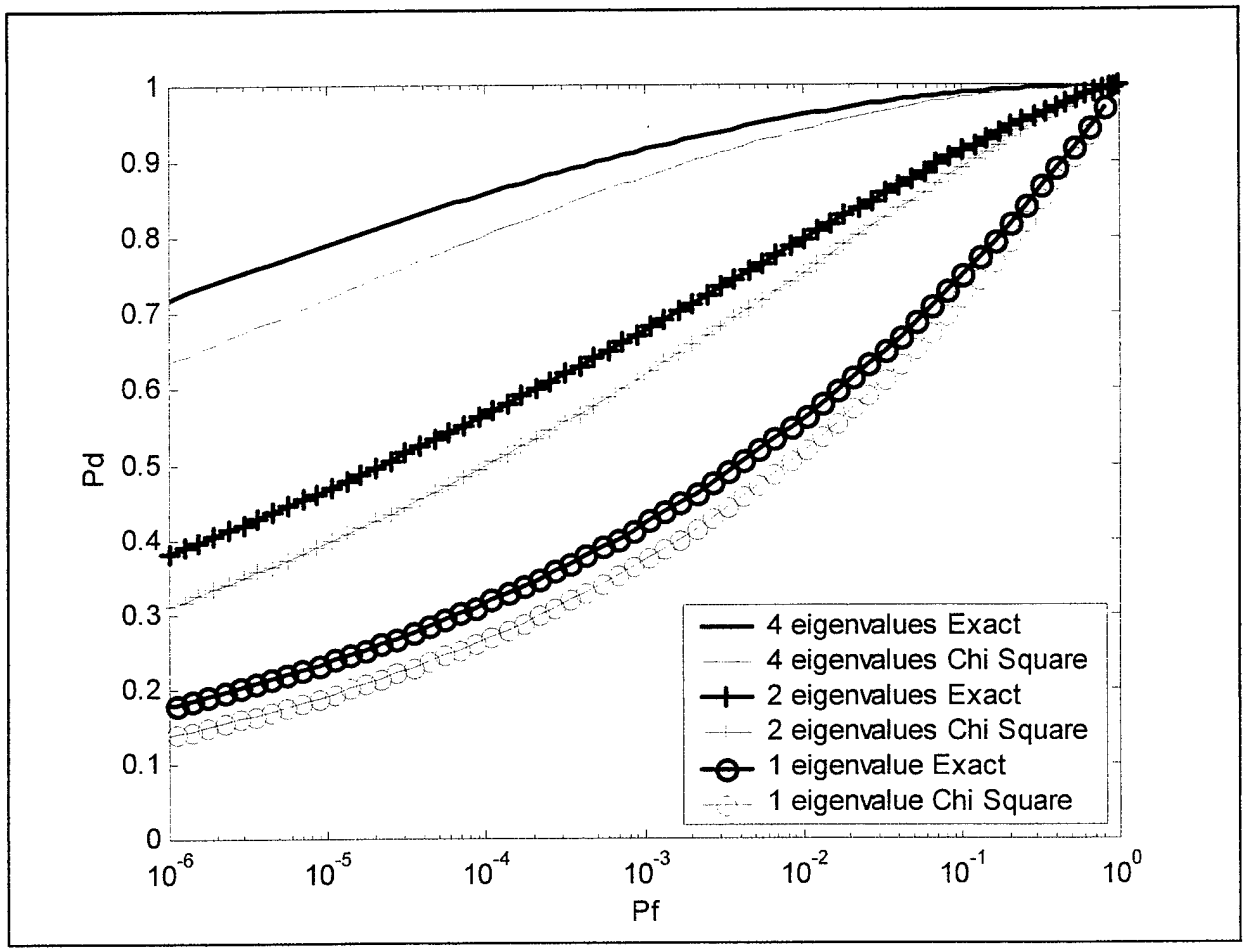

Figure 5 Comparison of ROC computation used in this thesis (exact) and the Chi Square approximation

3.5 The meaning of the whitened target covariance eigenvalues

As seen in equation 122 the eigenvalues of $\mathbf{R}_{yy}$ in the analytic case are just the ratio of target and reverberant scattering functions at each highlight location. The ROC curve depends only on these eigenvalues. Because the ROC is the most valid performance characterization for detectors, and the ROC depends only on the eigenvalues, these eigenvalues can be thought of as generalized, local, signal to noise ratios. Also, it is easy to see that the number of significant eigenvalues is closely related to the number of target highlights. For all the examples given in this thesis, the number of significant eigenvalues is equal to the number of significant highlights, regardless of the signal or its autoambiguity function shape. It was shown in section 3.2 that if the number of significant eigenvalues (and therefore the number of significant target highlights)

exceeds the number of digits of precision of the computer, there will be numerical problems computing the Heaviside coefficients necessary to compute the ROC curves.

As we saw in the previous section, when $K = I$, $\lambda_k^y = s_k^t / s_k^n$. Recall that

$$l|H_1 = \sum_N |v_{k_1}|^2 \lambda_k^y$$

Therefore, in this case, the likelihood is directly proportional to the sum of the energy in the scattering function, regardless of how that energy is distributed. A scatterer with one highlight of unit energy should be detected just as well as a scatterer with N_h highlights with $1/N_h$ unit energy each. Or, a scatterer with N_h highlights each of one unit energy should be much easier to detect than a scatterer with one highlight of one unit energy. In section 3.6 it is demonstrated that this is approximately true even when $K \neq I$.

3.6 An observation about the calculation of the covariance eigenvalues

Earlier, the reverberation covariance eigenvalues were found to be

$$\lambda_k^{rev} W_f u_k(x_i) = \sum_j K(x_i, x_j) S_{rev}(x_j, x_j) W_f u(x_j) \qquad \textbf{(129)}$$

where x_j represents the scale and delay of each highlight and $S(x_j, x_j)$ represents the strength of each highlight. $K(x_i, x_j)$ represents the autoambiguity function at the scale and delay corresponding to the distance between scales and delays x_i and x_j. Mathematically speaking

$$K(x, x') = \langle U(x) f, U(x') f \rangle_H$$

$$K(x, x') = \langle U(x * x') f, f \rangle_H$$

where $x * x'$ represents the difference in scale and delay between each highlight. This is the only place that the autoambiguity function is used in the calculation of the likelihood ratio. Thus one does not need to compute the entire autoambiguity function over the range of interest, but rather

one need only compute the points that correspond to the difference in scale and delay between each highlight.

3.7 Properties of the WTD-EC

The WTD-EC displays many of the advantages that one would expect. For all of the examples in this and the next chapter, signals will be referred to by their time-bandwidth product. Table 2 shows number of sample points in the transmit signal (N_s), time duration (T), bandwidth (B), and time-bandwidth product (TB) of the signals used in this work (for a sampling frequency of 4000Hz).

Table 2 Properties of transmit signals

N_s	T (ms)	B (Hz)	TB
201	50.25	1250	63
201	50.25	1093	55
201	50.25	937	47
201	50.25	625	31
49	12.25	1250	15
49	12.25	1093	13
49	12.25	937	11.5
49	12.25	625	7.5

Though the WTD-EC and sensitivity analysis developed in this thesis are valid for scatterers spread in scale, the computations are only implemented for scatterers spread in delay. Scattering functions are sampled in delay with the same sampling period as the signal. Thus the scattering function sampling period in distance D_s is $D_s = cT_s$ where c is the speed of sound in the medium and T_s is the sampling period. For a sampling frequency of 4000Hz the sampling period in time $T_s = 0.25\ (ms)$. For a speed of sound of c=1500m/s the sampling period in distance would be $D_s = 0.375m$.

Figure 6 compares the ROC of one-highlight EC to the WTD-EC for scatterers with N_h highlights and an SNR of $1/N_h$ compared to the one highlight case. Another way of saying this is that the ROC for the one highlight EC for one highlight of unit energy is being compared to the WTD-EC for a scatterer with one unit of total scattering strength distributed between N_h highlights.

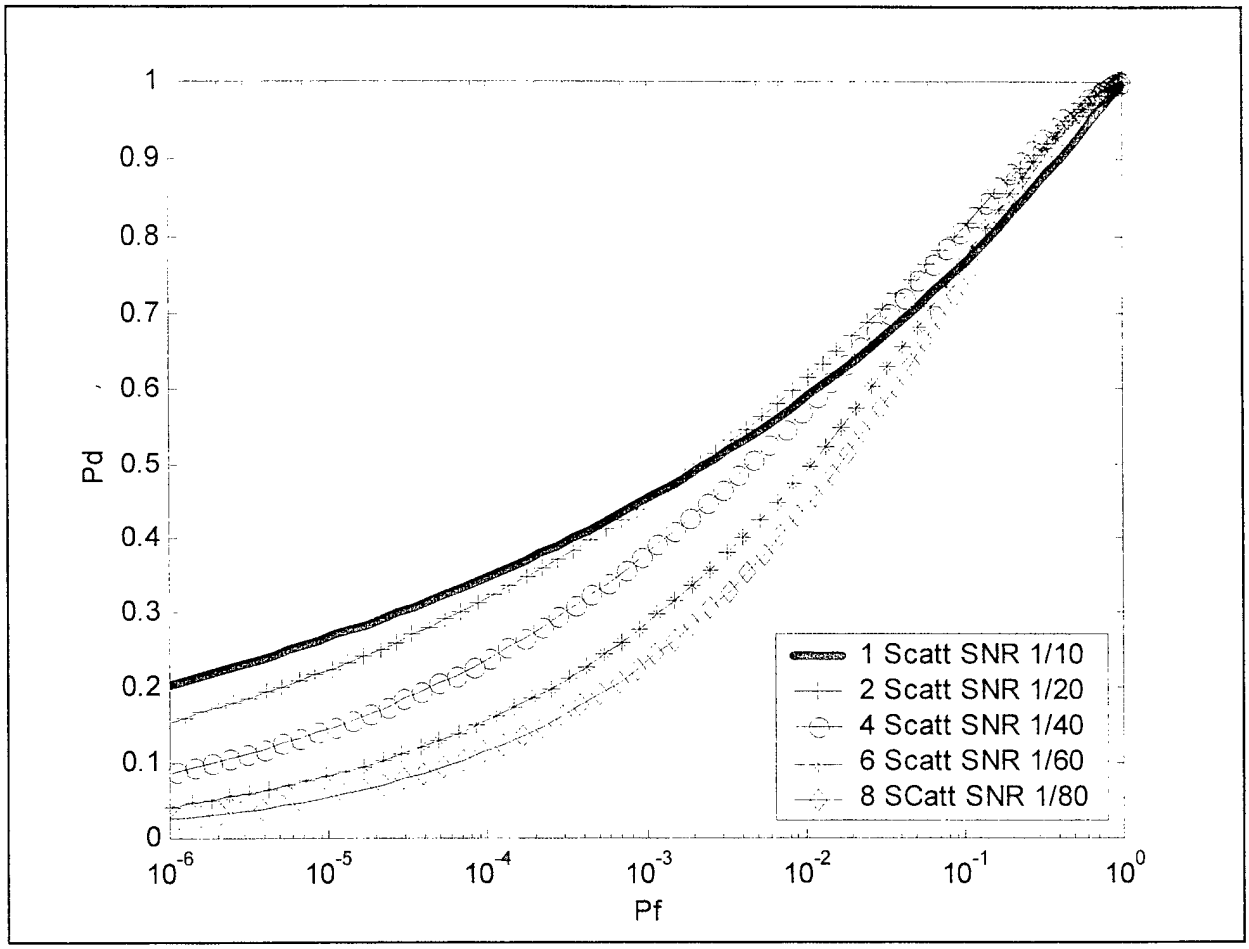

Figure 6 Performance for N_h highlights with SNR = $1/N_h$. Signal has TB = 15, highlights are 11 sample points apart.

As one might expect, for N_h highlights the WTD-EC has very similar performance as the one-highlight EC when the highlights have a scattering strength $1/N_h$ that of the one highlight case. In a way, it really can be said that it is N_h times better for N_h highlights. To put this in terms of processing gain, one can say that there is a $10\text{Log}_{10}(N_h)$ gain in output SNR. Additionally, one does not usually consider probabilities of detection smaller than 0.5 useful, and

thus the WTD-EC does slightly better in the useful detection range.

Framing the benefit of the WTD-EC in terms of processing gain leaves out much of the picture. Figure 7 compares the ROC for a normal (one highlight) EC with the WTD-EC for four highlights. If you consider the one scatterer for the one highlight EC to have a scattering strength of 1, the highest curve represents the ROC curve for a scatterer with 4 highlights each with a scattering strength of 1, the next curve would be for 4 highlights each with a scattering strength of ½, and so on.

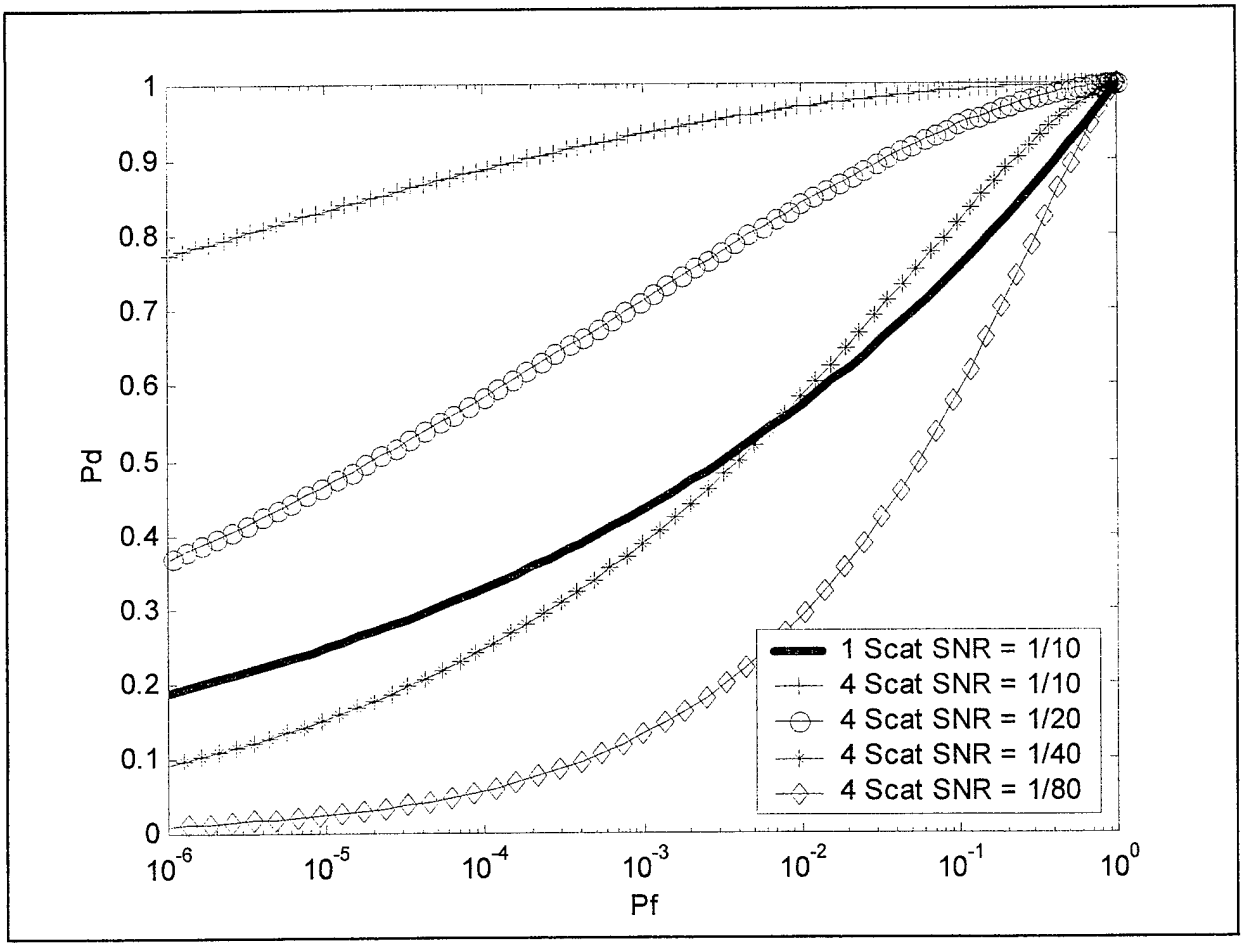

Figure 7 Comparing WTD-EC to the one highlight EC. Signal has TB = 15, highlights are 11 sample points apart, SNRs are Input SNRs.

In terms of processing gain, for four highlights, the WTD-EC yields a gain of 6 dB. For comparison, let's say that you chose to operate a single highlight detector with a probability of false alarm of 10^{-3}. This yields a probability of detection of 0.5. Using the WTD-EC would yield

a $P_d = 0.9$, which is an 80% improvement in P_d. Now let's say that you chose to operate the single highlight detector with a $P_f = 10^{-1}$, yielding a $P_d = 0.8$. To achieve a $P_d = 0.8$ the WTD-EC could operate at a P_f of 10^{-6}, a six order of magnitude improvement in P_f! This serves to show that there are important insights to be found in the ROC curve that are lost in scalar measure such as dB processing gain.

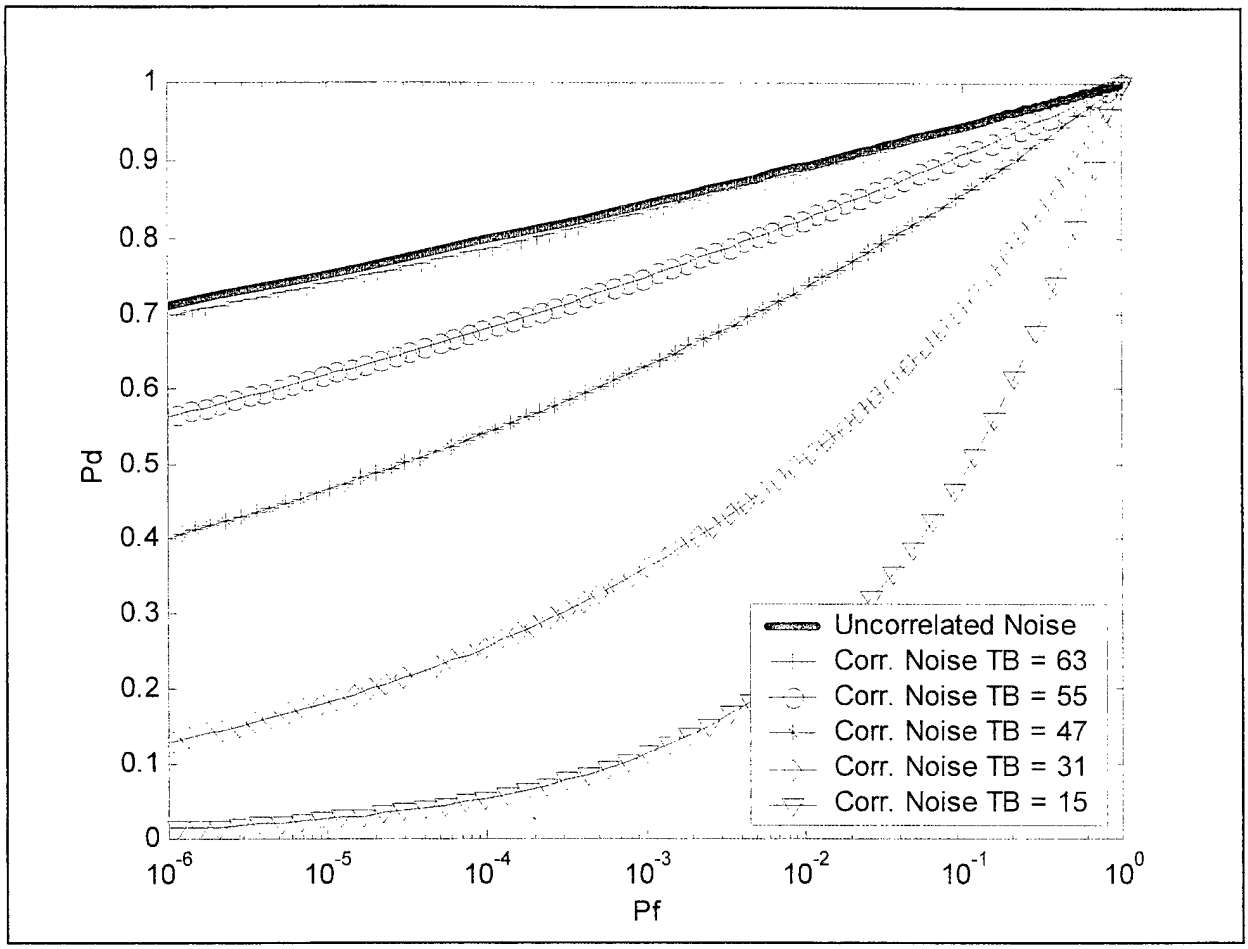

Figure 8 Dependence of ROC on Time-Bandwidth product. There is one highlight, and input SNR = -10dB.

Figure 8 shows the difference in ROC of the EC between when the noise is correlated, and when it is uncorrelated. When the transmit signal is perfectly resolvent (i.e. $K = I$) the reverberation is uncorrelated. In the section 2.3 it was shown that under these conditions it is true that: $\lambda_k^y = s_k^t / s_k^n$. If there is only one highlight, there will be only one non-zero whitened eigenvalue, and no need to do a Heaviside expansion. Under these conditions, the probability of

detection and false alarm are:

$$P_d = e^{\frac{-\gamma}{2\lambda^y}} \text{ and } P_f = e^{\frac{-\gamma}{2\lambda^y}(1+\lambda^y)}$$

which can be further simplified to $P_f = P_d^{1+D}$, where D is the ratio of the total signal energy to the noise covariance. This is the traditional result for the one highlight EC and the matched filter, and does not depend on any qualities of the transmit signal except its total energy. When the noise is correlated, this level of performance can no longer be attained, and serves as an upper bound on the EC performance under correlated noise. As shown, the performance of the EC under correlated noise increases with the TB of the signal.

For every example in this thesis, the reverberant scattering function has a magnitude of one (plus a small random number to avoid numerical problems) at each sample point. This is quite different than uncorrelated white noise. Having one reverberant highlight at each sample point does not lead to having the noise energy evenly distributed between the noise eigenvalues the way it would be for white noise. For low TB signals the noise energy is concentrated in a few eigenvalues - the energy becomes more and more evenly distributed as the TB increases, until the signal is perfectly resolvent, the energy is completely evenly distributed, and only then is it really uncorrelated white noise. Thus, all of the examples in this thesis are reverberation limited, not noise limited.

The point of the WTD-EC is to combine the energy from multiple highlights. Figure 9 shows that indeed the ROC improves with the number of highlights.

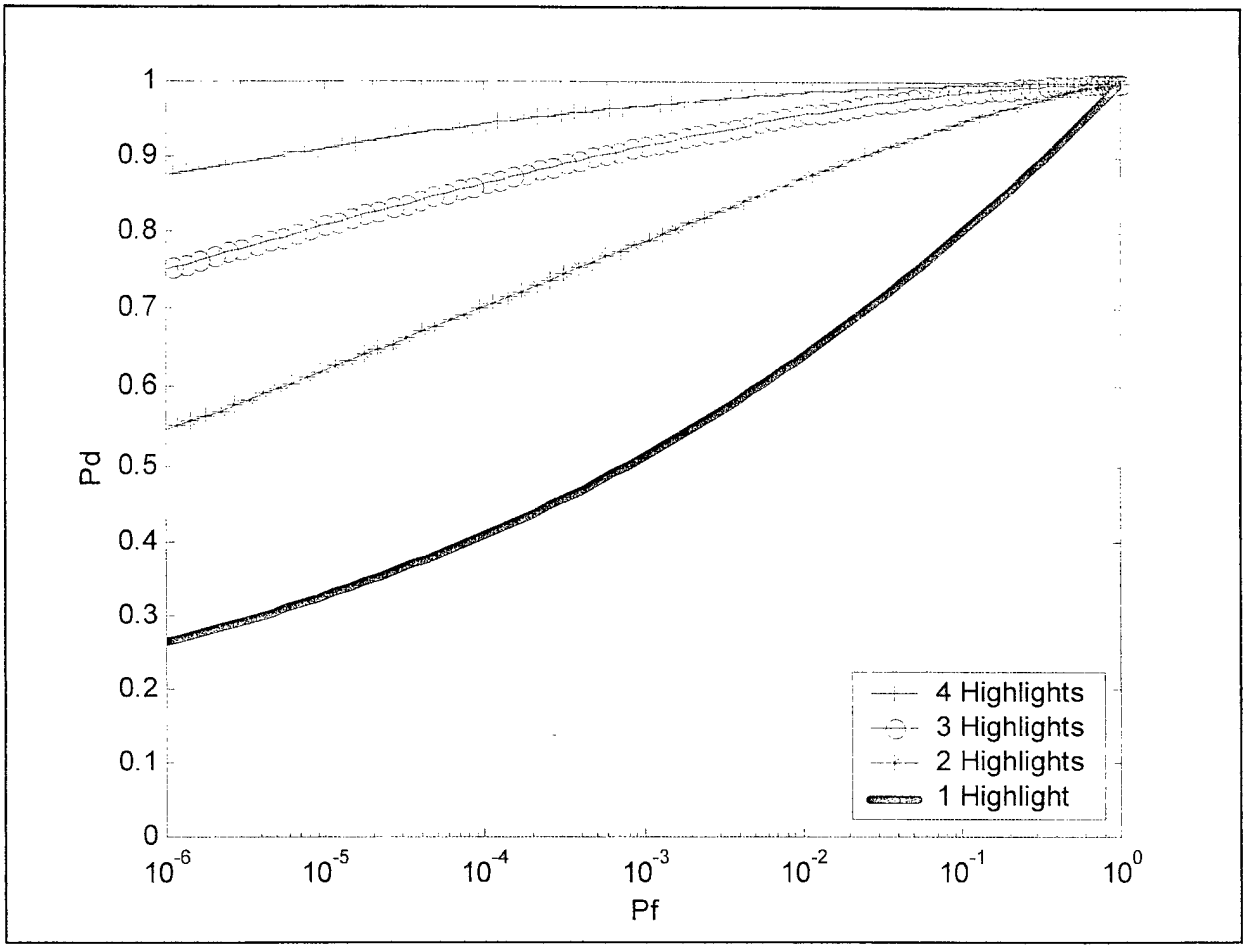

Figure 9 Dependence of ROC on number of highlights. Signal TB = 15, Input SNR = -10dB, Highlights separated by 10 sample points, and have equal strength.

When highlights are far apart compared to the width of the mainlobe of the transmit signal, the eigenvalues and eigenvectors behave much as if the autoambiguity function was a delta function. It would be difficult to predict analytically how the probability of detection changes when the highlights are closer than the width of the mainlobe.

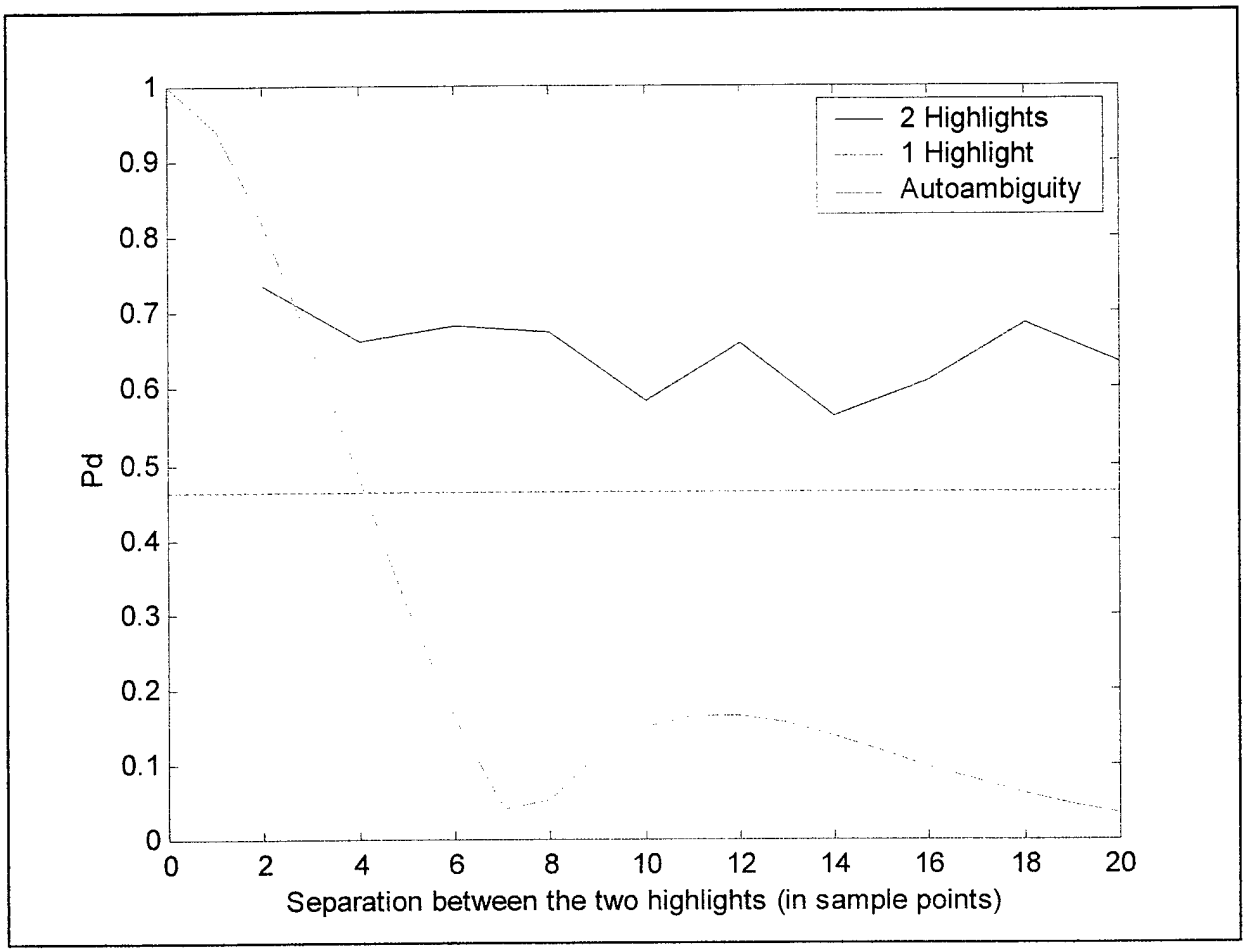

Figure 10 Dependence of Pd on Separation of Highlights for a transmit signal with TB = 7.5. SNR = -3dB.

Figure 10 shows the probability of detection for a probability of false alarm of 10^{-3} for a signal with TB = 7.5 and a scatterer with two highlights, and shows how the P_d depends on the separation between the two highlights.

Figure 11 shows the same graph for a signal with a TB = 15.

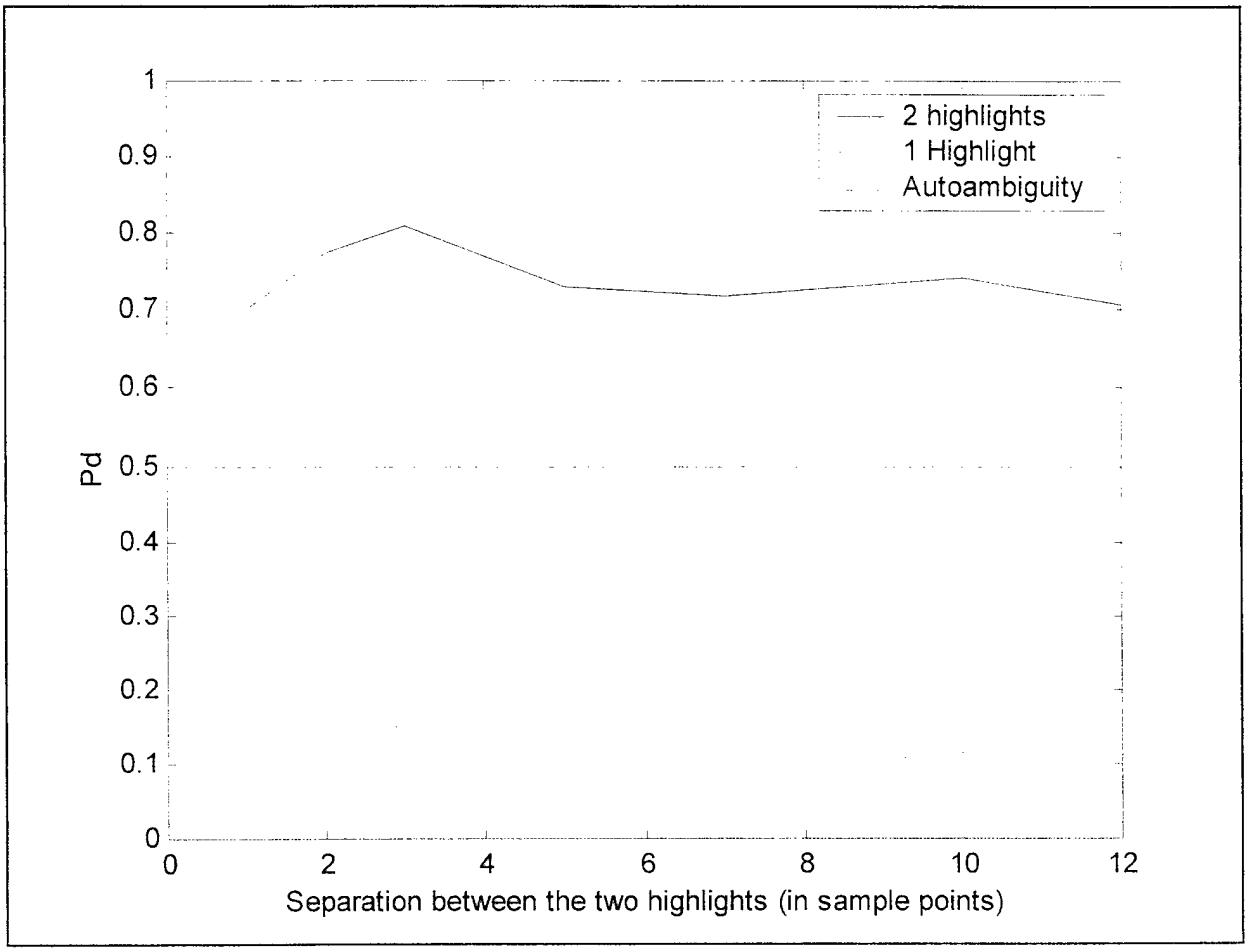

Figure 11 Dependence of Pd on Separation of Highlights for a transmit signal with TB = 7.5. SNR = -3dB.

Neither is the a large dependence on the separation, or an obvious correlation with the autoambiguity function.

Chapter 4

SENSITIVITY OF THE WAVELET TRANSFORM DOMAIN ESTIMATOR-CORRELATOR

4.1 Deriving the Sensitivity of the Wavelet Transform Domain EC

Incorporating the estimate of the scattering function into the EC can lead to dramatic detector gain. However, if that estimation contains errors, it will not reap the full benefits of making the a priori estimate. The critical question is: does the advantage of higher time-bandwidth product signals and recombining highlights outweigh the detriments caused by errors in the a priori estimate? For this reason, the sensitivity of the EC to errors in the a priori estimate is derived. Compelling evidence is given that the WTD-EC does in fact retain it's advantages even when the a priori estimate contains large errors. Preliminary results on this topic have been previously published by the author of this thesis [46], [47].

An expression for the ROC is now derived that takes into account errors in the assumed scattering function. The likelihood function derived before is:

$$l = \vec{r}^{\,H}\mathbf{U}_y\left(diag\left[\frac{\lambda_i^y}{1+\lambda_i^y}\right]\right)\mathbf{U}_y^H\vec{r} \tag{132}$$

For the case where the assumed scattering functions are incorrect, the affected variables are designated with the sub/superscript a. The assumed likelihood function is:

$$l^a = \vec{r}^{\,H}\mathbf{U}_{ya}\left(diag\left[\frac{\lambda_i^{ya}}{1+\lambda_i^{ya}}\right]\right)\mathbf{U}_{ya}^H\vec{r} \tag{133}$$

Note that we have not made any assumption about how the eigenvalues and eigenvectors are found. Thus, the sensitivity analysis derived here is true for any Estimator-Correlator, and not just the Wavelet Transform Domain Estimator-Correlator. U_{ya} in equation 133 does not whiten $\vec{r}$ because it is not based on the correct scattering function. $\vec{r}$ is now re-expressed in terms of a

whitened vector $\vec{z}^{\,a}$.

$$\vec{z}^{\,a} = \Lambda_r^{-1/2}\mathbf{U}_r^H\vec{r} \tag{134}$$

It is now shown that $\vec{z}^{\,a}$ is white

$$R_{zz} = E\{\vec{z}^{\,a}\vec{z}^{\,aH}\}$$

$$R_{zz} = E\{\Lambda_r^{-1/2}U_r^H\vec{r}\vec{r}^{\,H}U_r\Lambda_r^{-1/2}\}$$

$$R_{zz} = E\{\Lambda_r^{-1/2}U_r^H R_{rr}U_r\Lambda_r^{-1/2}\}$$

$$R_{zz} = \{\Lambda_r^{-1/2}U_r^H U_r\Lambda_r U_r^H U_r\Lambda_r^{-1/2}\}$$

$$R_{zz} = E\{\Lambda_r^{-1/2}\Lambda_r\Lambda_r^{-1/2}\} = \mathbf{I}$$

Rewriting r in terms of z and defining

$$\mathbf{D}_a = diag\left[\frac{\lambda_i^{ya}}{1+\lambda_i^{ya}}\right] \tag{140}$$

the likelihood ratio can be found in terms of z^a

$$l^a = (\vec{z}^{\,a}\Lambda_r^{1/2}\mathbf{U}_r^H)\mathbf{U}_{ya}\mathbf{D}_a\mathbf{U}_{ya}^H(\mathbf{U}_r\Lambda_r^{1/2}\vec{z}^{\,a}) \tag{141}$$

The terms in the middle can be collected and diagonalized. Defining new variables Λ_{ax}, and $\mathbf{U}_{ax}$:

$$\mathbf{U}_{ax}\Lambda_{ax}\mathbf{U}_{ax}^H = \Lambda_r^{1/2}\mathbf{U}_r^H\mathbf{U}_{ya}\mathbf{D}_a\mathbf{U}_{ya}^H\mathbf{U}_r\Lambda_r^{1/2} \tag{142}$$

$$l^a = \vec{z}^{\,a}\mathbf{U}_{ax}^H\Lambda_{ax}\mathbf{U}_{ax}\vec{z}^{\,a} \tag{143}$$

This can now be rewritten in terms of a new, unit variance, jointly Gaussian vector $\vec{x}^a = \vec{z}^a \mathbf{U}_{az}^H$

$$l^a = \sum_k \lambda_k^{ax} \left| x_k^a \right|^2 \tag{144}$$

Since x^a is jointly Gaussian one can derive a ROC curve for this likelihood ratio. But first x^a must be normalized. The expected value of x^a is:

$$\vec{x}^a = U_{ax}^H \vec{z}^a = U_{ax}^H \Lambda_r^{-1/2} U_r^H \vec{r}$$

$$E\{|x_i^a|^2\} = E\{\vec{x}^{aH} \vec{x}^a\}$$

$$E\{|\vec{x}^a|^2\} = E\{\vec{r}^H U_r \Lambda_r^{-1/2} U_{ax} U_{ax}^H \Lambda_r^{-1/2} U_r^H \vec{r}\}$$

$$E\{|\vec{x}^a|^2\} = E\{\vec{r}^H U_r \Lambda_r^{-1} U_r^H \vec{r}\}$$

Using the definition from section 2.8

$$\vec{z} = U_y^H \vec{r}$$

and the fact that

$$E\{|z_k|^2 | H_0\} = 1 \text{ and } E\{|z_k|^2 | H_1\} = 1 + \lambda_k$$

yields

$$E\{|x_k^a|^2 | H_0\} = \frac{1}{\lambda_k^r} \text{ and } E\{|x_k^a|^2 | H_1\} = 1$$

Rewriting x_k^a in terms of unit normalized values yields:

$$w_{k_0}^a = x_k^a \lambda_k^r \text{ and } w_{k_1}^a = x_k^a$$

$$l^a|H_0 = \sum_k |w_{k_0}^a|^2 \frac{\lambda_k^{ax}}{\lambda_k^r} \text{ and } l^a|H_1 = \sum_k |w_{k_1}^a|^2 \lambda_k^{ax}$$

The $w_{k_i}^a$ terms are unit variance, jointly Gaussian random variables (not to be confused with the spreading function $w(x)$). Thus the likelihood depends only on the assumed eigenvalues λ_i^{ax} and the actual eigenvalues λ_i^r. This expression includes information about both the correct scattering function and the assumed scattering function. Thus one can compare ROC curves for correct scattering functions and scattering functions with errors.

4.2 Estimating the Input SNR

The scattering function estimate is not just an estimate of where the highlights are, it also implies an estimate of what the overall input SNR is. The effect of guessing the wrong input SNR can be derived analytically. In section 3.3 it was derived that if $S^{ta} = aS^t$ then $\lambda_k^{ya} = a\lambda_k^y$, and that the eigenvectors will be the same for both the correct and assumed covariance matrices. Therefore equation 141 becomes

$$l^a = z^{aH} \Lambda_r^{1/2} D_a \Lambda_r^{1/2} z^a$$

and

$$\lambda_k^{ax} = \lambda_k^{ya} \frac{1+\lambda_k^y}{1+\lambda_k^{ya}}$$

Making the substitution $\lambda_k^{ya} = a\lambda_k^y$ yields:

$$\lambda_k^{ax} = a\lambda_k^y \frac{1+\lambda_k^y}{1+a\lambda_k^y}$$

or

$$\lambda_k^{ax} = \lambda_k^y \frac{\lambda_k^y + 1}{\lambda_k^y + 1/a}$$

If a=1 we get the sensible result that $\lambda_k^{ax} = \lambda_k^y$ and the performance is exactly the same as if the sensitivity analysis had not been done. If a<1 the denominator is greater than the numerator and $\lambda_k^{ax} < \lambda_k^y$. If a>1 then the denominator is smaller than the numerator and λ_k^{ax} is slightly larger than λ_k^y. As a approaches infinity the assumed eigenvalues converge to

$$\lim_{a \to \infty} \lambda_k^{ax} = \lambda_k^y + 1$$

One should not jump to the conclusion that performance must therefore be better. The λ_k^{ax} in the above expressions is really $\lambda_k^{ax} | H_1$. $\lambda_k^{ax} | H_0$ would be:

$$\lambda_k^{ax} | H_0 = \frac{\lambda_k^{ya}}{1 + \lambda_k^{ya}} = \frac{k\lambda_k^y}{1 + a\lambda_k^y} = \frac{\lambda_k^y}{\lambda_k^y + 1/a}$$

There is no obvious way to analytically derive the effect on the ROC curve so we will simply compute it. Figure 12 shows the effect of overestimating the input SNR.

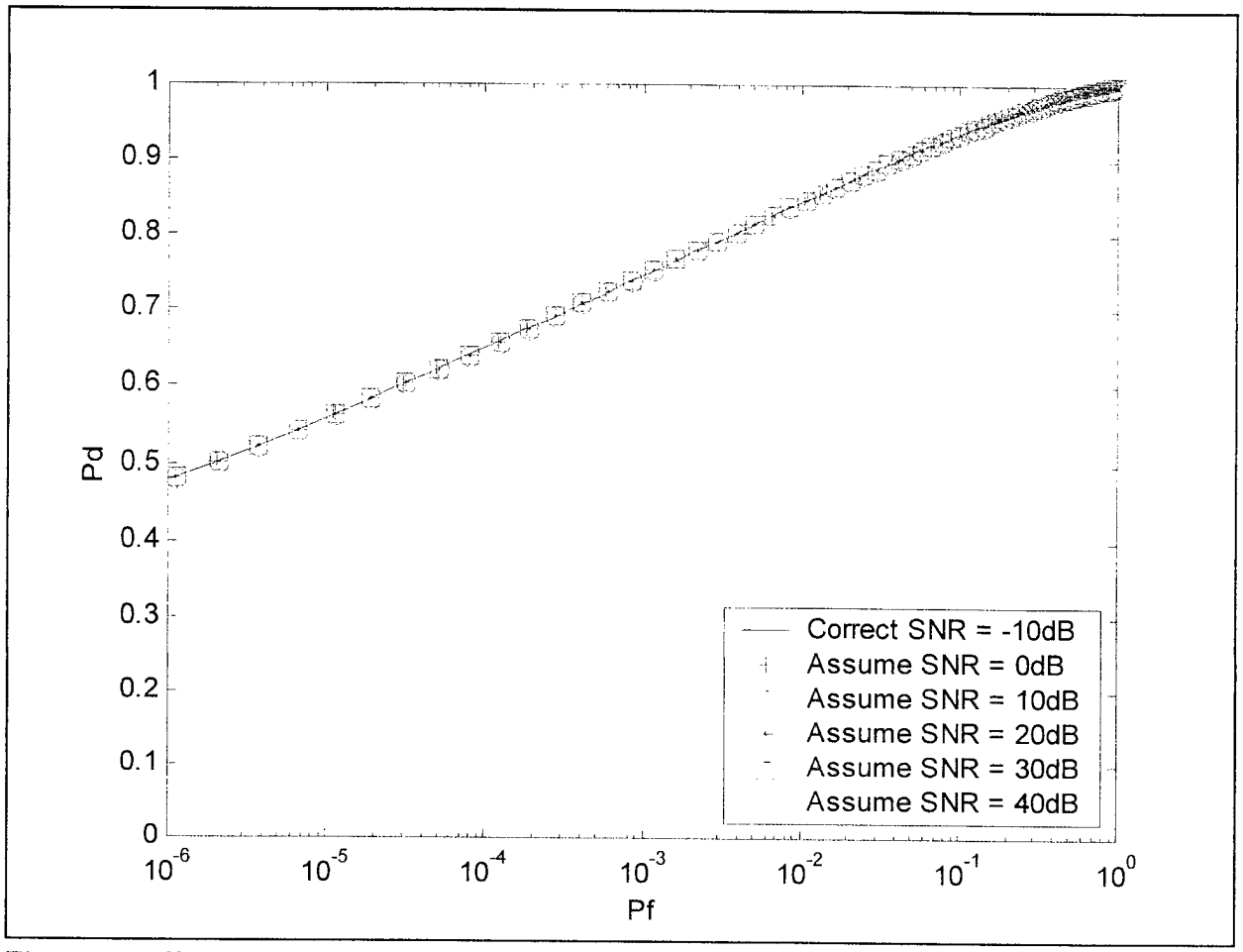

Figure 12 Effect of overestimating the input SNR. Scatterer has two highlights separated by 25 sample points, signal has TB = 15.

One can clearly see that the ROC curve is indistinguishably different when one overestimates the input SNR. This result was found by multiplying the target scattering function by a constant, no change was made to the reverberation scattering function. In the limit as one multiplies the target scattering function by as large a constant as numerically feasible, one is essentially estimating that there is no reverberation. Thus, in practice, it is not necessary to make any estimate of the reverberation scattering at all. This is advantageous in two ways. First, it requires less a priori knowledge of the scattering environment. Second, the bulk of the computation time is spent in computing eigenvalue decompositions, omitting the reverberation scattering function requires one less eigenvalue decomposition. Again, this result is true of any EC, not just the WTD-EC.

4.3 Validating the Sensitivity of the WTD-EC

The simplest way to test the sensitivity calculation is to set the assumed scattering function exactly equal to the correct scattering function. The resulting ROC curve should be the same as the ROC curve for the correct scattering function alone. This has been done for many different scattering functions.

One can also develop an analytic case similar to the one used to validate the correct likelihood calculation. Consider the case where $U = U_{ya} = U_r$. When this is true the expression in equation 142 becomes:

$$U_{ax}\Lambda_{ax}U_{ax}^{H} = \Lambda_r^{1/2}U^{H}UD_aU^{H}U\Lambda_r^{1/2}$$

or

$$U_{ax}\Lambda_{ax}U_{ax}^{H} = \Lambda_r^{1/2}D_a\Lambda_r^{1/2}$$

$$\lambda_k^{ax} = \lambda_k^{ya}\frac{1+\lambda_k^{y}}{1+\lambda_k^{ya}}$$

Substituting into the likelihood functions under hypothesis H_0 yields:

$$l^{a}|H_0 = \sum_k |w_{k_0}^{a}|^2\left(\lambda_k^{ya}\frac{1+\lambda_k^{y}}{1+\lambda_k^{ya}}\right)\frac{1}{1+\lambda_k^{y}}$$

or

$$l^{a}|H_0 = \sum_k |w_{k_0}^{a}|^2\frac{\lambda_k^{ya}}{1+\lambda_k^{ya}}$$

Notice that this is the same as the expression for the likelihood under H_0 for the correct scatterers, except the eigenvalues are replaced with the assumed eigenvalues.

Substituting the special case eigenvalues into the likelihood functions under hypothesis H_1 yields:

$$l^a | H_1 = \sum_k |w_{k_1}^a|^2 \lambda_k^{ya} \frac{1+\lambda_k^y}{1+\lambda_k^{ya}} \tag{161}$$

This is significantly different than the likelihood under H_1 for the correct scatterers which was

$$l | H_1 = \sum_k |v_{k_0}|^2 \lambda_k^y$$

As stated earlier, if the assumed scatterer is the same as the correct scatterer then the assumed and correct likelihood functions should be the same. If the assumed and correct scatterers are the same then the eigenvalues will also be the same $\lambda_k^{ya} = \lambda_k^y$. In which case the $1+\lambda$ terms in equation 161 cancel, and the assumed and correct likelihood functions are indeed equal. Another way to say this is that the likelihood is maximized when the guessed scattering function is the correct scattering function.

To test the case where the correct and assumed scattering functions are not equal, one needs to create a situation where $U = U_{ya} = U_r$. Just as in the case for validating the correct likelihood function, this can be done by setting $K = \mathbf{I}$. In this case the assumed eigenvalues are just the ratio of the assumed target highlights and the assumed reverberant highlights.

$$\lambda_k^{ya} = \frac{s_k^{ta}}{s_k^{na}}$$

As before the correct scatterers are:

$$\lambda_k^y = \frac{s_k^t}{s_k^n}$$

Again, just as was the case for validating the correct likelihood function, for the case where $U_{ya} \neq U_r$ one can still check the results by checking that eigenvector matrices are Hermitian and eigenvectors are real and positive.

4.4 Results

The purpose of the sensitivity analysis is to have some method of measuring what types of signals are best for what applications. What sort of signal should one use when you know the scattering function precisely, or when discriminating between very similar scatterers? What type of signal should one use when the scattering function is not well known? If there are sidelobes that correspond to the distance between highlights, is this a detriment, an enhancement, or irrelevant? Before doing a rigorous analysis, one might reasonably expect that the sensitivity to error is related to the autoambiguity function of the signal. That, as the guessed highlight moved outside of the mainlobe of the autoambiguity function centered on the correct highlight, probability of detection decreases. This has the unfortunate effect of reducing some of the gains made by having a high time-bandwidth product signal. As will be shown in this chapter, this is true to an extent, but luckily not so much so that errors in the scattering function outweigh the benefit of implementing the WTD-EC, or of using higher time-bandwidth product signals.

In figures 13 through 15 a simple example case is given to introduce the concept of a sensitivity graph, and to show it's connection to the assumed scattering functions. Figure 13 shows a set of scattering functions which will be used to generate ROC curves. The first scattering function is considered to be the correct scattering function. In successive scattering functions the guessed second highlight is further and further away from the correct highlight.

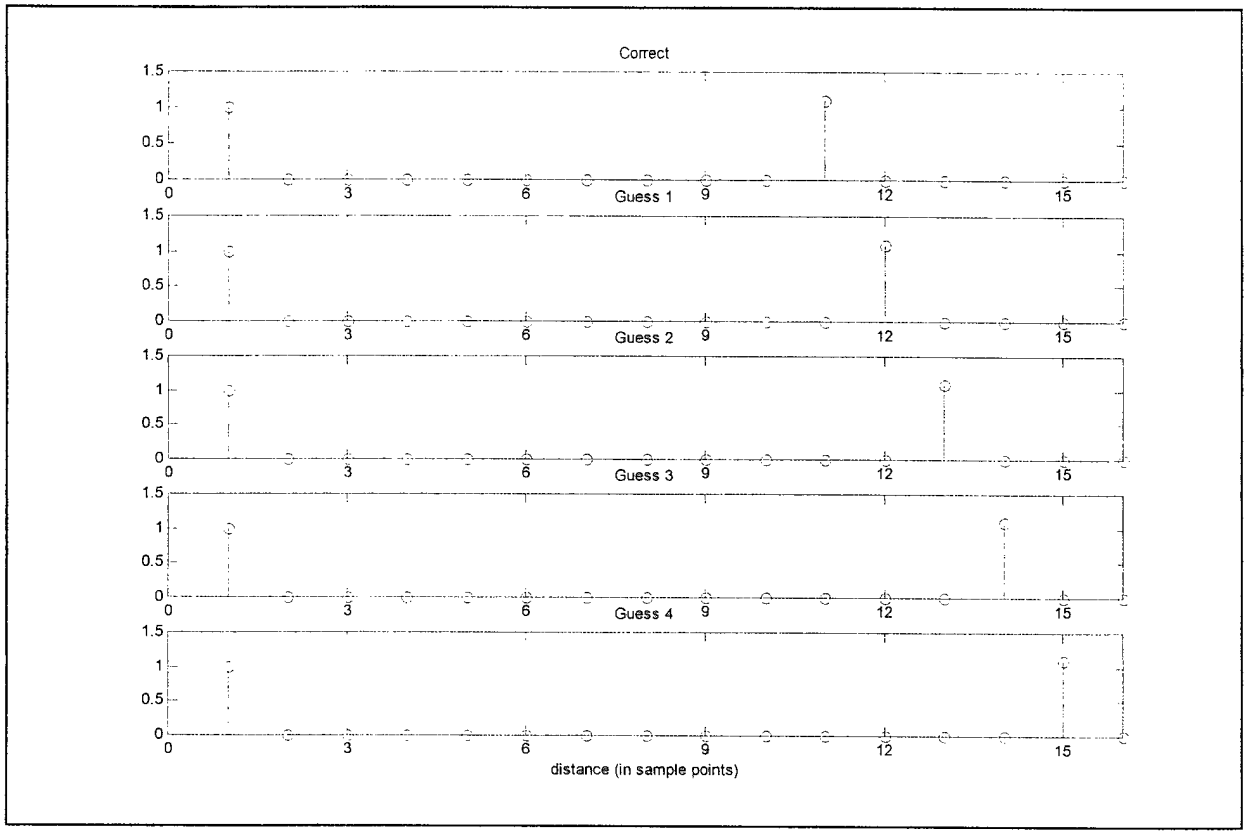

Figure 13 Scattering functions used to generate the next two graphs

Figure 14 shows the ROC curves corresponding to these scattering functions. The first curve corresponds to when the first scattering function is both the guessed scattering function and the correct scattering function, the next curve represents the second scattering function being guessed and the first is still the correct, the next curve is the third being guessed and the first correct, and so on.

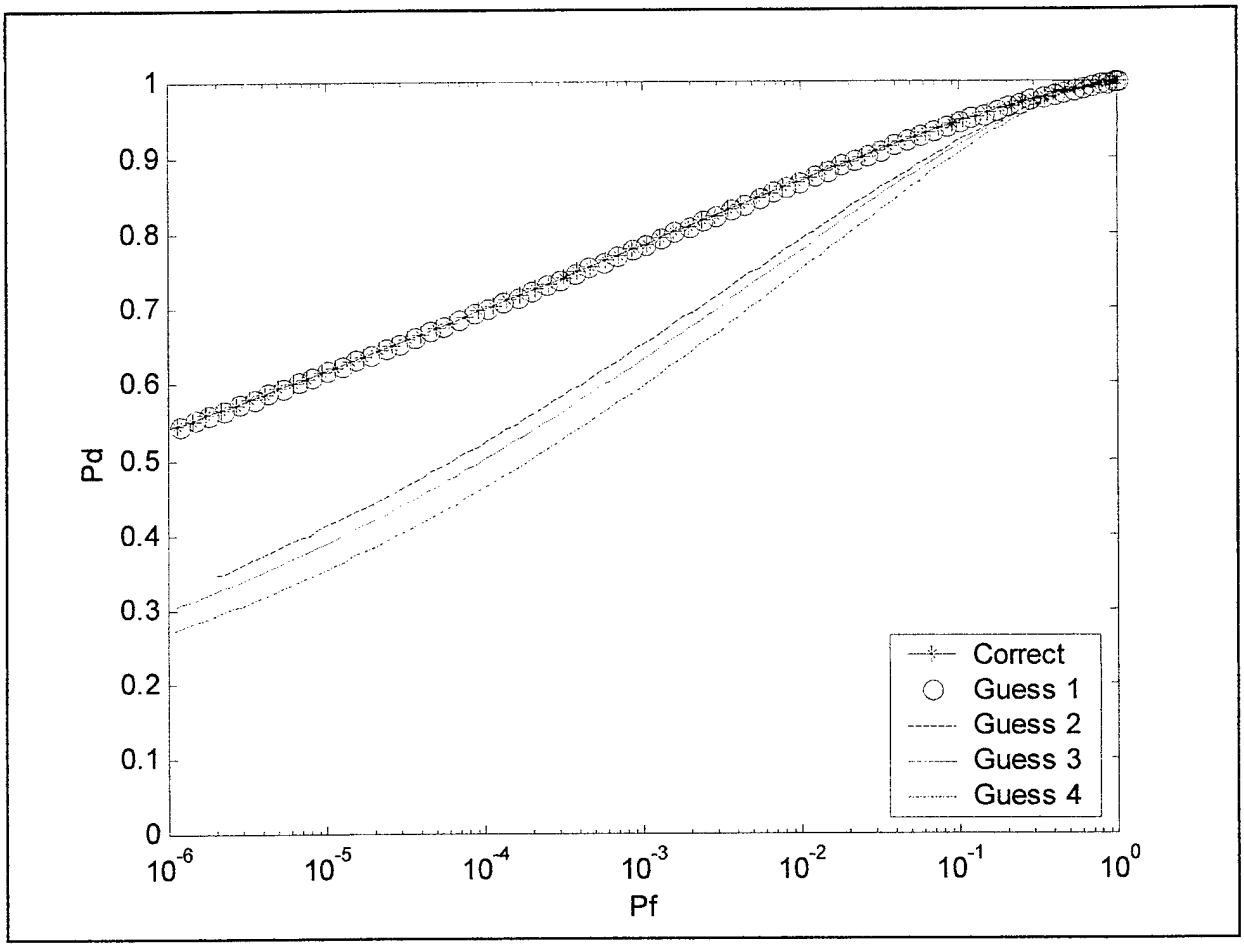

Figure 14 ROC curves corresponding to the scattering functions in figure 13

Graphs like figure 14 can be very muddled when the sensitivity does not depend monotonicly on the error (which is generally the case). To overcome this we will introduce a new kind of graph, which will be called a sensitivity graph. A sensitivity graph is generated by taking a graph such as figure 14 and slicing it vertically at a particular false alarm. Therefore a sensitivity graph is a plot of probability of detection versus error for a particular false alarm. For all of the sensitivity graphs in this thesis, the probability of false alarm is 10^{-3}.

Figure 15 shows the sensitivity graph corresponding to figure 14

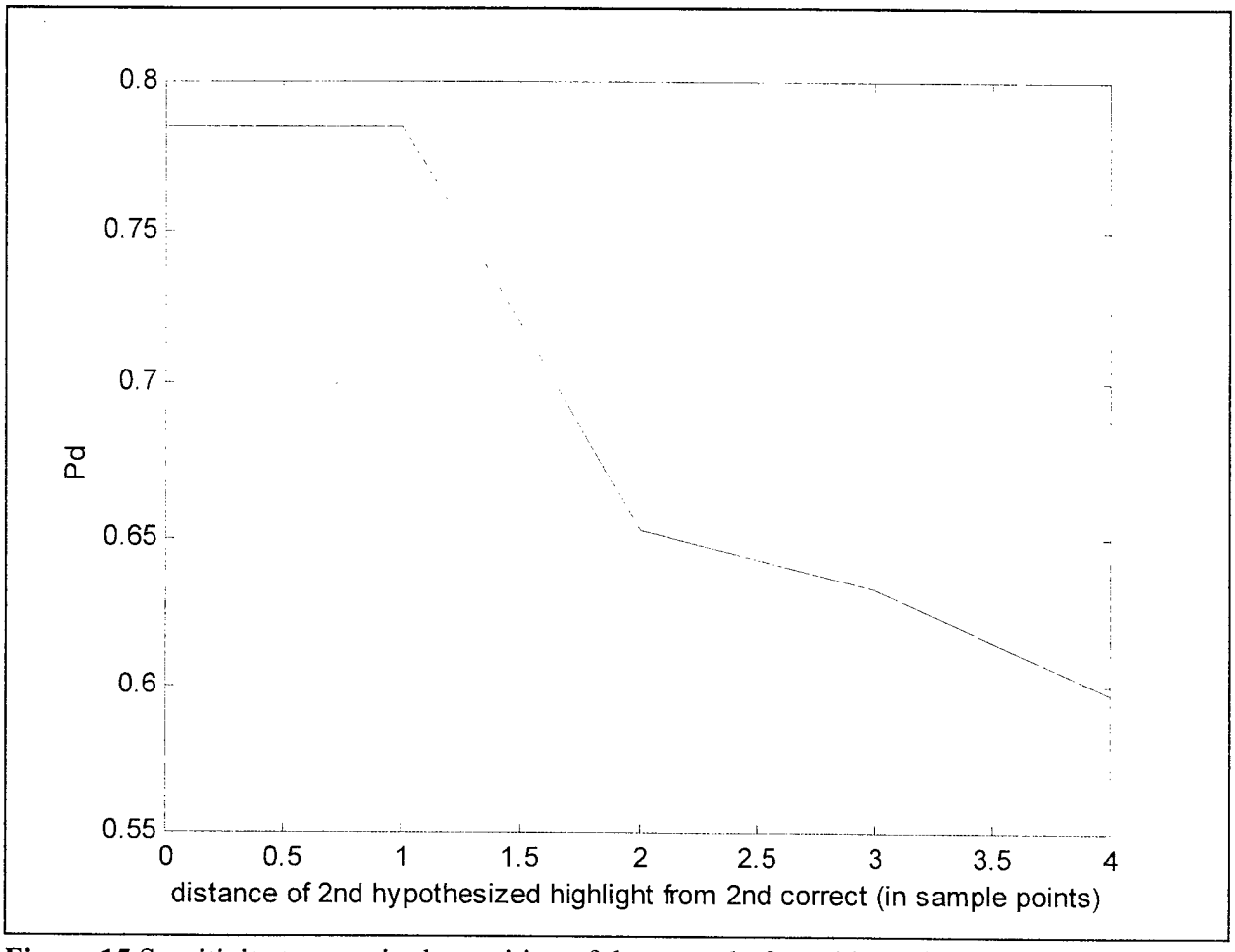

Figure 15 Sensitivity to error in the position of the second of two highlights for a signal of TB = 15

The sensitivity generally follows the autoambiguity function of the transmit signal. The wider the autoambiguity function, the less sensitive the detector to errors in the a priori scattering estimate. This is shown in figures 16 and 17

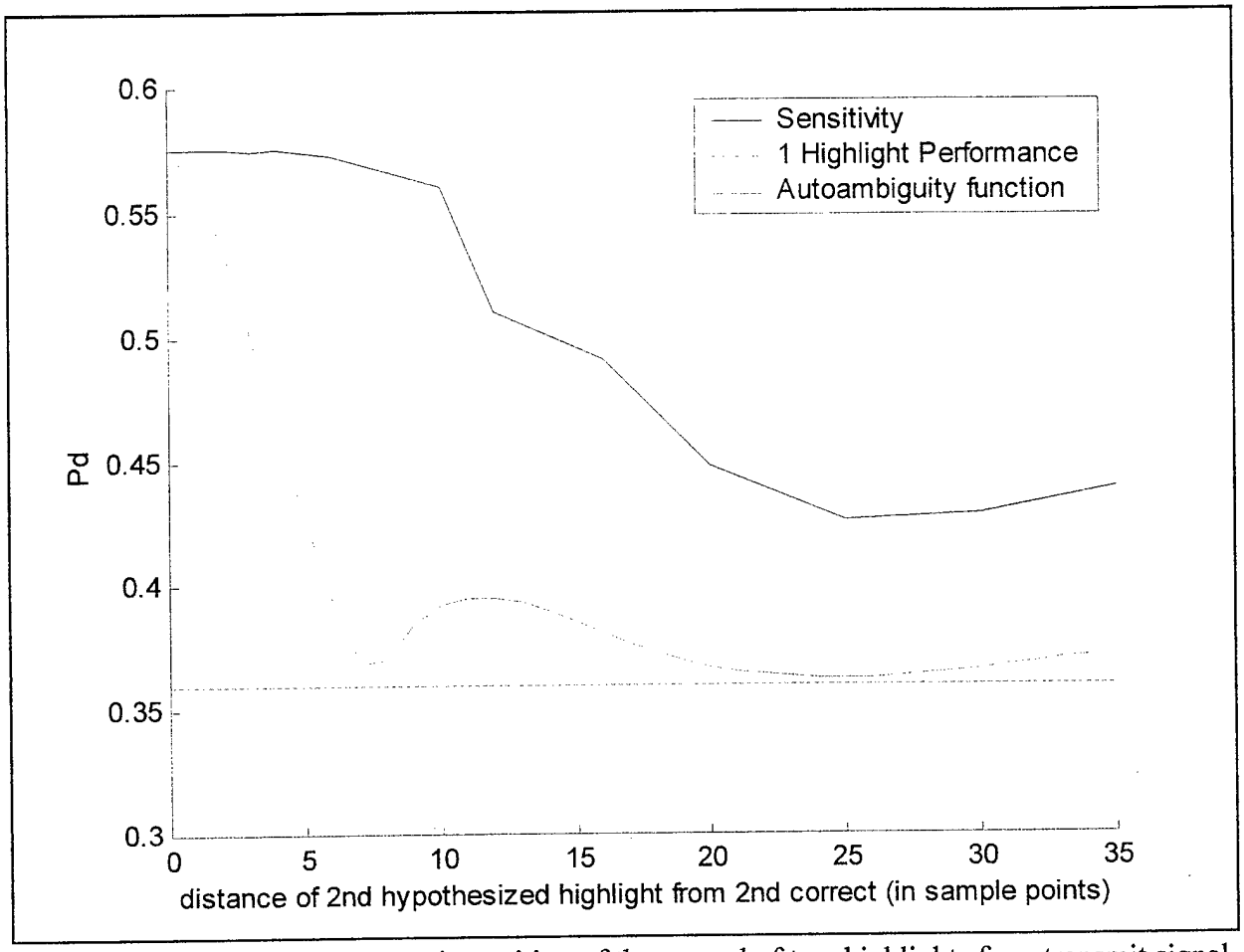

Figure 16 Sensitivity to the error in position of the second of two highlights for a transmit signal with TB = 7.5, input SNR of -3dB, two highlights separated by 50 points. The autoambiguity function is not plotted on the same vertical scale.

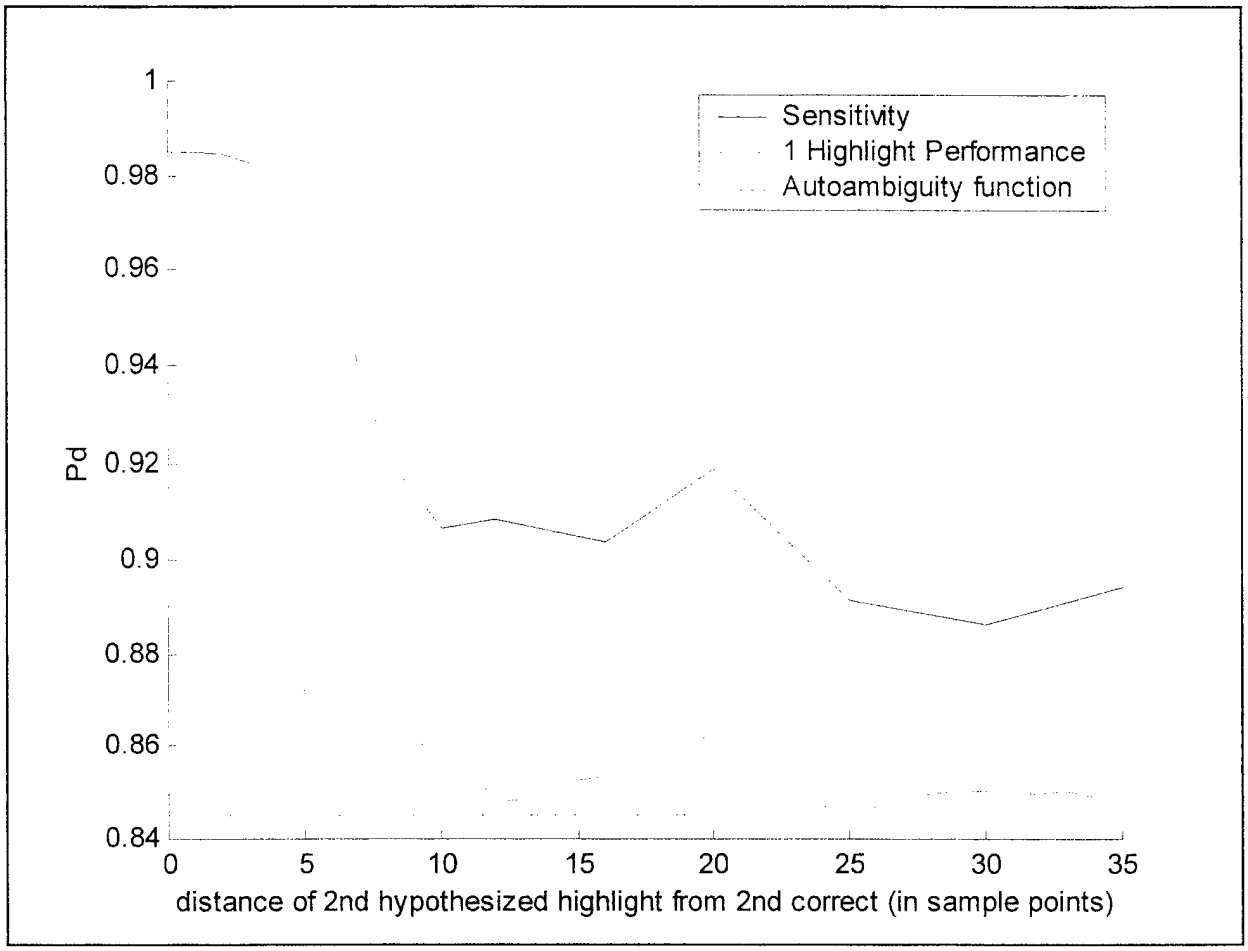

Figure 17 Sensitivity to the error in position of the second of two highlights for a transmit signal with TB = 15, input SNR of -3dB, two highlights separated by 50 points. The autoambiguity function is not plotted on the same vertical scale.

There are many things to note about these two graphs. First of all, the y axis does not extend from zero to one on either graph. Thus, even though the lower time-bandwidth product signal is less sensitive to error, the higher TB signal has a higher probability of detection everywhere. The dashed red line indicates the probability of detection when one guesses only one highlight, and uses the same transmit signal. Thus the one highlight detector sees only one of the two highlights, and therefore half the total scattered energy that the WTD-EC sees. One might guess, before having done this calculation, that the probability of detection for two highlights would converge to the performance for one highlight, when one of the guessed highlights is completely outside the mainlobe of the autoambiguity function. For this reason, the autoambiguity has been plotted on a

vertical scale such that it's maximum coincides with the probability of detection when both highlights are guessed correctly, and it's minimum coincides with the probability of detection when only one highlight is guessed. Thus figures 16 and 17 show that the probability of detection is even better than one might have expected. The probability of detection when guessing two highlights is always better than guessing only one, even when one is completely wrong about where the second highlight is.

Even though figures 16 and 17 may give us hope, it is not generally true that the sensitivity curve of a higher TB signal is everywhere better than the sensitivity curve for a lower TB signal. In figure 18 one can see that a signal with a time-bandwidth product of 13 does better than a signal with a TB of 15 for errors between 5 and 15 sample points, and is of comparable probability of detection for errors less than that. That, however, is not a very large difference in TB, and for significantly smaller time-bandwidths the probability of detection is uniformly worse. Thus there is no hard and fast rule saying that higher time-bandwidth product is always better. If you are trying to discern between very similar scattering functions, then you want the signal to be sensitive to errors, and it is probably best to pick the largest possible time-bandwidth product. If you want the detector to be robust to errors, then you may want to pick a slightly lower time-bandwidth product than the maximum allowed by the available equipment. There is a limit, however, to trading TB for robustness to error. One would not choose a time-bandwidth product of 11.5 for this scatterer because one could always do better by using a signal with TB of 15.

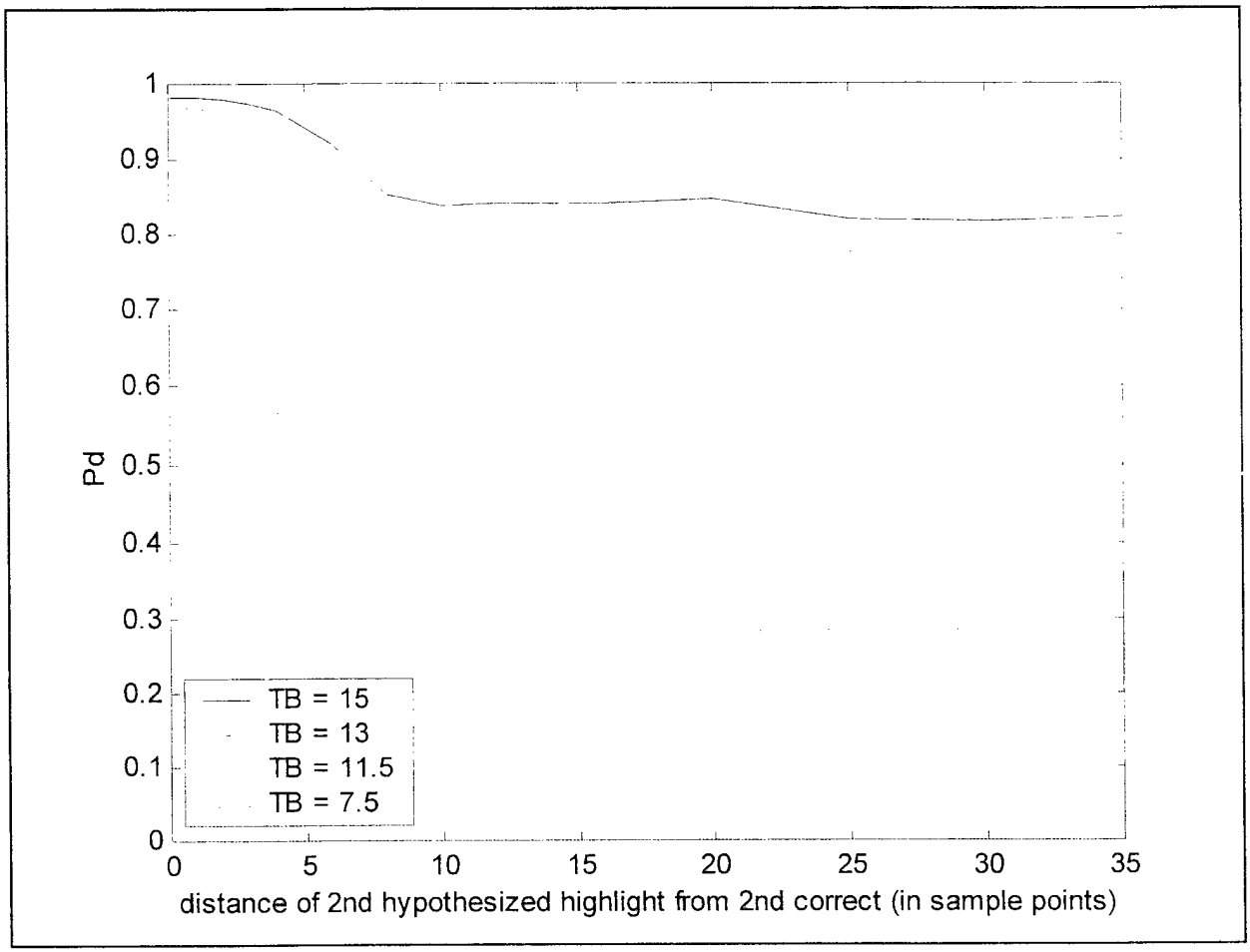

Figure 18 Sensitivity to error in position of the second of two highlights for transmit signals with various time-bandwidth products, input SNR of -3dB, two highlights separated by 50 points

While the oscillations in the sensitivity of the TB = 11.5 detector do, in fact, correspond in position to autoambiguity function sidelobes, it is not clear why they are so large. Figure 19 shows that the TB = 15 signal retains its advantage over signals with TB = 11.5 or lower, even when at very low input SNR.

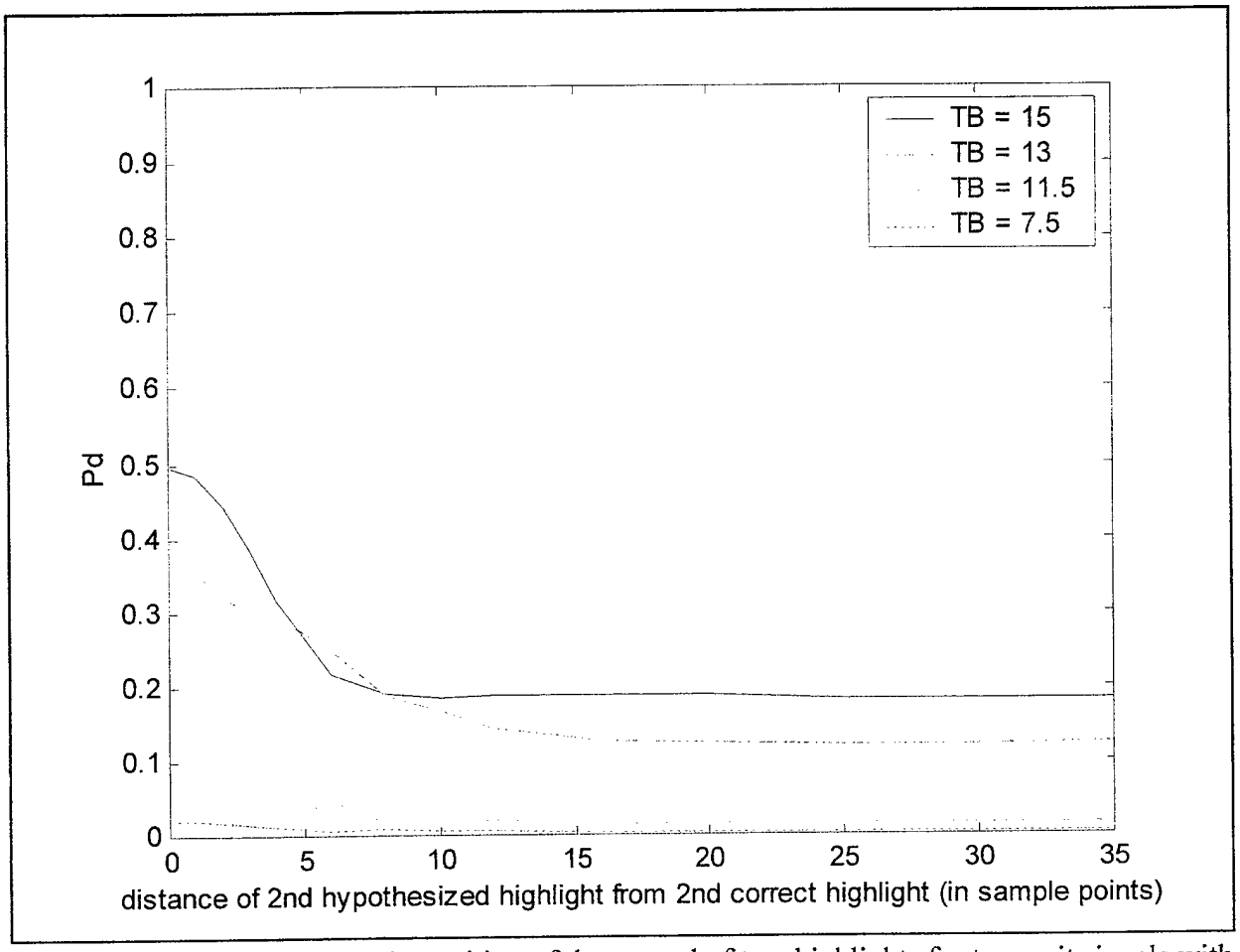

Figure 19 Sensitivity to error in position of the second of two highlights for transmit signals with various time-bandwidth products, input SNR of -13dB, two highlights separated by 50 points

Figure 20 shows more directly that the sensitivity does not change dramatically with the input SNR

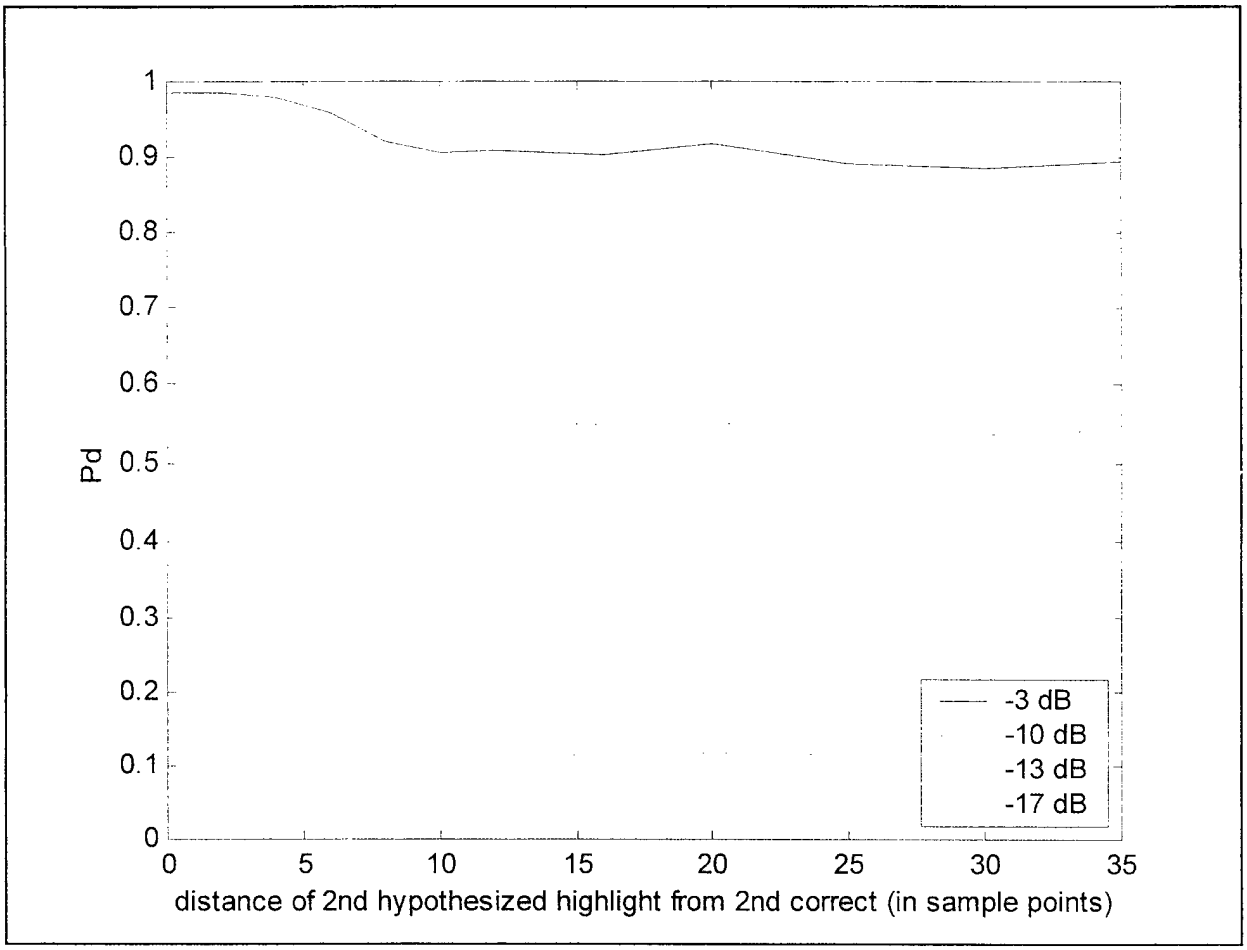

Figure 20 Sensitivity to the error in position of the second of two highlights for various input SNRs, a transmit signal with TB = 15, two highlights separated by 50 points.

It will now be demonstrated what happens when one is wrong both about the position and number of highlights. Figure 21 shows that probability of detection can only decrease if you hypothesize that there are three highlights when there are only two.

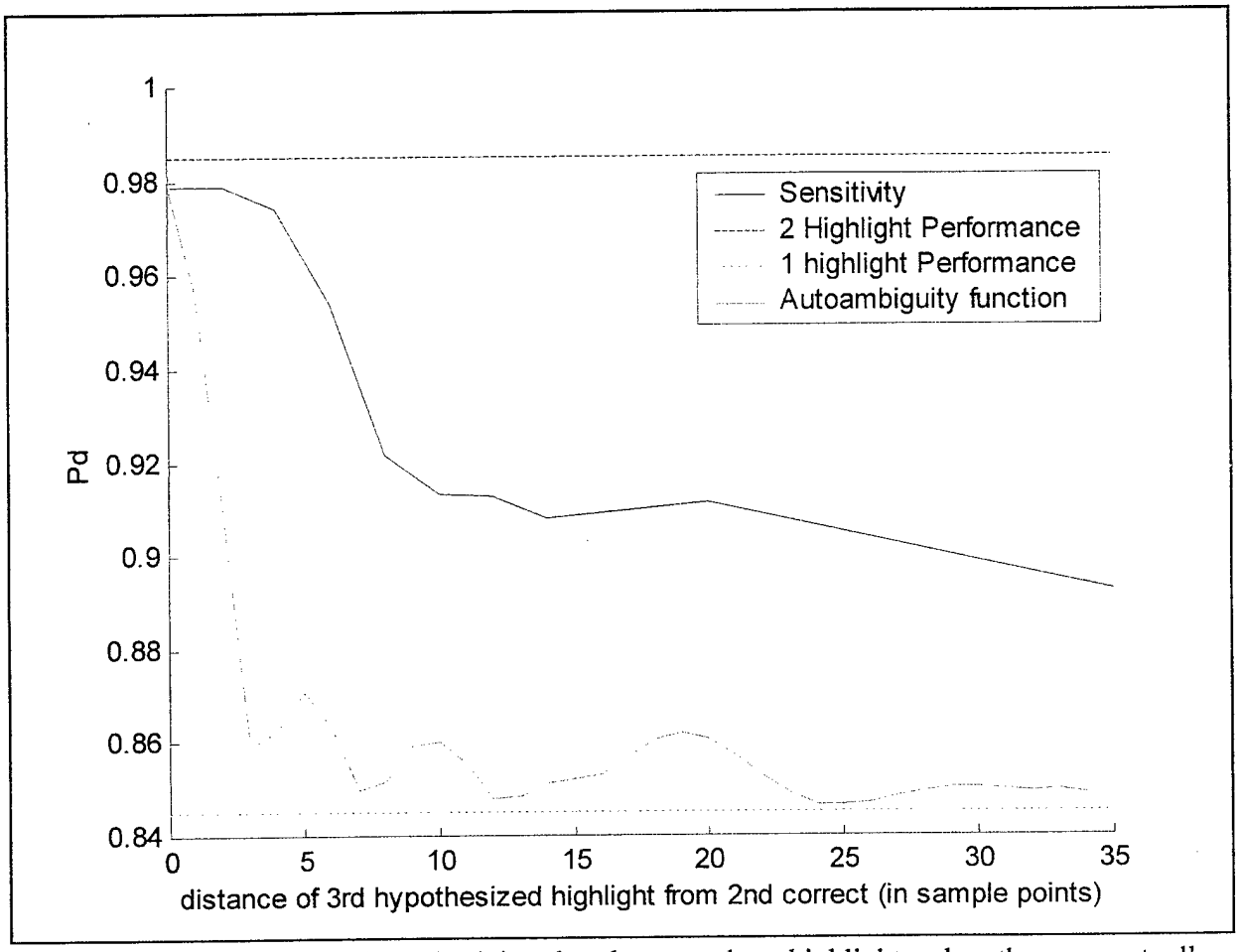

Figure 21 Sensitivity when hypothesizing that there are three highlights when there are actually two. Transmit signal has TB = 15, input SNR of -3dB. The two correct highlights are 50 sample points apart. The autoambiguity function is not plotted on the same vertical scale.

Figure 22 shows the sensitivity when there are three correct highlights, and there are only assumed to be two. The three correct highlights are separated by 12 sample points, the first hypothesized highlight is correct, the horizontal axis represents the distance of the second hypothesized highlight from the first.

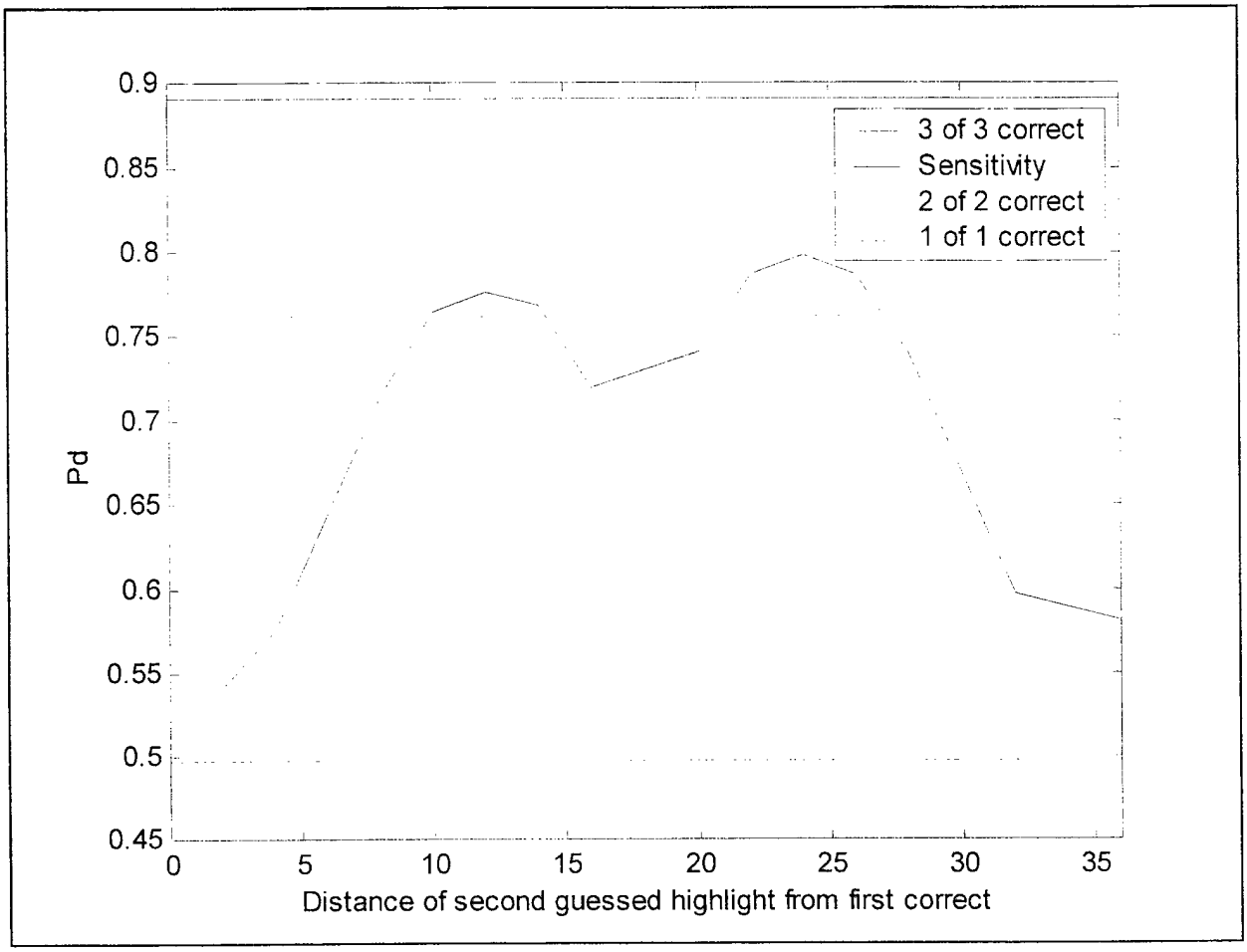

Figure 22 Sensitivity to the position of the second of two hypothesized highlights when there are three correct highlights. Signal has TB = 15, input SNR = -10dB, correct highlights are separated by 12 sample points.

In figures 21 and 22 the probability of detection is never less than probability of detection when only one highlight is hypothesized. In all of the examples in this thesis, when the correct scatterer has more than one highlight, it is always better to hypothesize more than one highlight, no matter how wrong you are about how many or where they are, than to guess only one highlight.

Roan [48] has suggested that a boot strap procedure could be used to find the scattering function that maximizes the probability of detection for a given observation vector. First, the maximum on the scale-delay map is considered to be a highlight. Next one hypothesizes a second highlight at each position further and further away from the first highlight. When a maximum in the likelihood ratio is found, a second highlight is added to the estimate. More highlights are

added to the estimate in a similar fashion. Figure 22 Shows there will indeed be maxima in the sensitivity when you get more than one (but not all) of the highlights estimated correctly. Thus, this bootstrap procedure has merit.

There is more to get wrong than the position of the highlights, one can also estimate the relative magnitudes of the highlights incorrectly. Figure 23 shows the sensitivity to estimating the magnitude of the second highlight incorrectly, for a scatterer with two highlights. Highlights are separated by 25 samples points, the signal has TB = 15.

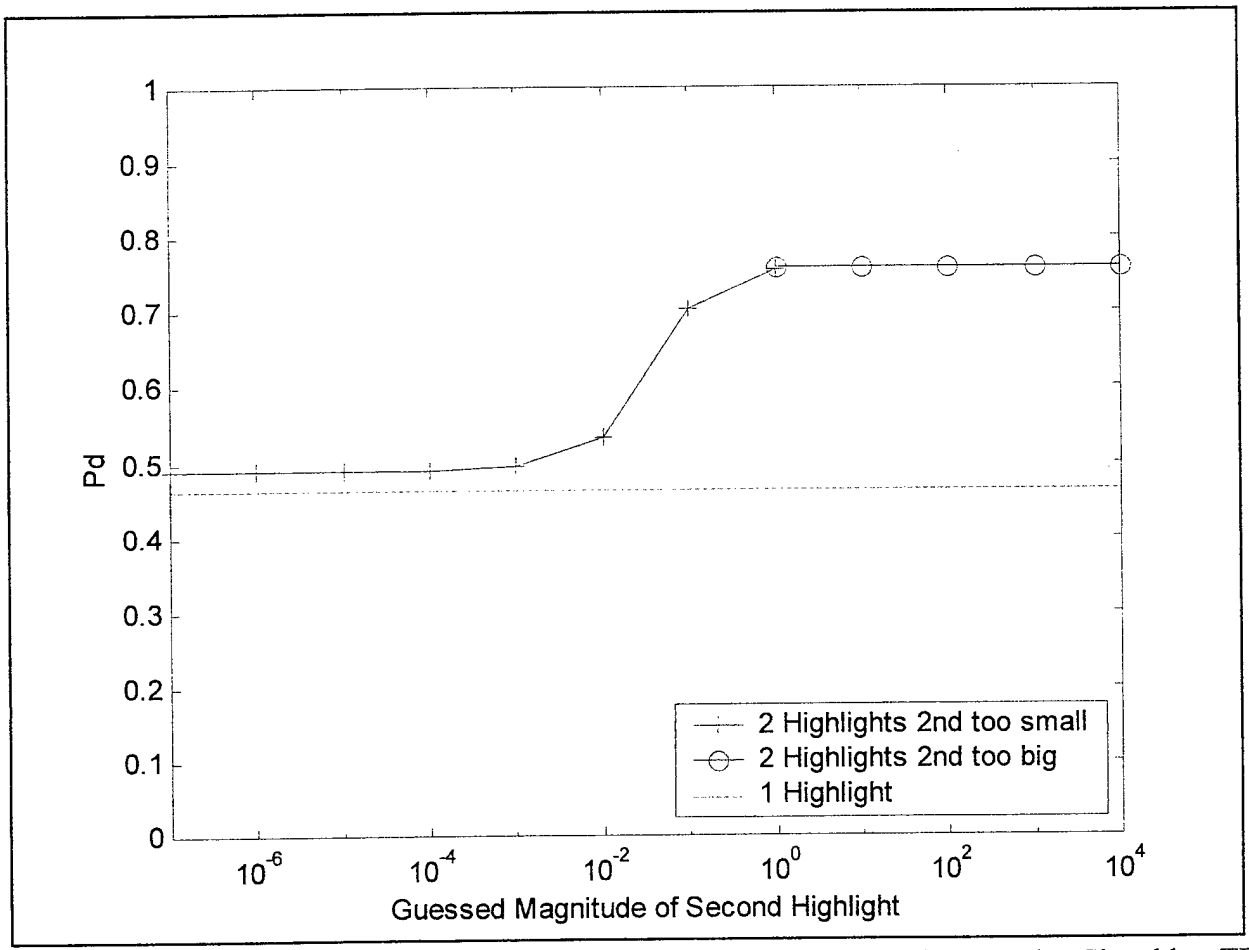

Figure 23 Sensitivity to estimating the relative magnitude of highlights incorrectly. Signal has TB = 15, highlights are separated by 25 sample points

This is an encouraging graph. It says that it does not matter if you overestimate, but still gives the sensible result that guessing too small is equivalent to guessing that there is only one highlight. Combined with the result of section 4.2, it can be concluded that one only need estimate the

position of target highlights.

Thus, the a priori knowledge needed by the EC is much less than is implied by the WTD-EC without doing a sensitivity analysis. Even though the mathematical form of the WTD-EC includes a detailed target and reverberant scattering function estimate, one need only estimate the position of target highlights. The relative magnitude of target highlights, and reverberation highlights need not be estimated at all.

Roan's thesis [17] tackles the problem of how to track a rotating distributed object. The sensitivity analysis can be used to find the sensitivity to error in the hypothesized rotation angle. Figure 24 shows how the highlights of a rotating object with one highlight at each end are projected onto the line of site of the transmit signal.

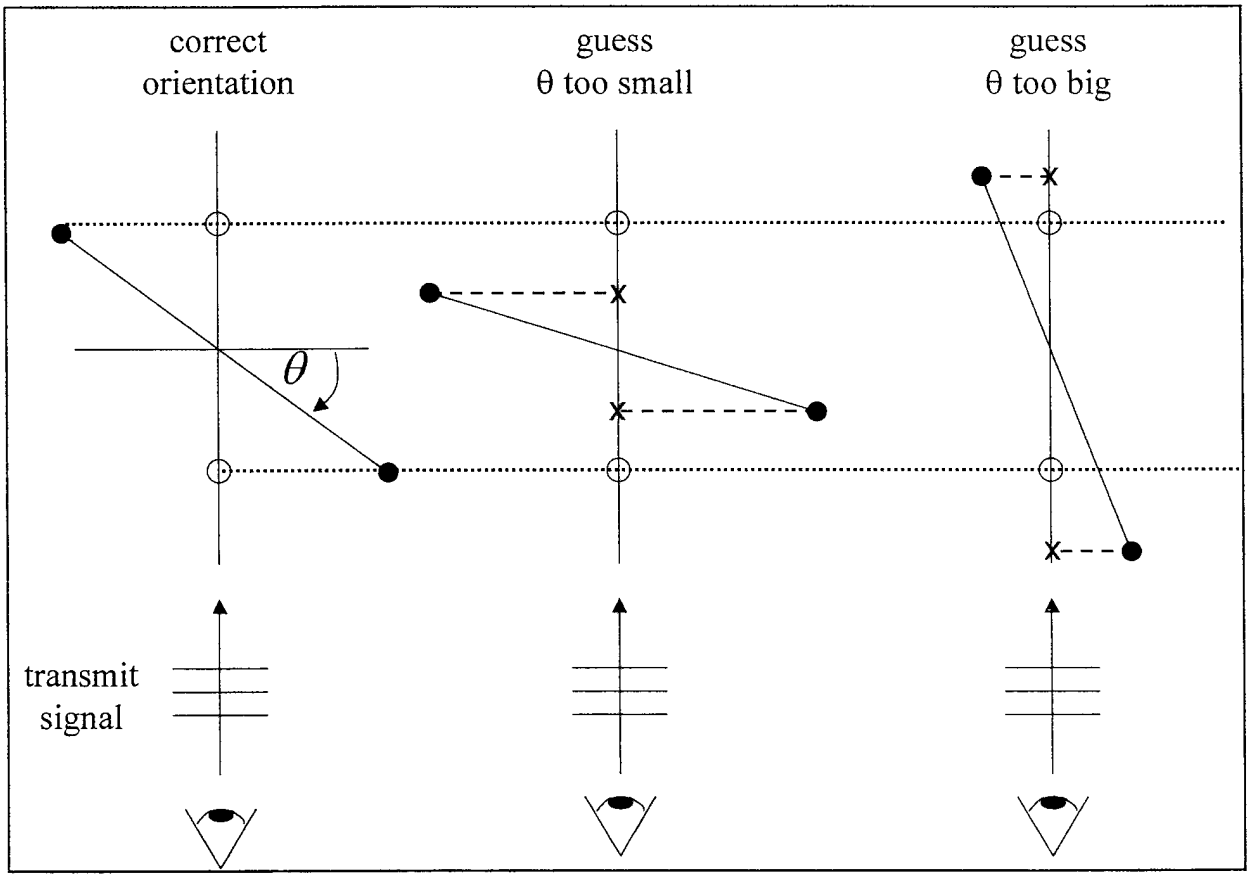

Figure 24 How highlights of a rotating objected are projected onto the line of site of the transmit signal.

When the rotation angle estimate is too small, the hypothesized highlights are closer together than the correct highlights. When the rotation angle estimate is too large, the hypothesized highlights are farther apart than the correct highlights.

The sensitivity to error in hypothesized rotation angle is now computed for an object with six highlights. Figures 25 and 26 show the correct and hypothesized scatterers used for this calculation. Note that the vertical scale of figure 25 is larger because at an angle of 90° the highlights combine to form a single highlight with magnitude six.

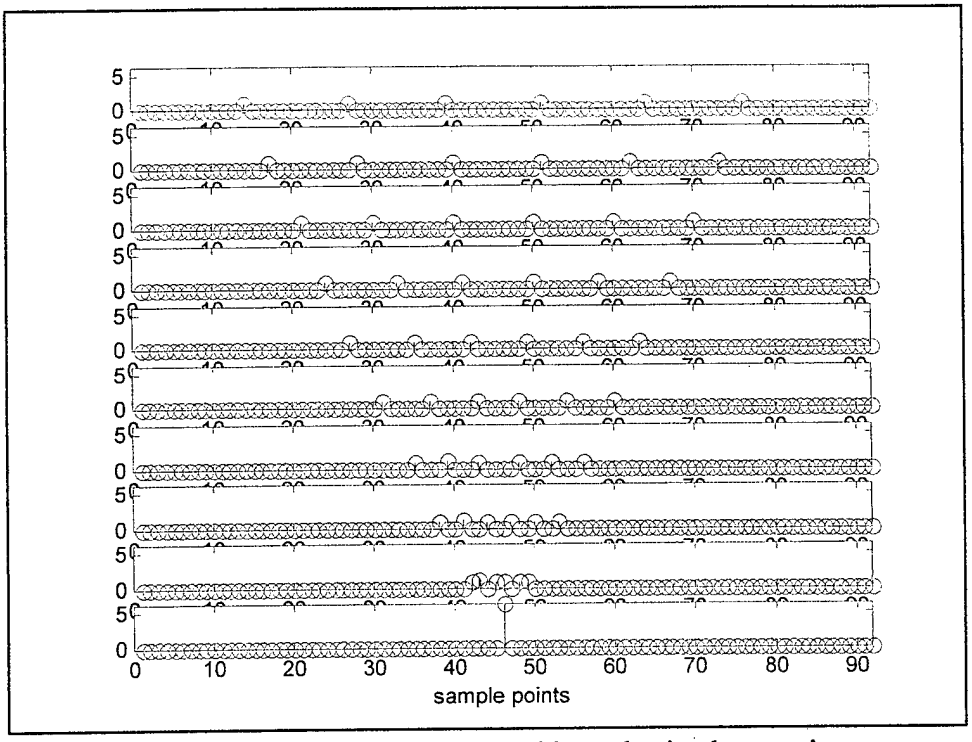

Figure 25 Correct scattering function, and hypothesized scattering functions with estimated angle too small.

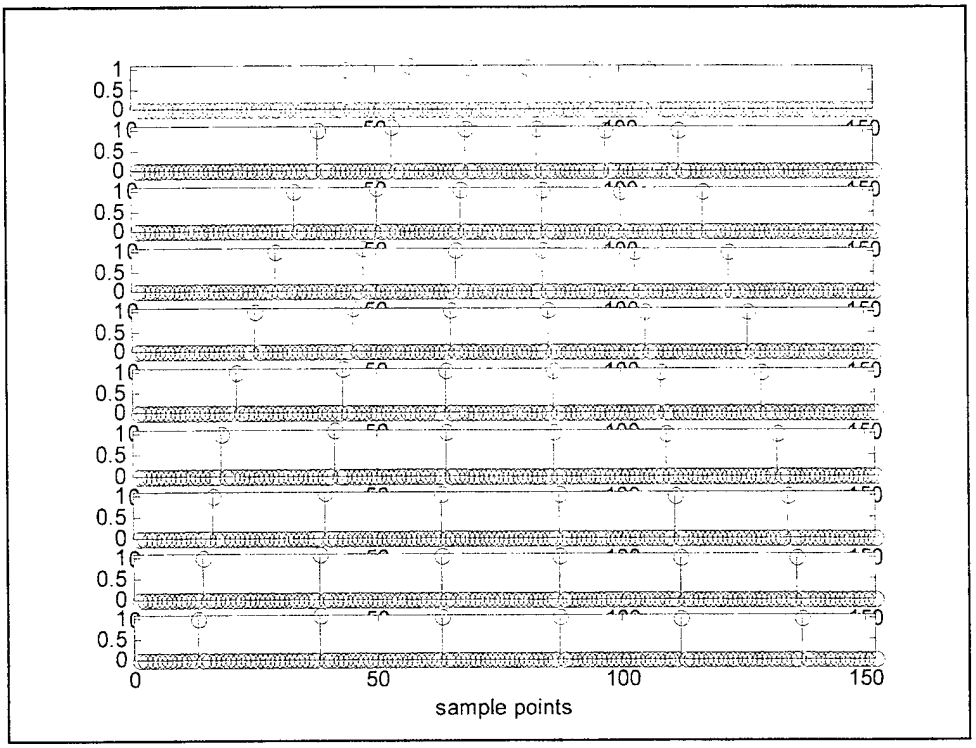

Figure 26 Correct scattering function, and hypothesized scattering functions with estimated angle too large.

Figures 27 through 30 show the sensitivity to error in the hypothesized rotation angle.

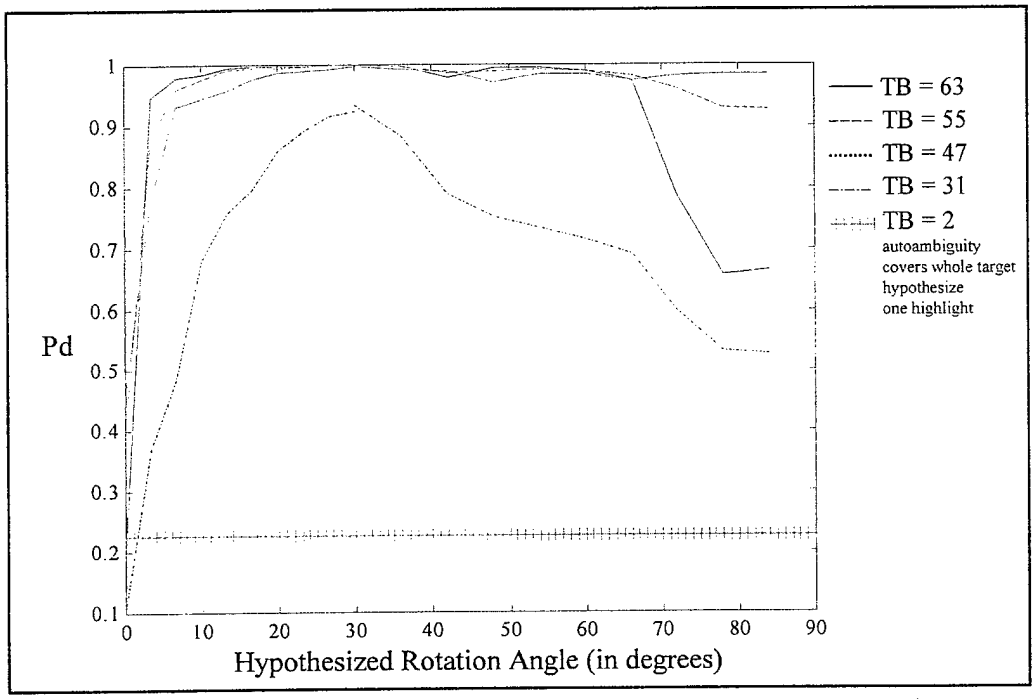

Figure 27 Sensitivity to hypothesized rotation angle. Input SNR = -10dB, correct angle = 30°.

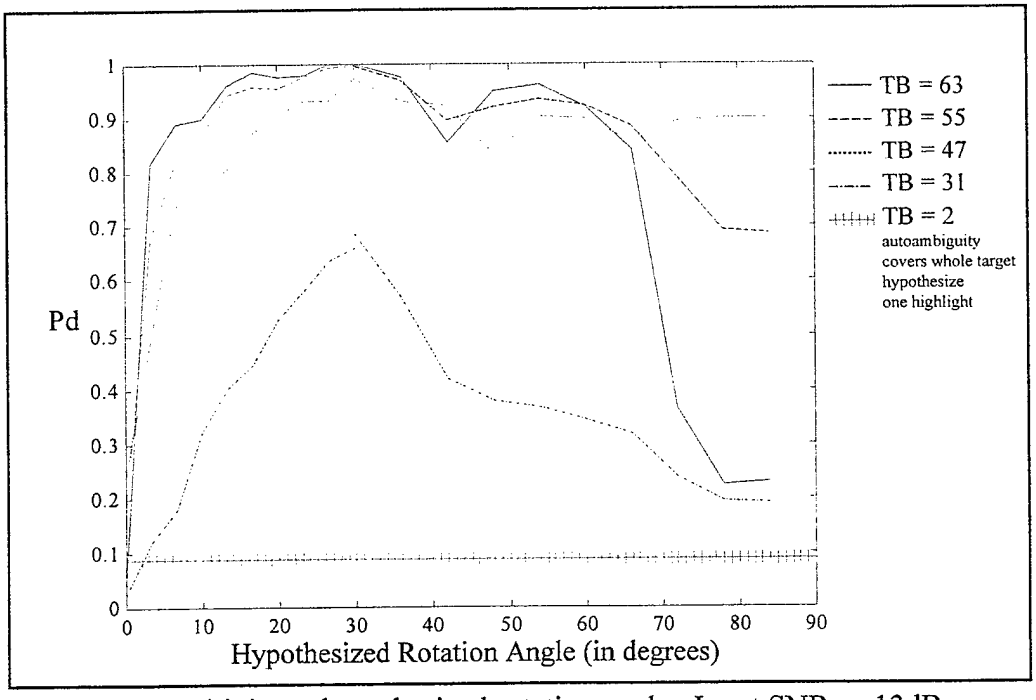

Figure 28 Sensitivity to hypothesized rotation angle. Input SNR = -13dB, correct angle = 30°.

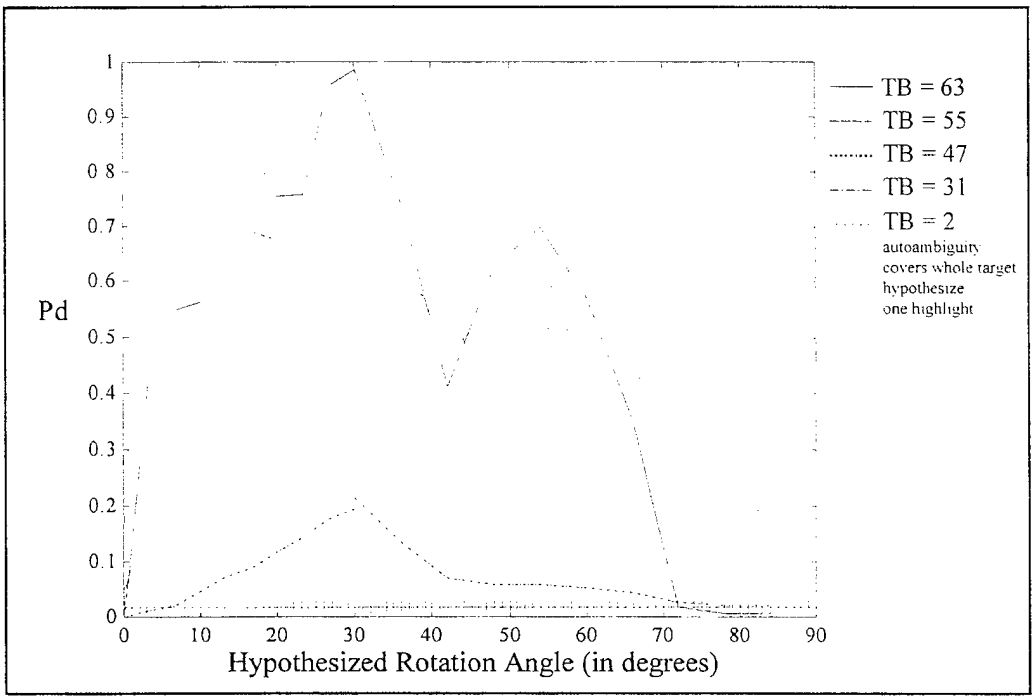

Figure 29 Sensitivity to hypothesized rotation angle. Input SNR = -16dB, correct angle = 30°.

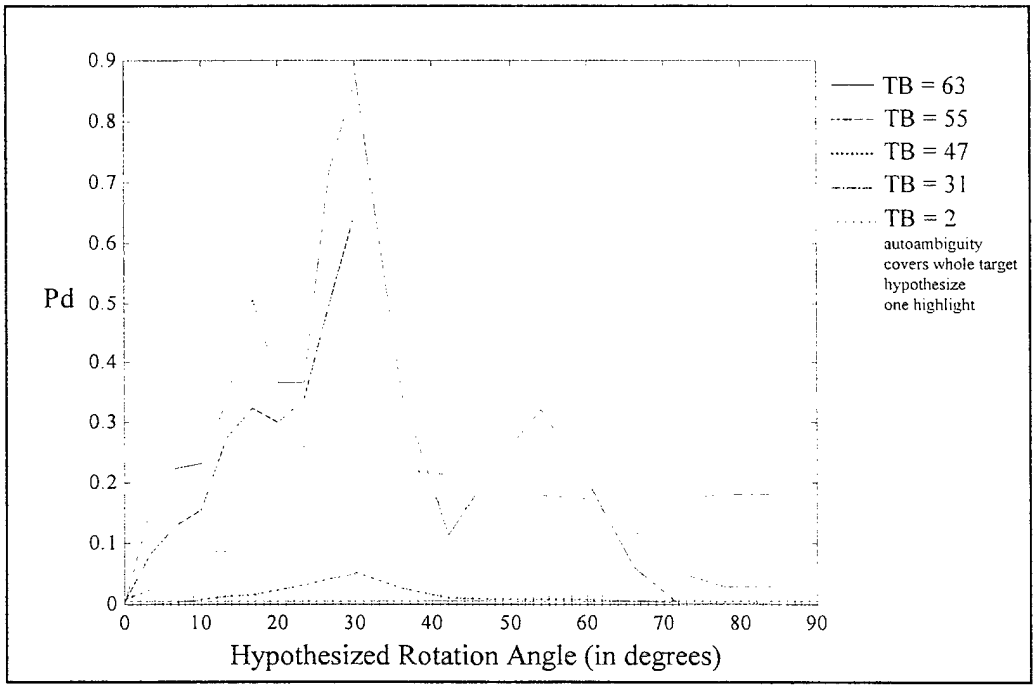

Figure 30 Sensitivity to hypothesized rotation angle. Input SNR = -20dB, correct angle = 30°.

Plotted in each figure is the probability of detection of a one highlight detector of TB = 2. This time-bandwidth product was chosen because its autoambiguity function is wide enough to cover all of the highlights. It sees the same total reflected energy as the WTD-EC. Thus the TB = 2 line represents the best the one highlight EC can do under correlated noise conditions. Therefore, even though the WTD-EC is less robust to error in rotation angle at very low input SNR, than at higher input SNR, it is still everywhere better than the one highlight EC because the one highlight EC is limited to a lower TB in order not to incur splitting loss. Furthermore, there is a clear relationship between time-bandwidth product, input SNR, and robustness.

Figures 27 through 30 were generated by first computing the sensitivity when the estimated angle is too small, and then when it is too big. This is why the scattering functions are split into to graphs in figures 25 and 26. Small random numbers are added to the scattering functions for numerical stability reasons. These small random numbers are different in each run, and thus sometimes the sensitivity to the angle being too small, and the sensitivity to it being too big, do not quite match in the middle (i.e. the TB = 31 line).

4.5 Summary

A sensitivity analysis has been derived which can be applied to any EC. It has been shown that it is not necessary to make an estimate of the reverberation scattering function. It has been demonstrated that the sensitivity of the EC mimics the autoambiguity function, but that the probability of detection does not degrade to the probability of detection of N_h-1 highlights when a hypothesized highlight is much farther away from its correct position than the width of the autoambiguity function. It was shown that one can trade off time-bandwidth product to gain robustness to error, but that for a given maximum TB there is a TB below which there is no benefit. It was demonstrated that making an estimate of the scattering function is always better than not making one (one highlight estimate), regardless of how wrong that estimate is. Finally, it was shown that one only needs to estimate the position of target highlights, no estimate of the relative magnitude of the highlights need be made.

Chapter 5
CONCLUSIONS

5.1 Implementing the WTD-EC

In Chapter 3 the Wavelet Transform Domain Estimator-Correlator derived by Roan and Sibul [4] was implemented. Many implementation and numerical problems were overcome. A fast method of inverting the inverse wavelet transformed eigenvector matrices was found. It was shown that small negative eigenvalues can arise from numerical errors, and that these must be omitted for the probability densities to be finite. A method of constructing and choosing the minimum size of the scattering matrix and eigenvectors for a given scattering function and transmit signal was presented.

It was shown that, because of numerical accuracy issues, there is a limit to the number of significant eigenvalues that can be used in the Heaviside expansion for the computation of the probability densities. The number of significant eigenvalues (which is roughly the same as the number of significant highlights) must be smaller than the number of digits of precision of the computer. It may be possible to approximate the Heaviside expansion with a Chi Square distribution, and some work in that direction is given in Appendix B.

Various methods of validating the numerical calculation were derived. It was shown that if the autoambiguity matrix is the identity function then the eigenvalues are the ratios of the target and reverberant scattering strengths. One can verify that the inverse wavelet transformed eigenvectors were correctly computed by verifying that $UU^H = cI$. Because covariance functions are positive definite, and positive definite matrices must have real non-negative eigenvalues, one can check the accuracy of the computation by seeing how close the actual computed eigenvalues come to meeting this condition. Lastly, the subsection of code that takes the eigenvalues as inputs and computes the probability distributions can be checked by giving it N eigenvalues that are close to the same value, and comparing the result to a Chi Squared distribution with N degrees of freedom. It was shown that the code used to generate the examples in this thesis meets all of these conditions.

Finally the properties of the WTD-EC were presented. It was shown that for N highlights the WTD-EC yields a $10Log_{10}(N)$ dB processing gain. Or, more precisely, the ROC curve for an N highlight target where each highlight has a scattering strength of 1/N is nearly identical to the ROC curve for one highlight with a scattering strength of 1. This is why one can not use just a scalar figure of merit to characterize the performance of the detector. Scatterers with the same total scattering energy can result in different ROC curves. The WTD-EC also has the expected properties of better performance for higher time-bandwidth product signals, and better performance for a larger number of highlights.

5.2 Sensitivity Analysis of the WTD-EC

A method was derived for finding the ROC curve of the EC for the case where the a priori estimate is not correct This result is not only true for the wavelet transform domain implementation of the EC, but for any method of finding the covariance function eigenvalues. This analysis has provided powerful evidence that the gains of the WTD-EC derived in Chapter 3 can actually be achieved in practice and provides a method of designing signals for specific applications.

Methods for validating the sensitivity calculation similar to those used in Chapter 3 were applied and met.

A new performance measure was introduced which we chose to call the sensitivity curve. The sensitivity curve is the probability of detection versus some measure of the error in the scattering function, at a given false alarm rate. It was shown that the sensitivity curve generally follows the autoambiguity function. That is, signals with a high resolution are more sensitive to errors in the scattering function estimate. This does not mean, however, that there is no advantage to using a high time-bandwidth product signal. Because the overall performance decreases as the resolution decreases, there is a limit to how much one can trade off resolution for robustness to error. For a signal with a sufficiently lower resolution, its performance will be worse no matter how large the error is. If you are trying to discern between a set of very similar scatterers, and you do not want robustness to error, it is always best to use the highest time-bandwidth product signal possible.

It was shown that the sensitivity does not depend on the input SNR.

Most importantly, it was shown that it is always better to make a scattering function estimate than not to, and less a priori information is needed than one would expect. It is not necessary to estimate the reverberation scattering function, or the relative magnitude of the scattering function highlights.

It was concluded that the WTD-EC can result in dramatic gains over the one highlight EC, and that these gains are not just theoretical. Errors in the scattering function estimate do not erase the gains made by using a high time-bandwidth product signal.

5.3 Future Work

Many questions remain that can be answered with the theory and computational code developed in this thesis. In Chapter 4 it was shown that if one guesses that there is an additional highlight which is close to a correct highlight, the performance will not be significantly degraded. Can one increase the robustness to error by doubling up highlights (that is, replace single highlights with several highlights packed together) ? Most of the examples in this thesis are for a small number of highlights. Some examples with a larger number of highlights has been computed by Ricker [19], but this should be demonstrated for a greater variety of examples. Also, does anything significant happen when a scatterer has some highlights that are within one mainlobe's distance of each other, and some that are not? Our derivation did not assume discrete scatterers, but all of our examples have been composed of discrete scatterers. What can be said about continuous scattering functions?

Most of the results in this thesis are empirical, they result from computing the performance for many combinations of transmit signals and scattering functions. It has been shown that the likelihood function increases in proportion to the energy in the scattering function (regardless of how it's distributed between highlights). In chapter 4 it was demonstrated that the sensitivity is related to the autoambiguity function. It would be nice to show this analytically. This would require either an exploration of the eigenvalue decomposition of the covariance matrices, or expanding those matrices in terms of a predetermined set of basis functions.

There is much room to improve the computational implementation of the theory. Though the WTD-EC and the sensitivity were derived for scatterers spread in both delay and scale, the computation was only implemented for scatterers spread in delay. The bulk of the computational

time is spent finding the eigenvalues and eigenvectors of the covariance matrices. This is done with the Matlab eig() function, which makes no assumptions about the form of the matrix. In this thesis though, quite a lot is known about the matrices. For example, in:

$$\lambda_k \psi_k = \underline{\underline{K}} S \psi_k$$

it is known a priori that S is diagonal, that K is composed of translated versions of the autoambiguity function, and that K is Hermitian. The whitened covariance matrix is composed of the eigenvalues and eigenvectors of the scattering and noise covariances. Certainly with all this a priori knowledge there is some more efficient way to compute the eigenvalues.

There is fertile ground for new research by relaxing some of the restrictions imposed in this work. In the very beginning it was assumed that the highlights in the scattering function were uncorrelated.

$$S(x,x') = S(x,x)\delta(x - x')$$

This made a matrix representation of the problem easy. However, there is no reason to assume that the computation could not be done without this restriction.

The WTD-EC can be combined with other methods in useful ways. Roan has developed a method of using Kalman filtering to track highlights. This could be used to generate the scattering function estimate used by the WTD-EC.

The WTD-EC can be combined with search algorithms in useful ways. It has been shown that the likelihood function is maximized when the guessed scattering function estimate is correct. Roan's boot strap algorithm could be implemented to find the scattering function which maximizes the likelihood ratio for a particular observation vector. This scattering function could be the first estimate used in the Kalman tracking method mentioned above.

A search algorithm could be used to find the optimum transmit signal given a particular scattering function and a bound on the scattering estimate error. Similarly, a search algorithm could find an optimum transmit signal to distinguish between similar scatterers.

The sensitivity analysis can be used to decide how large a library to build to distinguish between the same scatterer in different conditions. The same scatterer under different multipath

conditions will exhibit quite different highlight structure. One approach could be to build a library of scattering functions composed of the target at different positions in range and depth. The sensitivity analysis could tell you how finely you would need to sample in range and depth so that the performance is not severely degraded when the target is in between members of the library.

REFERENCES

1.Sibul, Leon H., Sidahmed, Stefan T., Dixon, Teresa L., Weiss, Lora G., "Wavelet Domain Implementation of the Estimator-Correlator and Weighted Wavelet Transforms", Proceedings of the 30th Annual Asilomar Conference on Signals, Systems, and Computers, Nov. 3 1997.

2.Dixon, Teresa L., Sibul, Leon H., "Wideband imaging and parameter estimation of distributed objects using the continuous wavelet transform", Signal Processing 54 (1996) 207-223.

3.Dixon, Teresa L., Sibul, Leon H., "A Parameterized Hough Transform Approach for Estimating the Support of the Wideband Spreading Function of a Distributed Object", Multidimensional Systems and Signal Processing, 7, 75-86 (1996).

4.Roan, Michael J., Sibul, Leon H., "Performance Quantification for the Wavelet Transform Domain Estimator-Correlator", Proc. 32nd Intnl. Conf. On Info. Sciences and Systs. Princeton Univ. March, 1998.

5.Bendat, Julius S., Piersol, Allan G., *Random Data Analysis Measurement Procedures*, John Wiley & Sons, 1986.

6. Weiss, Lora G., Sibul, Leon H., "Coherent Broadband Processing with Wavelet Transforms", Proc. Joint Math Meeting, American Math Society, January 8-11, 1997, San Diego, CA.

7.Weiss, L. G., Young, R. K., Sibul, L. H., "Wideband Processing of Acoustic Signals using Wavelet Transforms. Part I. Theory" J. Acoust. Soc, Am., Vol 96, No. 2, Prt. 1, August 1994.

8.Weiss, L. G., Young, R. K., Sibul, L. H., "Wideband Processing of Acoustic Signals using Wavelet Transforms. Part II. Efficient Implementation and Examples" J. Acoust. Soc, Am., Vol 96, No. 2, Prt. 1, August 1994.

9.Weiss, L. G., "Wavelets and Wideband Correlation Processing", IEEE Signal Processing Magazine, January 1994.

10.Weiss, L. G., "Wideband Inverse Scattering and Wideband Deconvolution of Acoustic Signals using Wavelet Transforms", Ph.D. Thesis in Acoustics, The Pennsylvania State University, May 1993.

11.Jin, Q., Wong, K. M., Luo, Z. Q., "Wideband Time Delay and Doppler Stretch Estimation: The Application of Wavelet Transform and the Optimum Signal", 1993 IEEE International Conference on Acoustics, Speech, and Signal Processing, 1993. ICASSP-93.,Volume: 1 , 1993 , Page(s): 241 -244.

12.Altes, R. A., "Some Invariance Properties of the Wideband Ambiguity Function", Journal of the Acoustical Society of America, Vol 53, No. 4, 1973.

13.Jourdain, G., Henrioux, J. P., "Use of Large Bandwidth-Duration Binary Phase Shift Keying Signals in Target Delay Doppler Measurements", Journal of the Acoustical Society of America, 90 (1), July 1991.

14.Ricker, D. W., "The Doppler Sensitivity of Large TW Phase Modulated Waveforms", IEEE Transactions on Signal Processing, Vol 40., No. 10, October 1992.

15.Glisson, Tildon H., Black, Charles I., Sage, Andrew P., "On Digital Replica Correlation Algorithms with Applications to Active Sonar", IEEE Trans. on Audio and Electroacoustics Vol. AU-17, No. 3, September 1969.

16.Tague, John A., Sibul, Leon H., "Estimator-Correlator Array Processing: Theoretical Underpinnings and Adaptive Implementation", Multidimensional Systems and Signal Processing, 2, 55-68, 1991.

17. Roan, Michael J., "A Kalman Filtering Approach to Wideband Scattering Function Estimation and Updating", Ph.D. Thesis in Acoustics, The Pennsylvania State University, May 1999.

18.Grove, Deborah M., Sensitivity of Scattering Function Estimates to Physical Parameter Measurement errors with Applications to the Wavelet Transform Domain Estimator-Correlator, Ph.D. thesis, Department of Acoustics, The Pennsylvania State University, 1998.

19. Ricker, Dennis W., Cutezo, Anthony J., "A Model-Based Estimator-Correlator (EC) Structure", IEEE Transactions of Signal Processing, Vol. 48, No. 10, October 2000.

20. Slepian, David, "On Bandwidth", Proceedings of the IEEE, Vol 64, No. 3, 1976, pp 292-300.

21. Slepian, David, "Some Comments on Fourier Analysis, Uncertainty, and Modeling", SIAM Review, Vol 25, No. 3, July 1983, p. 379-393.

22. Slepian, David, Pollack, Henry O., "Prolate Spheroidal Wave Functions, Fourier Analysis and Uncertainty - I", The Bell Systems Technical Journal, Vol 40, January 1961, P. 43-64.

23. Landau, Henry J., Pollack, Henry O., "Prolate Spheroidal Wave Functions, Fourier Analysis and Uncertainty - II", The Bell Systems Technical Journal, Vol 40, January 1961, P. 65-84.

24. Landau, Henry J., Pollack, Henry O., "Prolate Spheroidal Wave Functions, Fourier Analysis and Uncertainty - III", The Bell Systems Technical Journal, Vol 41, July 1962, P. 1295-1336.

25. Stewart, J. L., and Westerfield, E. C. "A Theory of Active Sonar Detection", Proc. IRE, pp. 872-881, May, 1959.

26. Knight, William C., Pridham, Roger G., Kay, Steven M., "Digital Signal Processing for Sonar", Proceedings of the IEEE, Vol. 69, No. 11, November 1981.

27.Sibul, L. H., Weiss, L. G., Dixon, T. L., "Characterization of Stochastic Propagation and Scattering Via Gabor and Wavelet Transforms", Journal of Computational Acoustics, Vol. 2, No. 3, 1994 345-369.

28. Daubechies, I., *Ten Lectures on Wavelets*, SIAM, Philadelphia, 1992.

29. Swick, D. A. "A Review of Wideband Ambiguity Functions", NRL Report 6994, 1969.

30. Van Trees, Harry L., *Detection, Estimation, and Modulation Theory Part 1*, John Wiley and Sons, New York, 1968.

31. Van Trees, Harry L., *Detection, Estimation and Modulation Theory Part 3*, John Wiley and Sons, New York, 1971.

32. McDonough, Robert N., Whalen, Anthony D., *Detection of Signals in Noise*, Academic Press, 1995.

33.Price, Robert, "Optimum Detection of Random Signals in Noise, with Application to Scatter-Multipath Communication, I", IRE Transactions on Information Theory, vol. IT-2, pp. 125-135. December 1956.

34.Esposito, R., "On a Relation between Detection and Estimation in Decision Theory", Information and Control, vol 12., 116-120, 1968.

35.Kailath, Thomas, "A General Likelihood-Ratio Formula for Random Signals in Gaussian Noise", IEEE Transactions on Information Theory, Vol IT-15, No. 3, May 1969.

36.Kailath, Thomas, "A Note on Least-Squares Estimates from Likelihood Ratios", Information and Control, vol 13, 534-540, 1968

37.Schwartz, Stuart C., "Conditional Mean Estimates and Bayesian Hypothesis Testing", IEEE Transactions on Information Theory, November 1975.

38.Schwartz, Stuart C., "The Estimator-Correlator for Discrete-Time Problems", IEEE transactions on Information Theory, Vol IT-23, No. 1, January 1977.

39.Middleton, David, "Simultaneous Optimum Detection and Estimation of Signals in Noise", IEEE Transactions on Information Theory, Vol. IT-14, No. 3, May 1968.

40.Chaiyasena, Arjuna Peter, "Radar and Sonar Ambiguity Functions and Group Theory", Ph.D. thesis, Department of Mathematics, The Pennsylvania State University, 1993.

41. Papoulis, Anthanasios, *Probability, Random Variables, and Stochastic Processes*, McGraw Hill, 1965.

42.Oppenheim, Alan V., Schafer, Ronald W., *Discrete-Time Signal Processing*, Prentice Hall, 1989, pg 166.

43. Spiegel, Murray R., Liu, John, *Mathematical Handbook of Formulas and Tables*, Second Edition, McGraw-Hill, 1999.

44.Scharf, Louis L., *Statistical Signal Processing: Detection, Estimation, and Time Series Analysis*, Addison-Wesley Publishing, 1991.

45.Lipschutz, Seymour, *Beginning Linear Algebra*, McGraw-Hill, 1997.

46. Schwenke, Roger W., Sibul, Leon H., "Sensitivity Analysis of a Detector for Multiple Highlight Targets", Proceedings of the 2000 Conference on Information Sciences and Systems, Vol 1.

47.Schwenke, Roger W., Sibul, Leon H., "Sensitivity Analysis of an Estimator Correlator", Journal of the Acoustical Society of America, Vol 107, No. 5, Pt. 2, May 2000 (abstract only)

48.Personal communication with Michael J. Roan.

49.Stewart, J. L., and Westerfield, E. C. "A Theory of Active Sonar Detection", Proc. IRE, pp. 872-881, May, 1959.

50.Golomb, Solomon W., Taylor, Herbert, "Two-Dimensional Synchronization Patterns for Minimum Ambiguity", IEEE trans. Info Theory, IT-28(4) July 1982, pp 600-604.

51.Titlebaum, E. L., "Time-Frequency Hop Signals Part I: Coding based Upon the Theory of Linear Congruences," IEEE Trans. Aerosp. & Elect. Systs. 17(4), pp 490-493, July 1981.

52.Titlebaum, Edward I., Sibul, Leon H., "Time-Frequency HOP Signals Part II: Coding based upon Quadratic Congruences", IEEE Trans. Aerosp. & Elect. Systs. 17(4), pp 494-499, July 1981.

53.Titlebaum, Edward I., Marić, Svetislav R., Bellegarda, Jerome R., "Ambiguity Properties of Quadratic Congruential Coding", IEEE Trans on Aerospace and Electronic Systems, Vol. 27, No. 1, January 1991.

54.Bellegarda, J. R., E.L.Titlebaum, "Time-Frequency Hop Codes Based Upon Extended Quadratic Congruences," IEEE Trans. Aerosp. & Elect. Systs. 24(6), pp 726-742, Nov. 1988.

55.Marić, S.V., E.L. Titlebaum, "Frequency Hop Multiple Access Codes Based Upon the Theory of Cubic Congruences," IEEE Trans. Aerosp. \& Elect. Systs. 25(6), pp 1035-42, Nov. 1990.

56.Bellegarda, Jerome R., Titlebaum, Edward I., "The Hit Array: An Analysis Formalism for Multiple Access Frequency Hop Coding", IEEE Trans. Aerosp. & Elect. Systs. 27(1), pp30-37, Jan. 1991.

57.Costas, J. P. "A Study of a Class of Detection Waveforms Having Nearly Ideal Range-Doppler Ambiguity Properties", Proc. of the IEEE, Vol. 72, No. 8, 1984, p 996.

58.Moreno, Oscar, Games, Richard A., Taylor, Herbert, "Sonar Sequences from Costas Arrays and the Best Known Sonar Sequences with up to 100 Symbols", IEEE Trans on Information Theory, Vol. 39, No. 6, November 1993.

59.Golomb, Solomon W., Taylor, Herbert, "Constructions and Properties of Costas Arrays", Proceedings of the IEEE, Vol. 72, No. 9, September 1984.

60.Bovbol, YE. I., Zaytseva YE. M., Kukharchik, P. D., "Costas Signals with Intrapulse Frequency Modulation", J. Communications Technology and Electronics 39(4), 1994.

61.Ricker, D.W., "A Logarithmic Frequency Allocation Algorithm for Wideband Discrete Frequency Pulse Trains," IEEE Trans. Aerosp. and Elect. Systs. 18(3), 1982, pp 347-349.

62.Freedman, Avraham, Levanon, Nadav, "Any Two NxN Costas Signals Must Have at Least One Common Ambiguity sidelobe if N > 3 - A Proof", Proceedings of the IEEE, Vol 73, No. 10, October 1985.

63.Chang, Weita, Scarbrough, Kent, "Costas Arrays with Small Number of Cross-Coincidences", IEEE Transactions on Aerospace and Electronic Systems, Vol AES-25, No. 1, January 1989.

64.Titlebaum, Edward L., Maric, Svetislav V., "Multiuser Sonar Properties for Costas Array Frequency Hop Coded Signals",

65.Titlebaum, Edward I., Marić, Svetislav R., "Multiuser Sonar Properties for Costas Array Frequency Hop Coded Signals", 1990 IEEE International Conference on Acoustics, Speech, and Signal Processing,, Vol. 5 Page(s): 2727 -2730, 1990.

66.Drumheller, David Mark, TitleBaum, Edward I, "Cross-Correlation Properties of Algebraically Constructed Costas Arrays", IEEE Trans on aerospace and Electrical Systems, Wol 27, No. 1 January 1991.

67.Mehta, Sanjay K., Titlebaum, Edward L., "A New Method for Measurement of the Target and Chanel Scattering Functions Using Costas Arrays and Other Frequency Hop Signals", 1991 International Conference on Acoustics, Speech, and Signal Processing,.Vol. 2, Page(s): 1337 -1340, 1991.

68.Gustafson, Michael J., "Uncertainty product scattering function estimation", A Masters Thesis in Acoustics, The Pennsylvania State University, 1993.

69.Naparst, Harold Lance, "Radar Signal Choice and Processing for a Dense Target Environment", Dissertation in Applied Mathematics, University of California, Berkeley, May 20, 1988.

70.Altes, Richard A., "Radar/Sonar Acceleration Estimation with Linear-Period Modulated Waveforms", IEEE Trans. On Aerospace and Electronic Systems, Vol. 26, No. 6, November 1990.

71.Altes, Richard A., "Optimum waveforms for Sonar Velocity Discrimination", Proceedings of the IEEE, November 1971.

72.Ricker, D. W., "Constrained Bandwidth Waveforms with Minimal Dilation Sensitivity", IEEE Trans. On Aerospace and Electronic Systems, Vol. 29, No. 3, July 1993.

73.Altes, Richard A., "Radar/Sonar Signal Design for Bounded Doppler Shifts", IEEE Trans. On Aerospace and Electronic Systems, Vol. AES-18, No. 4, July 1982.

74.Fenton, M. Brock, Bell, Gary P., "Echolocation and feeding behavior in four species of Myotis (Chiroptera)", Canadian Journal of Zoology, Vol. 57, 1979, p. 1271.

75.Kalko, Elisabeth K. V., Schnitzer, H.-U., "Plasticity in echolocation signals of European pipistrelle bats in search flight: implications for habitat use and prey detection", Behav. Ecol. Sociobiol (1993) 233:415-428.

76.Saillant, Preston A., Simmons, Jams A., Dear, Steven P., McMullen, Teresa A., "A computational model of echo processing and acoustic imaging in frequency-modulated echolocating bats: The spectrogram correlation and transformation receiver", Acoustical Society of America, 94 (5), November 1993, p. 2691.

77.Mahoney, J. F. , Sivazlian, B. D., "Partial fraction expansion: a review of computational methodology and efficiency", Journal of Computational and Applied Mathematics, 9, 1983, 247-269.

78. Chang, Fend-Cheng, "Recursive Formulas for the Partial Fraction Expansion of a Rational Function with Multiple Poles", Proceedings of the IEEE, August 1973.

79.Chang, Feng-Cheng, Mott, Harld, "On the Matrix Relatred to the Partial Fraction Expansion of a Proper Rational Function", Proceedings of the IEEE, August 1974.

80.Uraz, A., N-Ngay, F. L., Matrix Formulation for Partial-fraction Expansion of Transfer Functions", Journal of the Franklin Institute, Volume 297, Number 2, February 1974.

81.Deakin, Michael A. B., "Successive discoveries of the Heaviside expansion theorem", Int J. Math Educ. Schi. Technol., 1968, Vol. 17, No. 1, 51-60.

APPENDIX A

Signal Design

In 1959 Stewart and Westerfield published their paper "A Theory of Active Sonar Detection" [50] where the results of radar echo detection are applied to sonar. Stewart and Westerfield optimize a detection index, however the detection index is not a complete performance measure because it can not be used to uniquely identify the corresponding ROC curve. One needs the complete ROC curve to measure the performance of the detector because the total scattering strength no longer uniquely specifies the ROC curve. As shown in section 3.6, scattering functions with different highlight distributions, but the same total scattering energy result in different ROC curves.

One set of functions that has been optimized for different qualities is frequency hop codes. Hop codes have several desirable qualities such as energy efficiency and predictable sidelobe levels. They also have a large number of parameters which can be adjusted, namely the time that each frequency chip occurs in the signal. Hop Codes are typically designed to have a "thumb-tack" like autoambiguity function, but in the past the ROC has not been used in the criteria of the design. Also, the vast majority of frequency hop code work has used narrowband processing. Golomb and Taylor's "Two-Dimensional Synchronization Patterns for Minimum Ambiguity" [50, 59] provides a detailed review of the literature up to 1982.

Titlebaum's "Time-Frequency Hop Signals Part I: Coding Based Upon the Theory of Linear Congruences" [51] describes a code set where there is an upper bound on the cross-correlation between any two members of the set. In "Time Frequency HOP Signals Part II: coding Based Upon Quadratic Congruences" [52], Titlebaum and Sibul define signal efficiency as the ratio of average power to peak power and conclude that maximum signal efficiency is attained by frequency hop codes. In this frequency hop coding scheme the distance between successive chips increases quadratically. Chips wrap around in frequency when they surpass the desired bandwidth. Limits on the side lobe level for Quadratic Congruence codes are derived.

In "Ambiguity Properties of Quadratic Congruential Coding", by Titlebaum, Marić, and Bellegarda [53] it is shown that these codes have a thumbtack like auto-correlation function with a uniform upper bound on the plateau. It is shown that their cross ambiguity properties are better

than Costas codes (described below).

Further work along these lines is presented in Bellegarda and Titlebaums's "Time-Frequency Hop Codes Based Upon Quadratic Congruences" [54] and "Frequency Hop Multiple Access Codes Based Upon the Theory of Cubic Congruences", by Marić, and Titlebaum [55].

Bellegarda and Titlebaum, in their 1991 paper "The Hit Array: An Analysis formalism" [56], show that discretizing the time frequency representation of a signal provides a convenient method for analyzing them. They show that reflections and rotations of hop codes will produce the same reflection and rotation in the auto-correlation function. It is shown that this representation is valid when $N^2 << TB$ where N is the number of chips, T is the time duration of the signal, and B the bandwidth.

In 1984 Costas introduced what came to be known as Costas Codes, codes whose hit array has a maximum side lobe level of 1 [57]. A good overview of different methods of constructing Costas Codes has been written by Moreno, Games and Taylor [58]. Another such paper was written by Golomb and Taylor [50, 59]. Variations on Costas Codes have been suggested, such as "Costas Signals with Intrapulse Frequency Modulation" [60]. In this paper, each individual chip of the code is frequency modulated. The peak to side-lobe ratio is the same, but the main lobe is narrower. Ricker has shown that if hops are allocated logarithmically in frequency, instead of linearly, then the autoambiguity function is the same regardless of center frequency and bandwidth [61]. If hops are allocated linearly then the sidelobes interfere with each other in different ways depending on the center frequency and bandwidth.

One criteria often used to optimize signals is their cross-correlation properties. Freedman and Levanon have shown that "Any Two NxN Costas Signals Must Have at Least One Common Ambiguity Sidelobe if N > 3" [62]. Chang and Scarbrough have described a method of obtaining Costas arrays with a minimum number of cross-coincidences for a limited Doppler shift [63]. For an N x N Costas code, then q Costas codes can be found with a maximum cross-coincidence of one for a maximum Doppler shift of M where: $(M+1)q <= N$. Titlebaum and Marić have shown that if two cross coincidences are allowed, then Costas codes with minimum(2) cross coincidences can be found without limiting the allowed Doppler shift [64]. Certain constructions of Costas codes are shown to be better than others in this regard. In a separate paper they have

shown that certain sized Costas codes have better cross-correlation properties [65]. More work on this topic has been done by Drumheller and Titlebaum [66].

Another approach to optimizing the shape of the autoambiguity function is what is known as the Twin Processor or Uncertainty Product Function. In this approach more than one signal is transmitted into the environment, the scattering function is computed for each one, and then the two scattering functions are multiplied together. The effect is that real scatterers will add coherently, and spurious scatterers will be canceled. The drawback is that if the two signals are separated in time, then the velocity resolution is severely limited, and if they are separated in frequency the spacial resolution is severely limited. Work of this kind has been done by Mehta and Titlebaum [67], and Gustafson [69]. Naparst has worked on a system for combining information from several pings, where he uses the wideband processing and optimizes the shape of the autoambiguity function [69].

Signals have also been optimized to ignore, or "tolerate", certain conditions. Altes has derived signals which are acceleration tolerant [70] and velocity tolerant [71]. Ricker has derived signals which are Doppler tolerant [72]. Altes has also designed signals for use when Doppler shifts are bounded [73].

Research has been done on echolocation signals used by bats, in hopes that evolution has in some way optimized the signals used in ways that are useful to sonar designers. Fenton and Bell found that an LFM followed by a constant frequency portion is correlated to an increased detection range in the species Myotis Volnas [74]. Kalko and Schnitzer found that certain bats switch from narrowband signals in free flight to wideband signals when approaching prey or cluttered areas (such as cave entrances) [75]. Saillant et al. have created a computational model of the cochlea and echolocation system of the bat [76]. They claim that this model has higher resolution than simple cross correlation.

APPENDIX B

Alternatives to Computing the Probability of False Alarm

In Chapter 3 it was shown that there are numerical problems computing the Heaviside coefficients of:

$$\phi_{l_i}(\omega) = \prod_{k}^{N} (1 - j2\omega A_{k_i})^{-1}$$

Recall that

$$A_{k_0} = \frac{\lambda_k^y}{\lambda_k^y + 1} \text{ and } A_{k_1} = \lambda_k^y$$

If all of the A_{k_0} 's were precisely equal the corresponding probability function for the false alarm would be a Chi Squared distribution. It is now shown that the real characteristic function can be written as the Chi Squared distribution with a small correction.

$$\phi_{l_0} = \prod_{k}^{N} \frac{1}{1 - j2\omega A_{k_0}}$$

where

$$A_{k_0} = \frac{\lambda_k}{\lambda_k + 1} = \frac{1}{1 + 1/\lambda_k}$$

if λ_k is >>1 then $1/\lambda_k$ <<1. To emphasize this we will rename $1/\lambda_k = \varepsilon_k$

$$A_{k_i} = \frac{1}{1 + \varepsilon_k}$$

The characteristic function now becomes

$$\phi_{l_0} = \prod_k^N \frac{1}{1 - j2\omega/(1+\varepsilon_k)} = \prod_k^N \frac{1+\varepsilon_k}{1+\varepsilon_k - j2\omega}$$

$$\phi_{l_0} = \prod_k^N \frac{1+\varepsilon_k}{(1-j2\omega)+\varepsilon_k} = \prod_k^N \frac{1}{1-j2\omega}\left(\frac{1+\varepsilon_k}{1+\varepsilon_k/(1-j2\omega)}\right)$$

$$\phi_{l_0} = (1-j2\omega)^{-N}\prod_k^N \left(\frac{1+\varepsilon_k}{1+\varepsilon_k/(1-j2\omega)}\right)$$

The beginning term $(1-j2\omega)^{-N}$ is the characteristic function of a Chi Squared distribution of order N. The term it is multiplied by is one plus a small number, divided by one plus a small number, which is a number very close to one. This is highly suggestive of the fact that the false alarm may be approximated by a Chi Squared distribution. We will now show that $|1/(1-j2\omega)| \le 1$.

$$\left|\frac{1}{1-j2\omega}\right| = \left|\frac{1+j2\omega}{1+4\omega^2}\right|$$

$$= \frac{(1+4\omega^2)^{1/2}}{1+4\omega^2}$$

$$= \frac{1}{1+4\omega^2} \le 1$$

Expanding the expression for ϕ_{l_0}

$$\phi_{l_0} = (1-j2\omega)^{-N}\prod_k^N \frac{1}{1+\varepsilon_k/(1-j2\omega)} + \frac{\varepsilon_k}{1+\varepsilon_k/(1-j2\omega)}$$

$$\phi_{l_0} = (1 - j2\omega)^{-N} \prod_k^N \left(1 + \frac{\varepsilon_k}{1 - j2\omega}\right)^{-1} + \varepsilon_k \left(1 + \frac{\varepsilon_k}{1 - j2\omega}\right)^{-1}$$

Taylor expanding yields

$$\phi_{l_0} \approx (1 - j2\omega)^{-N} \prod_k^N 1 - \frac{\varepsilon_k}{1 - j2\omega} + \varepsilon_k - \frac{\varepsilon_k^{\,2}}{1 - j2\omega}$$

Dropping terms of order ε_k^2

$$\phi_{l_0} \approx (1 - j2\omega)^{-N} \prod_k^N 1 + \varepsilon_k \left(1 - \frac{1}{1 - j2\omega}\right)$$

$$\phi_{l_0} \approx (1 - j2\omega)^{-N} \prod_k^N 1 + \varepsilon_k \left(\frac{1 - j2\omega - 1}{1 - j2\omega}\right)$$

$$\phi_{l_0} \approx (1 - j2\omega)^{-N} \prod_k^N 1 + \varepsilon_k \left(\frac{-j2\omega}{1 - j2\omega}\right)$$

$$\phi_{l_0} = (1 - j2\omega)^{-N} [1 + \frac{j2\omega}{1 - j2\omega} \prod_k^N \varepsilon_k]$$

We now name these two terms:

$$\phi_{l_0} = \phi_{\chi^2} + \Delta\phi_{l_0}$$

$$\phi_{\chi^2} = (1 - j2\omega)^{-N}$$

$$\Delta\phi_{l_0} = (1 - j2\omega)^{-N} \frac{j2\omega}{1 - j2\omega} \prod_k^N \varepsilon_k$$

One approach we could take is to simply use the Chi Squared distribution, and drop any correction term. The ROC will still have information about the individual ε_k's because the probability of detection can be computed exactly.

The probability of false alarm for a chi squared probability density has already been derived by Van Trees 30.

$$P_{F\chi^2} = 1 - I_\Gamma\left(\frac{\gamma'''}{\sqrt{M+1}}, M\right)$$

where I_Γ is the incomplete gamma function which Van Trees defines as:

$$I_\Gamma(u, M) \equiv \int_0^{u\sqrt{M+1}} \frac{x^M}{M!} e^{-x} dx$$

It is important to note that this not the way that the incomplete gamma function is defined in Matlab. Van Trees also derives a approximation for large γ .

$$P_{F\chi^2 approx} \approx \frac{(\gamma''')^M e^{-\gamma'''}}{M!(1 - M/\gamma''')}$$

The notation with regards to γ is a bit tricky. The likelihood ratio used in this paper (equation 17) is equivalent to equation 398 on page 108 of Van Trees 30. Thus our γ is equivalent to his γ'. Van Trees then goes on to define:

$$\gamma''' = \frac{(\sigma_n^2 + \sigma_s^2)}{2\sigma_s^2}\gamma'$$

where σ_n^2 is the standard deviation of the noise and σ_s^2 is the standard deviation of the signal. In this work we have whitened the noise, so we take $\sigma_n^2 = 1$. The signal variance then corresponds to the eigenvalues of the whitened received signal $\sigma_s^2 = \overline{\lambda_s}$, where the bar denotes the average. Preliminary numerical results have shown that the chi squared approximation is not only a good approximation, but an upper bound and thus the computed ROC will never better than the true ideal. No analytic method has yet been found to confirm this. A typical Probability of false alarm for six eigenvalues between 5 and 50 is shown in figure ? in comparison to the exact Chi Squared distribution, and the approximate Chi Squared distribution:

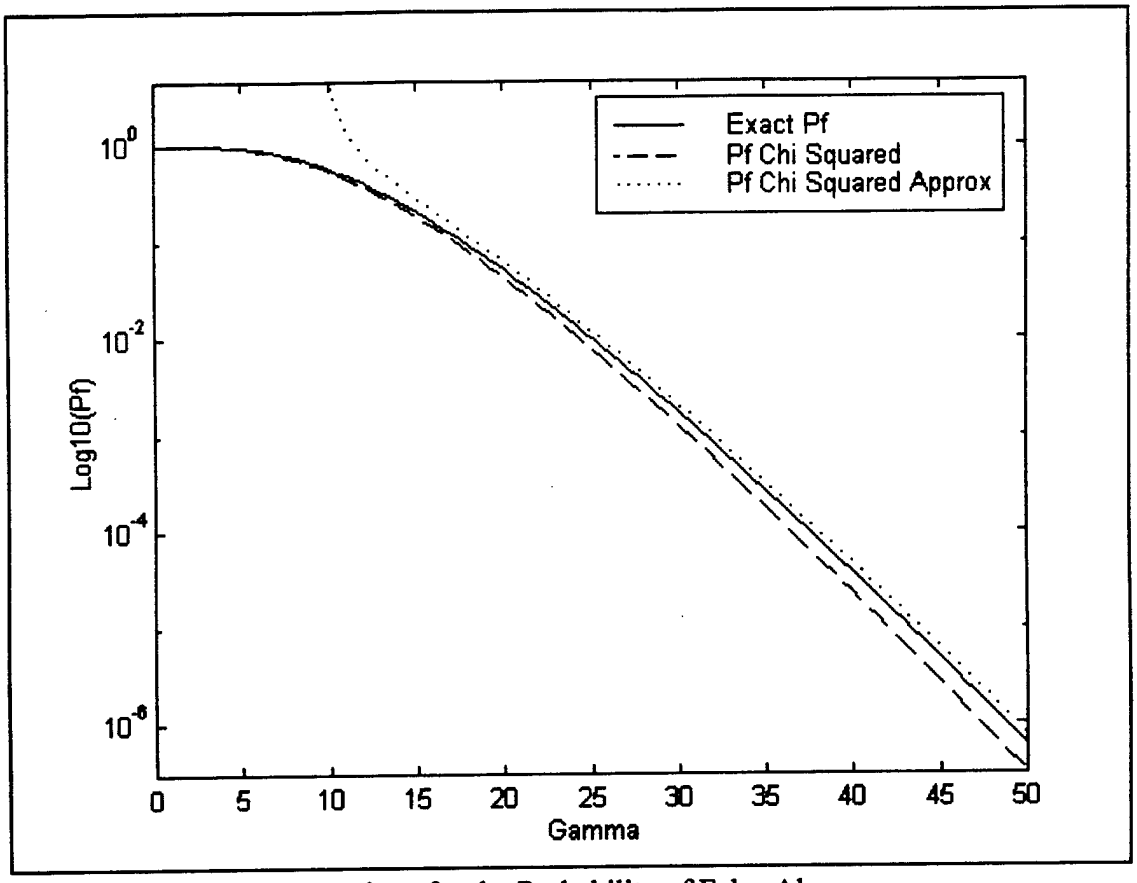

Figure 31 Different expressions for the Probability of False Alarm

We will now calculate the correction to the Chi Squared Probability of false alarm due to $\Delta\phi_{l_0}$. Defining $\varepsilon_T = \prod_k^N \varepsilon_k$

$$\Delta\phi_{l_0} = \frac{j2\omega\varepsilon_T}{(1-j2\omega)^{N+1}}$$

The corresponding probability distribution is

$$\Delta p_{l|H_0}(l|H_0) = \frac{1}{2\pi}\int_{-\infty}^{\infty}\frac{j2\omega\varepsilon_T}{(1-j2\omega)^{N+1}}d\omega$$

making the substitution $s = j\omega$, $ds = jd\omega$, $d\omega = ds / j$

$$\Delta p_{l|H_0}(l|H_0) = j\frac{1}{2\pi j}\int_{-\infty}^{\infty}\frac{2s\varepsilon_T}{(1-2s)^{N+1}}\frac{ds}{j}$$

writing in terms of an inverse Laplace transform $\mathcal{L}^{-1}\{\}$

$$\Delta p_{l|H_0}(l|H_0) = 2\varepsilon_T\mathcal{L}^{-1}\left\{\frac{s}{(1-2s)^{N+1}}\right\}$$

$$\Delta p_{l|H_0}(l|H_0) = 2\varepsilon_T\mathcal{L}^{-1}\left\{\frac{s}{(-2)^{N+1}(s-1/2)^{N+1}}\right\}$$

$$\Delta p_{l|H_0}(l|H_0) = \frac{2\varepsilon_T}{(-2)^{N+1}}\mathcal{L}^{-1}\left\{\frac{s}{(s-1/2)^{N+1}}\right\}$$

This transform can be found in standard tables. It is:

$$\mathcal{L}^{-1}\left\{\frac{1}{(s-1/2)^{N+1}}\right\} = \frac{l^N e^{-l/2}}{N!}$$

Using

$$\mathcal{L}^{-1}\{sf(s) - F(0)\} = F'(t)$$

we can write

$$\mathcal{L}^{-1}\left\{\frac{s}{(s-1/2)^{N+1}}\right\} = \frac{d}{dl}\frac{l^N e^{-l/2}}{N!} = \frac{1}{N!}\left(Nl^{N-1}e^{-l/2} - \frac{1}{2}l^N e^{-l/2}\right)$$

$$\Delta p_{l|H_0}(l|H_0) = \frac{2\varepsilon_T}{(-2)^{N+1}N!}\left(Nl^{N-1}e^{-l/2} - \frac{1}{2}l^N e^{-l/2}\right)$$

The corresponding correction to the false alarm is

$$\Delta P_F = \int_{\gamma}^{\infty} \Delta p_{l|H_0}(l|H_0)dl$$

$$\Delta P_F = \frac{2\varepsilon_T}{(-2)^{N+1}N!}\int_{\gamma}^{\infty}\left(Nl^{N-1}e^{-l/2} - \frac{1}{2}l^N e^{-l/2}\right)dl$$

$$\Delta P_F = \frac{2\varepsilon_T}{(-2)^{N+1}N!}\left[N\int_{\gamma}^{\infty} l^{N-1}e^{-l/2}dl - \frac{1}{2}\int_{\gamma}^{\infty} l^N e^{-l/2}dl\right]$$

using

$$\int_{\gamma}^{\infty} x^N e^{ax}dx = \frac{N!e^{a\gamma}}{a}\left(\sum_{k=0}^{N}\frac{(-1)^k\gamma^{N-k}}{a^k(N-k)!}\right)$$

The correction to the false alarm is:

$$\int_{\gamma}^{\infty} l^{N-1}e^{-l/2}dl = \frac{(N-1)!e^{-\gamma/2}}{-1/2}\left(\sum_{k=0}^{N-1}\frac{(-1)^k\gamma^{N-1-k}}{(-1/2)^k(N-1-k)!}\right)$$

$$\int_{\gamma}^{\infty} l^N e^{-l/2}dl = \frac{N!e^{-\gamma/2}}{(-1/2)}\left(\sum_{k=0}^{N}\frac{(-1)^k\gamma^{N-k}}{(-1/2)^k(N-k)!}\right)$$

$$\Delta P_F = \frac{2\varepsilon_T}{(-2)^{N+1}N!}\left[N\frac{(N-1)!e^{-\gamma/2}}{-1/2}\left(\sum_{k=0}^{N-1}\frac{(-1)^k\gamma^{N-1-k}}{(-1/2)^k(N-1-k)!}\right) - \frac{1}{2}\frac{N!e^{-\gamma/2}}{(-1/2)}\left(\sum_{k=0}^{N}\frac{(-1)^k\gamma^{N-k}}{(-1/2)^k(N-k)!}\right)\right]$$

$$\Delta P_F = \frac{2\varepsilon_T N!e^{-\gamma/2}}{(-2)^{N+1}(-1/2)N!}\left[\left(\sum_{k=0}^{N-1}\frac{(-1)^k\gamma^{N-1-k}}{(-1/2)^k(N-1-k)!}\right) - \frac{1}{2}\left(\sum_{k=0}^{N}\frac{(-1)^k\gamma^{N-k}}{(-1/2)^k(N-k)!}\right)\right]$$

$$\Delta P_F = \frac{2\varepsilon_T e^{-\gamma/2}}{(-2)^N}\left[\left(\sum_{k=0}^{N-1}\frac{(-1)^k\gamma^{N-1-k}}{(-1/2)^k(N-1-k)!}\right) - \frac{1}{2}\left(\sum_{k=0}^{N}\frac{(-1)^k\gamma^{N-k}}{(-1/2)^k(N-k)!}\right)\right]$$

$$\Delta P_F = \frac{2\varepsilon_T e^{-\gamma/2}}{(-2)^N}\left[\left(\sum_{k=0}^{N-1}\frac{(-1)^k\gamma^{N-1-k}}{(-1)^k(1/2)^k(N-1-k)!}\right) - \frac{1}{2}\left(\sum_{k=0}^{N}\frac{(-1)^k\gamma^{N-k}}{(-1)^k(1/2)^k(N-k)!}\right)\right]$$

$$\Delta P_F = \frac{2\varepsilon_T e^{-\gamma/2}}{(-2)^N}\left[\left(\sum_{k=0}^{N-1}\frac{2^k\gamma^{N-1-k}}{(N-1-k)!}\right)-\frac{1}{2}\left(\sum_{k=0}^{N}\frac{2^k\gamma^{N-k}}{(N-k)!}\right)\right]$$

Alternatives to Computing the Probability of False Alarm: Advanced Methods of Computing the Heaviside Expansion

A number of different methods of computing the Heaviside coefficients have been developed, unfortunately, the vast majority of them focus on computational efficiency and not on numerical accuracy. Also all of them compute coefficients which are equal to the coefficients found in the traditional manner, and are thus still limited by the machines precision. These schemes usually find some way to express the expansion in terms of a matrix inversion. Unfortunately, the case where all the roots are nearly equal correspond to a matrix whose rows are all nearly equal, which is also numerically difficult to compute. Mahoney and Sivazlian 76 wrote a review of these methodologies as of 1983. Chang has developed a non-matrix recursive method 77, however the coefficients are still equivalent to the traditional coefficients. Matrix algorithms have been developed by Chang and Mott 78, and Uraz and N-Nagy 79. Deakin has written a paper on the history of the heaviside expansion 80.

Vita

Roger W Schwenke received an advanced studies degree from Thomas Jefferson High School for Science and Technology in Fairfax Virginia in 1991. He received a Bachelor of Science with Honors in Physics from the College of William and Mary in 1995. During the summers between 1990 and 1995 he worked as a programmer for Mission Research Corp. While at Penn State University he was awarded the Kenneth T Simowitz Memorial Citation given by Graduate Department in Acoustics in recognition for presentations of papers in professional meetings. He served on the student council of the Acoustical Society of America representing the Interdisciplinary Technical Group on Signal Processing. In 2000 Mr. Schwenke won second prize for the best student paper award in underwater acoustics given by the Acoustical Society of America for "Sensitivity Analysis of an Estimator Correlator" given at the 139th meeting of the Acoustical Society of America, Atlanta Georgia. Mr. Schwenke is a member of the Acoustical Society of America, and the Audio Engineering Society.